National Library
of Canada

Acquisitions and
Bibliographic Services Branch

395 Wellington Street
Ottawa, Ontario
K1A 0N4

Bibliothèque nationale
du Canada

Direction des acquisitions et
des services bibliographiques

395, rue Wellington
Ottawa (Ontario)
K1A 0N4

Your file Votre référence

Our file Notre référence

NOTICE

The quality of this microform is heavily dependent upon the quality of the original thesis submitted for microfilming. Every effort has been made to ensure the highest quality of reproduction possible.

If pages are missing, contact the university which granted the degree.

Some pages may have indistinct print especially if the original pages were typed with a poor typewriter ribbon or if the university sent us an inferior photocopy.

Reproduction in full or in part of this microform is governed by the Canadian Copyright Act, R.S.C. 1970, c. C-30, and subsequent amendments.

AVIS

La qualité de cette microforme dépend grandement de la qualité de la thèse soumise au microfilmage. Nous avons tout fait pour assurer une qualité supérieure de reproduction.

S'il manque des pages, veuillez communiquer avec l'université qui a conféré le grade.

La qualité d'impression de certaines pages peut laisser à désirer, surtout si les pages originales ont été dactylographiées à l'aide d'un ruban usé ou si l'université nous a fait parvenir une photocopie de qualité inférieure.

La reproduction, même partielle, de cette microforme est soumise à la Loi canadienne sur le droit d'auteur, SRC 1970, c. C-30, et ses amendements subséquents.

Canada

UNIVERSITY OF ALBERTA

CHARACTERIZATION OF THE IMMUNOGENIC PROPERTIES OF THE MENGO VIRION

BY

© DARWYN L. KOBASA

A thesis submitted to the Faculty of Graduate Studies and Research in partial fulfillment of the requirements for the degree of DOCTOR OF PHILOSOPHY.

DEPARTMENT OF BIOCHEMISTRY

Edmonton, Alberta
Fall 1994

National Library of Canada
Acquisitions and Bibliographic Services Branch
395 Wellington Street
Ottawa, Ontario
K1A 0N4

Bibliothèque nationale du Canada
Direction des acquisitions et des services bibliographiques
395, rue Wellington
Ottawa (Ontario)
K1A 0N4

Your file Votre référence

Our file Notre référence

The author has granted an irrevocable non-exclusive licence allowing the National Library of Canada to reproduce, loan, distribute or sell copies of his/her thesis by any means and in any form or format, making this thesis available to interested persons.

L'auteur a accordé une licence irrévocable et non exclusive permettant à la Bibliothèque nationale du Canada de reproduire, prêter, distribuer ou vendre des copies de sa thèse de quelque manière et sous quelque forme que ce soit pour mettre des exemplaires de cette thèse à la disposition des personnes intéressées.

The author retains ownership of the copyright in his/her thesis. Neither the thesis nor substantial extracts from it may be printed or otherwise reproduced without his/her permission.

L'auteur conserve la propriété du droit d'auteur qui protège sa thèse. Ni la thèse ni des extraits substantiels de celle-ci ne doivent être imprimés ou autrement reproduits sans son autorisation.

ISBN 0-315-95210-5

Canada

Name Darwyn Kobasa

Dissertation Abstracts International is arranged by broad, general subject categories. Please select the one subject which most nearly describes the content of your dissertation. Enter the corresponding four-digit code in the spaces provided.

	0982
SUBJECT TERM	SUBJECT CODE

U·M·I

Subject Categories

THE HUMANITIES AND SOCIAL SCIENCES

COMMUNICATIONS AND THE ARTS

Architecture	0729
Art History	0377
Cinema	0900
Dance	0378
Fine Arts	0357
Information Science	0723
Journalism	0391
Library Science	0399
Mass Communications	0708
Music	0413
Speech Communication	0459
Theater	0465

EDUCATION

General	0515
Administration	0514
Adult and Continuing	0516
Agricultural	0517
Art	0273
Bilingual and Multicultural	0282
Business	0688
Community College	0275
Curriculum and Instruction	0727
Early Childhood	0518
Elementary	0524
Finance	0277
Guidance and Counseling	0519
Health	0680
Higher	0745
History of	0520
Home Economics	0278
Industrial	0521
Language and Literature	0279
Mathematics	0280
Music	0522
Philosophy of	0998
Physical	0523
Psychology	0525
Reading	0535
Religious	0527
Sciences	0714
Secondary	0533
Social Sciences	0534
Sociology of	0340
Special	0529
Teacher Training	0530
Technology	0710
Tests and Measurements	0288
Vocational	0747

LANGUAGE, LITERATURE AND LINGUISTICS

Language	
General	0679
Ancient	0289
Linguistics	0290
Modern	0291
Literature	
General	0401
Classical	0294
Comparative	0295
Medieval	0297
Modern	0298
African	0316
American	0591
Asian	0305
Canadian (English)	0352
Canadian (French)	0355
English	0593
Germanic	0311
Latin American	0312
Middle Eastern	0315
Romance	0313
Slavic and East European	0314

PHILOSOPHY, RELIGION AND THEOLOGY

Philosophy	0422
Religion	
General	0318
Biblical Studies	0321
Clergy	0319
History of	0320
Philosophy of	0322
Theology	0469

SOCIAL SCIENCES

American Studies	0323
Anthropology	
Archaeology	0324
Cultural	0326
Physical	0327
Business Administration	
General	0310
Accounting	0272
Banking	0770
Management	0454
Marketing	0338
Canadian Studies	0385
Economics	
General	0501
Agricultural	0503
Commerce-Business	0505
Finance	0508
History	0509
Labor	0510
Theory	0511
Folklore	0358
Geography	0366
Gerontology	0351
History	
General	0578
Ancient	0579
Medieval	0581
Modern	0582
Black	0328
African	0331
Asia, Australia and Oceania	0332
Canadian	0334
European	0335
Latin American	0336
Middle Eastern	0333
United States	0337
History of Science	0585
Law	0398
Political Science	
General	0615
International Law and Relations	0616
Public Administration	0617
Recreation	0814
Social Work	0452
Sociology	
General	0626
Criminology and Penology	0627
Demography	0938
Ethnic and Racial Studies	0631
Individual and Family Studies	0628
Industrial and Labor Relations	0629
Public and Social Welfare	0630
Social Structure and Development	0700
Theory and Methods	0344
Transportation	0709
Urban and Regional Planning	0999
Women's Studies	0453

THE SCIENCES AND ENGINEERING

BIOLOGICAL SCIENCES

Agriculture	
General	0473
Agronomy	0285
Animal Culture and Nutrition	0475
Animal Pathology	0476
Food Science and Technology	0359
Forestry and Wildlife	0478
Plant Culture	0479
Plant Pathology	0480
Plant Physiology	0817
Range Management	0777
Wood Technology	0746
Biology	
General	0306
Anatomy	0287
Biostatistics	0308
Botany	0309
Cell	0379
Ecology	0329
Entomology	0353
Genetics	0369
Limnology	0793
Microbiology	0410
Molecular	0307
Neuroscience	0317
Oceanography	0416
Physiology	0433
Radiation	0821
Veterinary Science	0778
Zoology	0472
Biophysics	
General	0786
Medical	0760

EARTH SCIENCES

Biogeochemistry	0425
Geochemistry	0996
Geodesy	0370
Geology	0372
Geophysics	0373
Hydrology	0388
Mineralogy	0411
Paleobotany	0345
Paleoecology	0426
Paleontology	0418
Paleozoology	0985
Palynology	0427
Physical Geography	0368
Physical Oceanography	0415

HEALTH AND ENVIRONMENTAL SCIENCES

Environmental Sciences	0768
Health Sciences	
General	0566
Audiology	0300
Chemotherapy	0992
Dentistry	0567
Education	0350
Hospital Management	0769
Human Development	0758
Immunology	0982
Medicine and Surgery	0564
Mental Health	0347
Nursing	0569
Nutrition	0570
Obstetrics and Gynecology	0380
Occupational Health and Therapy	0354
Ophthalmology	0381
Pathology	0571
Pharmacology	0419
Pharmacy	0572
Physical Therapy	0382
Public Health	0573
Radiology	0574
Recreation	0575
Speech Pathology	0460
Toxicology	0383
Home Economics	0386

PHYSICAL SCIENCES

Pure Sciences

Chemistry	
General	0485
Agricultural	0749
Analytical	0486
Biochemistry	0487
Inorganic	0488
Nuclear	0738
Organic	0490
Pharmaceutical	0491
Physical	0494
Polymer	0495
Radiation	0754
Mathematics	0405
Physics	
General	0605
Acoustics	0986
Astronomy and Astrophysics	0606
Atmospheric Science	0608
Atomic	0748
Electronics and Electricity	0607
Elementary Particles and High Energy	0798
Fluid and Plasma	0759
Molecular	0609
Nuclear	0610
Optics	0752
Radiation	0756
Solid State	0611
Statistics	0463

Applied Sciences

Applied Mechanics	0346
Computer Science	0984
Engineering	
General	0537
Aerospace	0538
Agricultural	0539
Automotive	0540
Biomedical	0541
Chemical	0542
Civil	0543
Electronics and Electrical	0544
Heat and Thermodynamics	0348
Hydraulic	0545
Industrial	0546
Marine	0547
Materials Science	0794
Mechanical	0548
Metallurgy	0743
Mining	0551
Nuclear	0552
Packaging	0549
Petroleum	0765
Sanitary and Municipal	0554
System Science	0790
Geotechnology	0428
Operations Research	0796
Plastics Technology	0795
Textile Technology	0994

PSYCHOLOGY

General	0621
Behavioral	0384
Clinical	0622
Developmental	0620
Experimental	0623
Industrial	0624
Personality	0625
Physiological	0989
Psychobiology	0349
Psychometrics	0632
Social	0451

UNIVERSITY OF ALBERTA

RELEASE FORM

NAME OF AUTHOR: Darwyn L. Kobasa

TITLE OF THESIS: Characterization of the Immunogenic Properties of the Mengo Virion

DEGREE: Doctor of Philosophy

YEAR THIS DEGREE GRANTED: 1994

Permission is hereby granted to the University of Alberta to reproduce single copies of this thesis and to lend or sell such copies for private, scholarly or scientific research purposes only.

The author reserves all other publication and other rights in association with the copyright in the thesis, and except as hereinbefore provided neither the thesis nor any substantial portion thereof may be printed or otherwise reproduced in any material form whatever without the author's prior written permission.

Darwyn Kobasa

Box 1202
Fairview, Alberta
T0H 1L0
Canada

Aug 30, 1994

UNIVERSITY OF ALBERTA

FACULTY OF GRADUATE STUDIES AND RESEARCH

The undersigned certify that they have read, and recommend to the Faculty of Graduate Studies and Research for acceptance, a thesis entitled CHARACTERIZATION OF THE IMMUNOGENIC PROPERTIES OF THE MENGO VIRION submitted by DARWYN KOBASA in partial fulfillment of the requirements for the degree of DOCTOR OF PHILOSOPHY.

D G Scraba

Dr. Douglas G. Scraba

R C Bleackley

Dr. R. Chris Bleackley

Stephen G. Rice

Dr. Stephen Rice

Robert S Hodges

Dr. Robert Hodges

R B Hodgetts

Dr. Ross Hodgetts

Fred Brown

Dr. Fred Brown

Aug 30, 1994

To my family
for their constant
support and encouragement

ABSTRACT

Mengo virus, a natural pathogen of mice, is a member of the cardiovirus genus of the picornaviruses, a family of viruses causing a variety of diseases in humans and animals. The Mengo virion is composed of 60 copies of each of four structural proteins (VP1, VP2, VP3 and VP4) symmetrically arranged into a spherical icosahedral capsid approximately 30 nm in diameter; its structure has been determined to 3 Å resolution. The capsid encloses a single stranded RNA genome of approximately 7780 nucleotides. In this study we have investigated the immunogenic structures of the Mengo capsid which are recognized by the B and T-helper lymphocyte components of the murine immune system. As well, a preliminary analysis of the mechanisms by which anti-Mengo virus monoclonal antibodies neutralize viral infectivity has been undertaken.

First, four neutralizing monoclonal antibodies were generated from mice immunized with viral capsid subunits and used to select naturally occurring mutants of the virus able to escape neutralization. Sequencing of the genome of each mutant virion was performed to identify amino acid mutations in the capsid which conferred neutralization resistance; these define the position of the binding site (epitope) for the antibody used to select the mutant. Three of the antibodies recognized an immunodominant region (antigenic determinant) in VP2 (Site 1) while the other bound to an epitope within VP3 (Site 2).

The analysis of the B cell epitopes was extended to examine the murine B cell response to an actual infection with live Mengo virus. Five neutralizing monoclonal antibodies were generated from mice immunized with an attenuated strain of the virus whose capsid structure is identical to that of wild-type virus. Two of these antibodies recognized the previously identified immunodominant determinant in VP2 while another bridged this site and Site 2 in VP3. The other two antibodies bound to regions within VP1 (Sites 3 and 4).

To examine the murine T-helper cell response to Mengo virus, lymph node cells from mice immunized with inactivated virus were stimulated *in vitro* with overlapping peptides representing the entire sequences of the four capsid proteins. Peptides representing sequences which are recognized by T-helper cells stimulated the proliferation of the cells and defined eight T-helper cell epitopes in VP2 and five epitopes in VP3. Unlike the B cell epitopes, which comprise surface residues, the T-helper cell epitopes were found largely in interior regions of the capsid.

ACKNOWLEDGEMENTS

I would like to express my deepest gratitude to my supervisor, Dr. Douglas G. Scraba, for his assistance, advice and support during the course of my graduate studies and in the preparation of this thesis.

I would also like to express my appreciation to Ulrike Boege for her help and for teaching me many of the laboratory techniques and skills which were required for my research projects.

The technical assistance of Roger Bradley and Perry d'Obrenan to produce the photographs and many of the diagrams used in publications, presentations and in this thesis is also appreciated.

I would like to thank Pat Carpenter and Ramona Hancharyk for their technical assistance in the laboratory particularly in the maintenance of cell cultures.

Stan Moore put considerable effort into assisting me with the production of the ribbon diagrams used in Chapter III of this thesis for which I am very grateful.

I would also like to thank Maya Shmulevitz and Jo Parrish for their participation, as summer students, towards the completion of the B cell epitope mapping project.

I would like to express my appreciation to Mike Mulvey for many useful discussions of projects while we worked together in Dr. Scraba's laboratory and well as for proofreading my thesis and providing helpful comments.

Susie Muir taught me the procedures and techniques required for the helper T cell epitope mapping project and I would like to thank her for her participation in the project.

I am also grateful to Mae Wylie for typing and formatting Chapter II.

Finally I would like thank Alison Darmon for her support and encouragement during the production and defense of my thesis.

Financial support from the Alberta Heritage Foundation for Medical Research and the Department of Biochemistry is gratefully acknowledged.

TABLE OF CONTENTS

CHAPTER I. GENERAL INTRODUCTION 1

- Picornavirus Classification 1
- General Physical Properties of the Picornaviruses 1
- Pathogenesis of the Cardioviruses 1
- Attachment of Cardioviruses to Cellular Receptors 3
- Initiation of Infection 4
- Mengo Virus Genome Organization 4
- Mengo Viral Proteins: Polyprotein Processing and Function 7
- Structure of Mengo Virus 8
- Capsid Proteins 8
- Protomers and Pentamers 11
- B Lymphocytes and the Antibody Mediated Response to Mengo Virus Infection 12
- Antibody Molecular Structure 13
- Nature of the Interaction Between Antibody and Antigen. 15
- Mechanisms of Antibody Mediated Neutralization of Picornaviruses 17
- T Lymphocytes 18
- Cytotoxic T Cells 19
- Helper T Cells 20
- B and T-helper Cell Interaction 22

REFERENCES 23

CHAPTER II. CHARACTERIZATION OF MENGO VIRUS NEUTRALIZATION EPITOPES 31

INTRODUCTION 31

METHODS 32

- Monoclonal antibodies 32
- Mutant selection 33
- Radiolabeled virus preparations 33
- RNA isolation 33
- RNA sequence determinations 34
- Cross neutralization 35
- Isoelectric focusing 35
- Nomenclature 35

RESULTS 35
DISCUSSION 47
REFERENCES 54

CHAPTER III. FURTHER CHARACTERIZATION OF MENGO VIRUS NEUTRALIZATION EPITOPES 60
INTRODUCTION 60
METHODS 60
Hybridoma Production for Anti-Mengo Virus Monoclonal Antibodies 61
Preparation of SP2/O Conditioned Medium 62
Cloning Cells Secreting Anti-Mengo Virus Antibodies 63
Freezing and Thawing Aliquots of Hybridoma Cells 63
Enzyme-Linked Immunoabsorbant Assays (ELISA) 64
A. Direct ELISA 64
B. Direct Peptide ELISA 64
C. Peptide Competition ELISA 65
D. Determination of Monoclonal Antibody Isotype 65
E. Antibody Competition ELISA 65
Micro-Neutralization Assays 66
Western Blots 66
Selection of Mutant Mengo Virions Which Escape Neutralization 67
Preparation of Mutant Mengo Virus for RNA Extraction 67
RNA Isolation 67
RNA Sequence Determination 67
Cross Neutralization Assays 67
Ribbon Diagrams 68
RESULTS 68
DISCUSSION 80
REFERENCES 95

CHAPTER IV. IDENTIFICATION OF MENGO VIRUS T-HELPER CELL EPITOPES 98
INTRODUCTION 98
METHODS 99
Mice 99
Virus purification and inactivation 99

Immunization 99
Detection of anti-Mengo virus antibodies 100
Serum-neutralizing assay 100
Peptide Synthesis 100
Isolation and purification of individual capsid proteins VP1, VP2 andVP3 101
In vitro T cell proliferation assay 101
Immunological characterization of T-lymphocyte population 102
Computer analysis of Mengo capsid protein sequences to predict T-cell sites 102
RESULTS 103
DISCUSSION 115
REFERENCES 120

CHAPTER V. MECHANISMS OF NEUTRALIZATION BY MONOCLONAL ANTIBODIES 124
INTRODUCTION 124
METHODS 125
Antibody Purification 125
Standard plaque assay 125
Determination of the ND95 of Purified Monoclonal Antibody Preparations 126
Determination of the Antibody:Virus Ratios Required For Neutralization 126
Electron microscopy of monoclonal antibody-Mengo virus complexes 126
Attachment inhibition assays 126
Antigen Capture ELISA 127
RESULTS 127
DISCUSSION 138
REFERENCES 136
APPENDIX A 140
APPENDIX B 141

LIST OF TABLES

Table I-1. Picornaviridae 2

Table II-1. Frequency of escape mutations 37

Table II-2. Changes in nucleotide sequence, amino acid sequence and isoelectric points for the external capsid proteins of Mengo virus escape mutants 44

Table II-3. Silent mutations found in Mengo escape mutants 46

Table II-4. A comparision of the locations of neutralization epitopes in picornaviruses 49

Table III-1 Monoclonal hybridoma cell lines generated against live attenuated Mengo virus 69

Table III-2. Changes in nucleotide sequence and amino acid sequence of Mengo virus escape mutants 74

Table III-3. Cross neutralization data 75

Table IV-1. Summary of T cell epitopes in BALB/c mice 109

Table V-1. Effect of antibody:virion ratio on the efficiency of neutralization by antibody JEL 370 131

Table V-2. Effect of antibody 3A on virion attachment to cells and neutralization of virions 132

LIST OF FIGURES

Figure I-1. Schematic representation of the Mengo virus genome 5
Figure I-2. Schematic representation of the surface of the Mengo virus capsid 9
Figure I-3. Computer graphics representation of the surface of the Mengo capsid 10
Figure I-4. Basic structure of an IgG molecule 14
Figure II-1. Cross neutralization data 38
Figure II-2. Isoelectric focusing profiles of the capsid proteins of wild type Mengo virus and neutralization mutants. 39
Figure II-3. Mutant virus sequence information 41
Figure II-4. Position of mutants in neutralization escape mutants. 42
Figure II-5. Surface map of one crystallographic asymmetric unit of the Mengo virus capsid 50
Figure II-6. Diagrammatic representation of the Mengo virus capsid 52
Figure III-1. Plaque assay of 3A mutants 72
Figure III-2. Western blot analysis of antibody 6A from tissue culture hybridoma supernatant 77
Figure III-3. Antibody competition analysis 79
Figure III-4. Ribbon diagram representation of Mengo capsid protein VP1 82
Figure III-5. Surface map of one crystallographic asymmetric unit of the Mengo virus capsid 83
Figure III-6. Ribbon diagram representation of Mengo capsid protein VP2 85
Figure III-7. Ribbon diagram representation of Mengo capsid protein VP3 86
Figure III-8. Ribbon diagram representation of a biological protomer indicating the positions of the immunogenic determinants of the Mengo virion 88
Figure IV-1. Specificity of the T lymphocyte response 104
Figure IV-2. Mengo virus specific proliferation of CD4$^+$ T lymphocytes 105
Figure IV-3. Proliferative responses of VP1, VP2 or VP3 primed lymph node cells 107
Figure IV-4. Proliferative responses of UV-inactivated Mengo virus primed lymph node cells from BALB/c mice to VP2 and VP3 synthetic peptides 108
Figure IV-5. Location of T cell epitopes 111
Figure IV-6. Relationship between B and T cell epitopes 112
Figure IV-7. Haplotype restriction of T cell epitopes 113
Figure IV-8. Prediction of T cell epitopes in VP2 and VP3 114
Figure V-1. Purification of monoclonal antibodies 128
Figure V-2. Electron micrographs of antibody-virion complexes 130

LIST OF ABBREVIATIONS

Å	Ångstrom (10^{-10})
AFC	antibody forming cell
AMV	avian myeloblastosis virus
APC	antigen presenting cell
BCIP	bromochloroindolyl phosphate
BEV	bovine enterovirus
BME	modified Basal Medium Eagle
BSA	bovine serum albumin
C terminal	carboxyl terminal
CAPS	3-(cyclohexylamine)-1-propanesulfonic acid
CD	cluster of differentiation
CDR	complimentarity determining region
C_H	heavy chain constant region
Ci	curie
C_L	light chain constant region
CPM	counts per minute
ddNTP	dideoxynucleotide triphosphate (N = A, C, G or T)
DME	Dulbecco's modified Eagle's medium
DMSO	dimethylsulfoxide
DNA	deoxyribonucleic acid
DTT	dithiothreitol
dNTP	deoxynucleotide triphosphate (N = A, C, G or T)
EDTA	ethylenediaminetetraacetic acid
ELISA	enzyme linked immunosorbant assay
EMCV	encephalomyocarditis virus
Fab	antigen binding fragment
Fc	fragment crystallizable
FCS	fetal calf serum
FMDV	foot-and-mouth disease virus
HPLC	high performance liquid chromatography
Ig	immunoglobulin
IL	interleukin
IP	intraperitoneal
IRES	internal ribosome entry segment

kDa	kilodalton
kV	kilovolt
LN	lymph node
ME virus	Maus-Elberfeld virus
MEM	minimal essential medium
MHC	major histocompatibility complex
N terminal	amino terminal
NBT	nitroblue tetrazolium
ND$_{95}$	antibody required to neutralize 95% of virus
NP40	nonidet P40
PBS	phosphate buffered saline
PEG	polyethylene glycol
PFU	plaque-forming unit
pI	isoelectric point
PVDF membrane	polyvinylidene difluoride membrane
rpm	revolutions per minute
S	Svedberg constant
SDS	sodium dodecyl sulphate
SI	stimulation index
TAP	transporter of antigenic peptides
Tc cell	cytotoxic T cell
TCR	T cell receptor
TEMED	N, N, N', N'-tetramethylethylene diamine
Th cell	helper T cell
UV	ultraviolet
VCAM	vascular cell adhesion molecule
V_H	heavy chain variable region
V_L	light chain variable region
VP	viral polypeptide
VPg	viral genome protein
xg	centrifugal force relative to gravity

CHAPTER I

GENERAL INTRODUCTION

Picornavirus Classification

The family name *Picornaviridae* is derived from 'pico' (Gk. small) and RNA (ribonucleic acid-containing) to describe a family of related vertebrate and insect viruses (Porterfield, 1989; Francki *et al.*, 1991). Originally divided into four genera (Enteroviruses, Cardioviruses, Rhinoviruses and Aphthoviruses) on the basis of physical characteristics, pathogenesis and antigenicity, the picornaviruses have more recently been reorganized on the basis of additional information provided by genome sequencing. This includes the assignment of Theiler's virus to the cardiovirus genus (Pevear, 1988; Palmenberg, 1989) and the formation of the Hepatovirus genus for the hepatitis A viruses (Francki *et al.*, 1991). The creation of the Echovirus 22 genus for echovirus 22 and the Cricket Paralysis virus genus for the first classification of an insect picornavirus, cricket paralysis virus has been proposed by Koonin and Dolja (1993). Table I-1 gives a brief summary of the *Picornaviridae* and distinguishing properties of each genus.

General Physical Properties of the Picornaviruses

The picornaviruses share a number of distinguishing physical characteristics. Virions consist of an unenveloped icosahedral protein capsid approximately 30 nm in diameter. The capsid is made up of a symmetrical arrangement of 60 copies of each of four viral proteins designated VP1, VP2, VP3 and VP4 with approximate molecular masses of 34, 30, 25, and 7 kDa, respectively (Rueckert 1990). With the exception of a molecule of myristic acid covalently attached to the amino terminal end of each VP4 there is no lipid or carbohydrate associated with the picornavirion (Rueckert, 1990).

The capsid surrounds the genome, one copy of a positive sense single-stranded RNA between 7100 and 8500 nucleotides in length (Koonin and Dolja, 1993). The genome includes a 5'-untranslated region (700-1300 residues) and a template encoded 3'-poly(A) (50-130 residues). The RNA genome is infectious and acts directly as a messenger RNA for the virally encoded proteins.

Pathogenesis of the Cardioviruses

The cardioviruses are a serologically related group of viruses which cause disease in rodents, pigs and monkeys and are associated with a wide variety of species including man, a variety of domestic animals, birds and mosquitoes (Dick, 1948; Hubbard *et al.*,

Table I-1[a]

Picornaviridae

Genus		Distinguishing Characteristics[b]
Enterovirus	Poliovirus (3) Human Coxsackie A viruses (23) Human Coxsackie B viruses (6) Human echoviruses (32) Human enteroviruses (4) Vilyuisk virus Bovine enteroviruses (2) Simian enteroviruses (18) Porcine enteroviruses (8)	-stable at acid pH -buoyant density in CsCl=1.30-1.34 g/cm^3 -empty capsids produced *in vivo* -shut off host cell protein synthesis by cleavage of host cell protein p220 with viral protease 2A
Hepatovirus	Human hepatitis A virus Simian hepatitis A virus	-very stable, acid resistant -stable at 60° for 10 min. -buoyant density in CsCl=1.32-1.34 g/cm^3
Cardiovirus	Encephalomyocarditis (EMC) virus Mengo virus Murine encephalomyelitis (ME) virus Columbia SK virus MM virus Theiler's murine encephalomyelitis virus (3)	-unstable at pH5-6 in presence of 0.1M Cl$^-$ or Br$^-$ -buoyant density in CsCl=1.33-1.34g/cm^3 -no empty capsids produced *in vivo* -5' untranslated region of genome has poly(C)tract of 61-250 bases (exception Theiler'sviruses)
Rhinovirus	Human rhinoviruses (>110) Bovine rhinoviruses (2)	-unstable below pH 5-6 -buoyant density in CsCl=1.38-1.42g/cm^3
Aphthovirus	Foot-and-mouth disease viruses (7)	-unstable below pH 5-6 -buoyant density in CsCl=1.43-1.45g/cm^3 -poly(C) tract (100-170 bases) in 5' untranslated region of genome
Echovirus 22[c]	Echovirus 22	-similar to enteroviruses but does not shut off host cell protein synthesis
Cricket Paralysis Virus[c]	Cricket paralysis virus	-buoyant density in CsCl=1.34 g/cm^3 -sediments at 167S -27 nm icosahedral capsid -ssRNA genome of MW 2.5-2.8x10^6

[a] adapted from Francki *et al.*, 1991.

[b] physical properties of cricket paralysis virus described in Moore, 1985.

[c] proposed genera (Koonin and Dolja, 1993)

1992; Dea *et al.*, 1991; Scraba, 1994). The natural reservoir of the viruses appears to be rodents, and cardioviruses are distributed world-wide. The pathogenic consequences of infection with different cardioviruses are dependent on differing tissue tropism (Morishima, 1982). For example, in mice one strain of EMC virus can cause diabetes, one strain of Theiler's virus can cause chronic demyelinating disease of neurons, and intraperitoneal injection of Mengo virus or EMC virus can cause a rapid and fatal encephalitis (Duke, 1990).

The first step in cardiovirus pathogenesis is the primary infection which results from the ingestion of enteric secretions from another infected animal (Rotbart and Kirkegaard, 1992). Mengo virus replicates in the gastrointestinal tract then spreads to the bloodstream by an as yet unknown mechanism. If the virus is not rapidly cleared by the immune system a secondary infection will occur. In mice, Mengo virus causes infection in many tissues such as the central nervous system, cardiac muscle, thymus, pancreas, kidneys, salivary glands and exorbital glands. Symptoms such as hind limb paralysis develop quickly and the mice usually die from a severe meningoencephalitis (Guthke, 1987).

Attachment of Cardioviruses to Cellular Receptors

Picornaviruses have structures on the surface of the capsid which are involved specifically in recognition of and attachment to particular proteins on the surface of susceptible cells. However, if the genome or a cDNA copy of the genome is injected directly into nonsusceptible cells live infectious virus can be produced in most cell types, indicating that the cellular machinery for virus production is present in the cells but sometimes not accessible because the virus does not always recognize cell surface glycoproteins (Rotbart and Kirkegaard, 1992). Expression of the particular surface receptor recognized by the virus varies between cell types and determines the tissue tropism of the virus. In mice all tissues are susceptible to infection with Mengo virus.

The cell surface receptor for Mengo virus has not yet been identified. Mengo is capable of binding to human erythrocytes causing hemagglutination (although Mengo virus can not productively infect erythrocytes), and it is the membrane sialoglycoprotein, glycophorin A, which is recognized by the virus. Sialic acid forms part of the active binding site on the receptor and can be modeled to fit into a surface depression on the virion called the "pit" (Burness and Pardoe, 1983; Luo *et al.*, 1987). Vascular cell adhesion molecule 1 (VCAM-1) was recently identified to be a cell surface receptor molecule on murine vascular endothelial cells for the D variant of encephalomyocarditis virus (EMCV-D), a very closely related member of the cardiovirus genus (Huber, 1994).

When a picornavirus binds to its cellular receptor the capsid undergoes an irreversible conformational change which is believed to initiate the extensive alteration required for capsid dissociation and the release of the genomic RNA. It has been shown for poliovirus that the conformational change includes extensive alteration of the capsid protein structure, externalization of the N-terminal region of VP1 and loss of VP4 molecules from the virion (Roivainen *et al.*, 1993). The conformational changes are irreversible. If the virus detaches from the receptor it is unable to reattach to a receptor molecule and is therefore noninfectious. (Fricks and Hogle, 1990; Rotbart and Kirkegaard, 1992).

Initiation of Infection

Once bound to a cell, the virus must transfer its genome to the cellular cytoplasm. Two mechanisms have been proposed by which this could occur (Rueckert, 1990):

1) Fusion of the virion with the plasma membrane might permit the RNA to pass directly into the cell. For example, when poliovirions undergo the conformational change upon receptor binding the VP1 N-termini are exposed, making the outer surface of the virion more hydrophobic; this may make it possible for them to insert into the membrane (Fricks and Hogle, 1990; Mirzayan and Wimmer, 1994).

2) Most experiments with picornaviruses suggest that receptor mediated endocytosis is responsible for entry. Virions are believed to uncoat in endocytic vesicles, as a result of the conformational changes in the virion induced by receptor binding and perhaps additional conformation changes induced by acidic pH in vesicles (Madshus *et al.*, 1984; Rotbart and Kirkegaard, 1992). Once the genome is released into the cytoplasm of the cell the synthesis of viral proteins and RNA begins. The replicative process has been reviewed in Rueckert (1990) and the role of the nonstructural proteins in this process is discussed by Porter (1993).

Mengo Virus Genome Organization

A schematic diagram of the organization of the RNA genome of Mengo virus is shown in Figure I-1 (sequence data provided by G.M. Duke and A.C. Palmenberg, University of Wisconsin). At the 5' end of the genome is a stretch of 758 untranslated nucleotides which is important for replication and translation of the genome and pathogenicity of the virus. At the 5' end of the RNA a small protein composed of 20 amino acid residues, designated VPg, is covalently linked through a phosphodiester bond

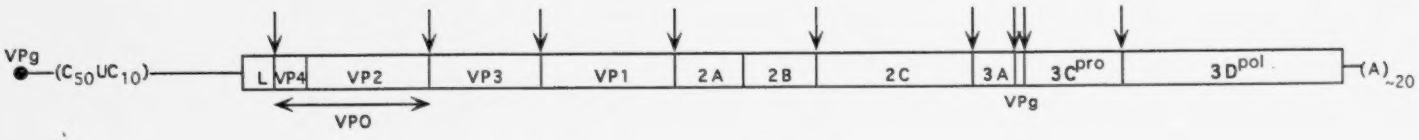

Figure I-1. Schematic representation of the Mengo virus genome (redrawn from Scraba, 1994). The region coding for the polyprotein is indicated by the boxed sequence. The vertical arrows indicate the sites of cleavage of the polyprotein by the viral protease $3C^{pro}$. There are 70 amino acid residues in VP4, 256 in VP2, 231 in VP3 and 277 in VP1. Not including the poly (A) tail the Mengo virus genome is 7761 nucleotides in length.

between the 5'-pU residue of the genome and the phenolic oxygen of a tyrosine residue (Wimmer, 1982; Brinton and Heinz, 1990). VPg is uridylated during viral replication and may act as a primer for initiation of RNA synthesis by the viral RNA polymerase (3D) (Mirzayan and Wimmer, 1994; Andino *et al.*, 1993). VPg may also play a role in initiating assembly of progeny virions through protein-protein interactions between VPg and the interior surface of a pentamer (Reuer *et al.*, 1990; Scraba, 1994).

VPg attachment precludes the formation of a 5' "cap" structure ($m^7G(5')ppp(5')Np$) associated with most eucaryotic and viral mRNAs, and required for the formation of a stable translation initiation complex between the mRNA and ribosomes. For conventional mRNAs the ribosome assembly scans for the first AUG codon and begins translation from that location. By contrast, the initiation of translation of picornaviral mRNAs occurs through the binding of ribosomes to an internal site in the 5'-untranslated region of the genome (Pelletier and Sonenberg, 1988; Jang and Wimmer, 1990). A segment of approximately 450 nucleotides termed the IRES (internal ribosome entry segment) is involved in forming the binding site for the 40S ribosome. While the position of the IRES element varies with respect to the position of the authentic initiation codon among different picornaviruses, for the cardioviruses it is believed that ribosomes are directed to bind the AUG initiation codon which lies closest to the 3' end of the IRES element (Hunt *et al.*, 1993).

Another distinctive feature of the untranslated region which is found only in the cardioviruses (with the exception of Theiler's virus) and aphthoviruses is the presence of a poly (C) tract of 60 to 250 nucleotides located about 150 to 330 bases from the 5' end (Duke and Palmenberg, 1989). The sequence of the poly (C) tract varies between viral isolates (insertion of bases other than C within this region) and, at least in the case of the cardioviruses, has been demonstrated to play a role in determining the pathogenicity of the virus *in vivo*. The Mengo virus poly (C) tract begins at nucleotide 148 from the 5' end and has the sequence $C_{50}UC_{10}$. Shortening the poly (C) tract to $C_{13}UC_{10}$ reduces the LD_{50} of intraperitoneal injection from approximately 10^5 PFUs for the wild-type virus to approximately 10^{11} PFUs in mice (Duke and Palmenberg, 1989; Duke *et al.*, 1990).

Following the 5' untranslated region of the Mengo virus genome is the virus protein coding region comprising nucleotides 759 to 7637. This region has only one termination codon (UAA) located at bases 7638-7640, thus all the protein products of the genome are cotranslated as one large polyprotein which is later processed by proteolytic cleavages. A 3' untranslated region of 124 bases follows the coding region of the Mengo virus genome and at nucleotide 7762 a template encoded poly (A) tract begins (Duke and Palmenberg, 1989).

Mengo Viral Proteins: Polyprotein Processing and Function

As mentioned above, the Mengo virus genome (which is typical of the picornaviruses) contains a single open reading frame which is initially translated into a single long polyprotein. The individual viral proteins, structural and non-structural, are generated by a series of post-translational proteolytic cleavages. The exact nature of the cleavage events, whether autocatalytic or mediated by viral protease(s), differs only slightly among the different groups of the picornaviruses. In the case of Mengo virus, the first cleavage event occurs at the junction between 2A and 2B (Figure I-1). The tetrapeptide NPGP at this site is believed to be intrinsically unstable resulting in the cleavage between the P and G residues. As might be expected, this sequence is very rare in nature and occurs no where else in the genome. With one exception (see below) the remainder of the cleavages of the Mengo virus polyprotein are effected by the viral protease 3C. This protease frees itself from the polyprotein autocatalytically and is then available to act on the remainder of the polyprotein (Palmenberg, 1990).

The final event in the polyprotein processing is termed the maturation cleavage and occurs during the assembly of progeny virions. In this step VP0 is cleaved into VP2 and VP4. The mechanism of this process is not understood but it is believed to be catalyzed by the arrangement of amino acids at the cleavage site in association with the viral RNA; *i.e.* by an RNA-aided cleavage mechanism (Palmenberg, 1990).

VP1, VP2, VP3 and VP4 are the structural proteins of the virion; the remainder of the virus-encoded proteins primarily play roles in the replication of the viral RNA either as individual proteins or as partially processed complexes. For example it has been shown that, for some of the picornaviruses, the complex of 2BC has a role in replication distinct from that of the separate 2B and 2C proteins. The same has been shown to be true for 3CD activity even though 3C (protease) and 3D (RNA polymerase) have well defined roles as the individual proteins. The roles of the various structural proteins and some of the partially processed precursors have been reviewed by Porter (1993). Of the nonstructural proteins, 3D is of particular interest in the context of the Mengo virus B cell epitope mapping project. 3D is an RNA-dependent RNA polymerase responsible for the replication of progeny viral genomes It does not have proof-reading (3'→5' exonuclease) activity. As a result the estimated error frequency in copying the genome of the virus is approximately one incorrect nucleotide per 10,000 or about one mistake per viral genome. The resulting abundance of naturally occuring viral mutants makes the selection of mutants which are capable of escaping neutralizing monoclonal antibodies (through a mutation in the antibody binding site) possible from the natural replicating stock of virus.

Structure of Mengo Virus

The structures of a large number of picornaviruses have been determined at atomic resolution. The crystallographic structure of Mengo virus was solved at a resolution of 0.30 nm in 1987, as a representative member of the cardioviruses, (Luo *et al.*, 1987). Figure I-2 shows a schematic representation of the organization of the capsid proteins of Mengo virus. One copy of each capsid protein (VP1, VP2, VP3 and VP4) is organized into a structural unit referred to as a protomer. Five protomers form a stable virion assembly subunit called the pentamer. Each VP1 molecule in the five protomers is clustered in the center of the pentamer about the five-fold axis of rotation. VP4 is located entirely on the interior surface of the pentamer (and the assembled capsid).

Crystallographic determination of picornavirion structures has aided in understanding the functions of the capsid to encapsidate the genome during morphogenesis, protect it once it is outside of the cell and deliver it intact to a new cell. It has also permitted an understanding of virion assembly through protomer and pentamer structural intermediates, the role the capsid plays in initiating infection of new host cells and how the immune system of the host animal can attempt to prevent the infection of cells through the recognition of specific elements of the capsid proteins to identify and clear a viral infection.

Capsid Proteins

The three major capsid proteins VP1, VP2 and VP3 are each organized into an eight-stranded antiparallel β-barrel structural motif that has also been found with the capsid proteins of most other spherical RNA viruses. This structural motif is well conserved among the picornaviruses (Rossmann and Johnson, 1989). It is likely that the picornaviruses have evolved from a common ancestor with the least sequence divergence occuring in the β-barrel central structural motif of the proteins, since this is required to maintain structural and functional integrity of the capsid. The major differences between the capsid proteins of different picornaviruses are primarily in the segments connecting the β-strands, which are responsible for characteristic features (knobs, loops and depressions) on the exterior surface of the virions. Figure I-3 is a ball model representation of the virion showing the relatively smooth surface of the capsid with

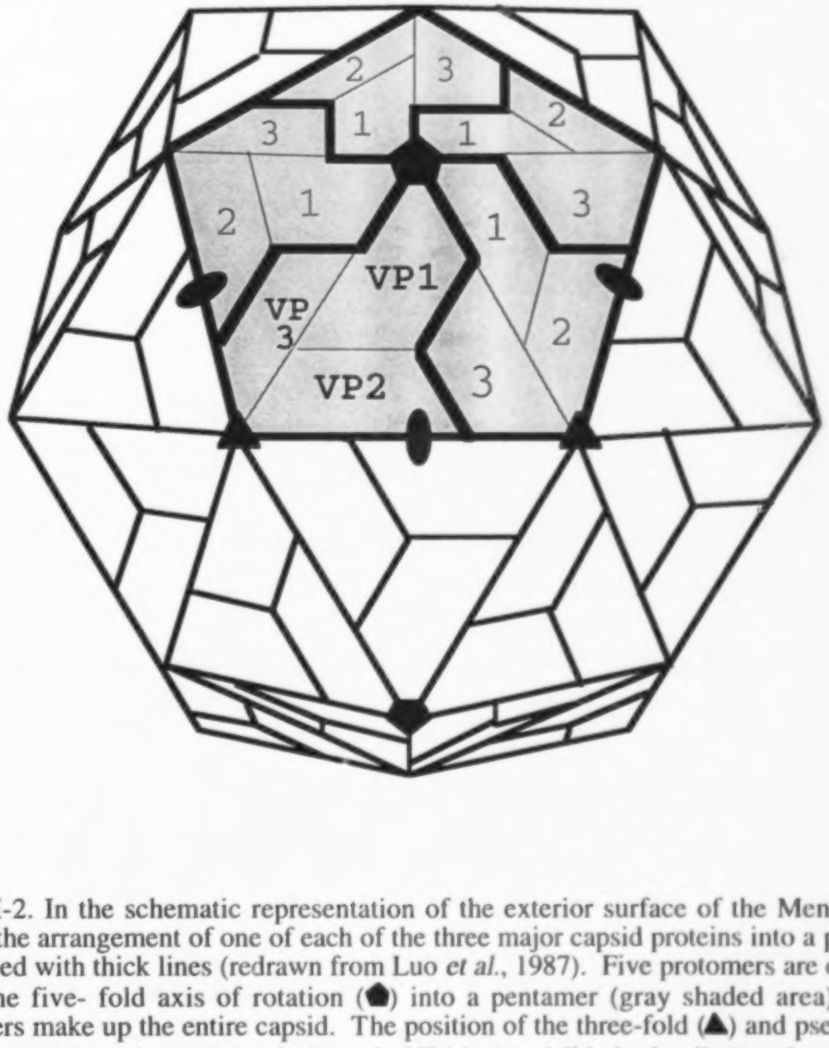

Figure I-2. In the schematic representation of the exterior surface of the Mengo virus capsid, the arrangement of one of each of the three major capsid proteins into a protomer is outlined with thick lines (redrawn from Luo *et al.*, 1987). Five protomers are clustered about the five- fold axis of rotation (⬟) into a pentamer (gray shaded area) and 12 pentamers make up the entire capsid. The position of the three-fold (▲) and pseudo-two fold (⬮)axes of rotation are also indicated. VP4 is not visible in the diagram because it is located internally in the capsid.

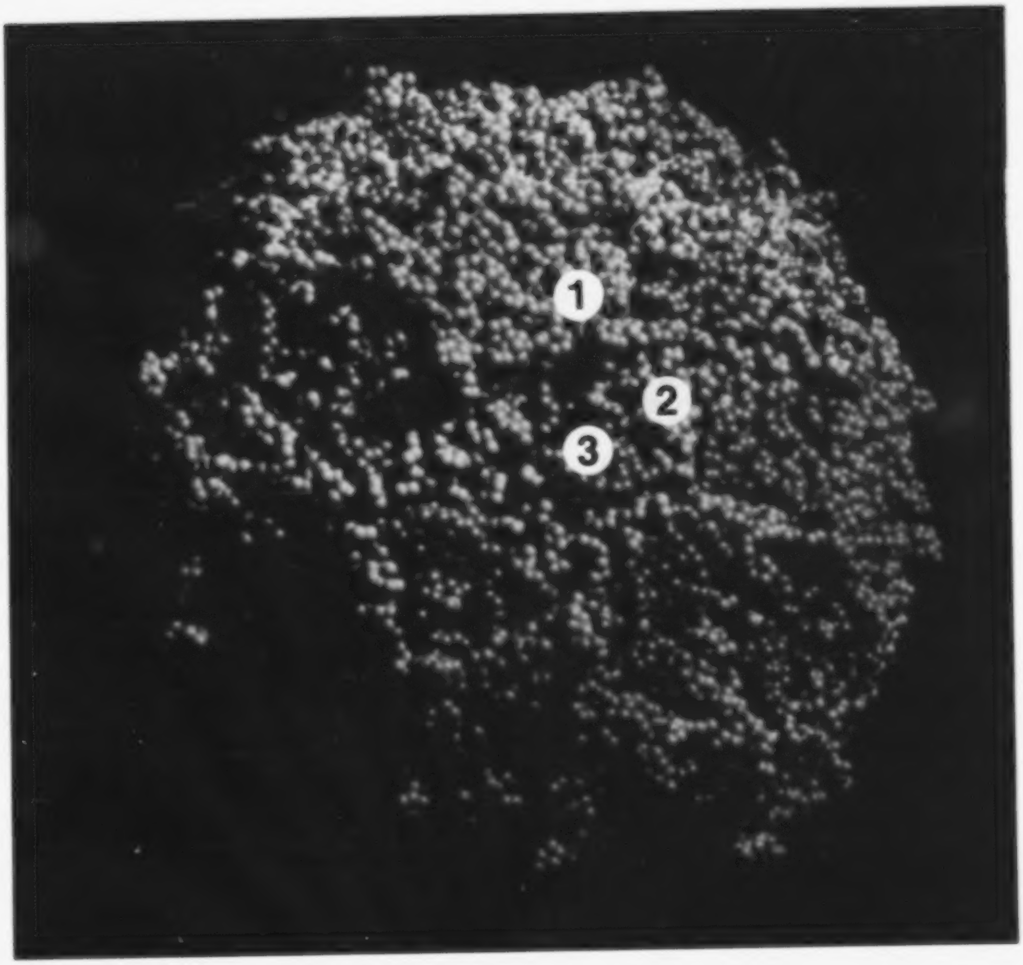

Figure I-3. Computer graphics representation of the surface of the Mengo capsid. The position of one protomer is indicated by the numbers 1, 2 and 3 representing capsid proteins VP1, VP2 and VP3 respectively. The individual balls represent α-carbon atoms in the polypeptide chains.

small surface depressions and protrusions. The sequences on the surface which form flexible protrusions, are sites of hypervariability. This hypervariability allows the virus to alter regions recognized by circulating antibodies, produced in response to viral infection, and thereby evade host immune surveillance.

Protomers and Pentamers

The contacts between the three major structural proteins within a protomer unit are extensive and stable, being susceptible to dissociation only by heating in the presence of SDS (Mak *et al.*, 1974). VP1 and VP3 interact most extensively as result of an association between the amino terminal segments of each. VP4 has few interactions in the protomer and does not contribute to protomer stability (Krishnaswamy and Rossmann, 1990).

In the pentamer the contacts between the structural proteins are not as extensive as they are within the protomer, therefore pentamers can be dissociated under milder conditions (2M urea) into protomers while protomers remain intact (Mak *et al.*, 1974). However, each VP4 polypeptide is important in the assembly of pentamers from protomers by interacting along its length with VP1 near the five-fold axis, through to the amino terminus of VP3 and then with the amino terminus of VP2 in a neighbouring protomer (Luo *et al.*, 1987; Krishnaswamy and Rossmann, 1990).

The interactions between the structural proteins of one pentamer with a neighbouring pentamer are the least extensive of all, with no stabilizing salt bridges and only VP2 and VP3 forming significant hydrogen-bond interactions between pentamers primarily about the three-fold axis. Because of the weak interactions virions will dissociate into pentamers in the presence of 140 mM Cl^- or Br^- at pH 6-6.5. The dissociation is believed to be the result of the substantial conformational changes which occur at the proposed receptor attachment site and result in the loss of the RNA and VP4 from the capsid (Kim *et al.*, 1990). The changes observed *in vitro* are assumed to be similar to those which occur when Mengo binds its cellular receptor and the release of the RNA is initiated.

One very important feature of the surface of the Mengo virion is a 22 Å deep and 30 Å wide pit. Five of these pits are located about the five-fold axis of each pentamer (Luo *et al.*, 1987). The existence of a similar structure on rhino and polio viruses in the form of a continuous groove or canyon encircling each five-fold axis led to the proposal of the "canyon hypothesis " (Rossmann *et al.*, 1985; Luo *et al.*, 1987; Rossmann, 1989). It was suggested that the cellular receptor would fit into the canyon and interact with the residues lining it. Antibody molecules, produced by the host in response to infection, would be too large to fit into the canyon. Residues lining the canyon would not be under immune selective pressure to mutate to avoid immune recognition. In this way the virus is able to maintain its receptor specificity while being to evade immune surveillance by mutating residues on the surface of the virion. The pit was proposed to play the same role in the interaction of Mengo virus with its receptor (Kim *et al.*, 1990). Convincing evidence for the role of the canyon of rhinovirus 16 as its receptor binding site was recently provided using a combination cryoelectron microscopy and x-ray crystallography to show that its cellular receptor does bind in the canyon of the virion (Olson *et al.*, 1993).

B Lymphocytes and the Antibody Mediated Response to Mengo Virus Infection

Lymphocytes are the cellular components of the immune system which are responsible for the antigen-specific adaptive response to pathogens. Although all lymphocytes are derived from bone marrow stem cells, the site of development for T cells is the thymus while for B cells it is the bone marrow. Using a cell surface immunoglobulin as an antigen receptor, each B cell is capable of specifically recognizing a particular antigen. During the invasion of a host animal by a foreign antigen such as a virus, B cells which recognize the antigen are stimulated to divide and develop into mature antibody forming cells (which secrete soluble antigen specific immunoglobulin molecules) or memory B cells (which remain in circulation after the primary response and provide a very fast response to any future invasion of the host by the same antigen). For a given antigen there will be a number of B cells which will respond (a polyclonal response) to various sites on the antigen's surface, and each will be induced to mature and secrete antibodies capable of binding to their epitope (binding site). The response of B cells to the first invasion of the host by the foreign antigen is called the primary response. There are four phases of the primary antibody response to virus:

1) a lag phase after infection during which no antibody is detected in the serum of the infected host;
2) a log phase during which the antibody titre rises logarithmically;
3) a plateau phase where the antibody titre is held at its peak titre for a period; and
4) a decline phase where the antibody and antibody producing cells are cleared because it is bound to antigen or removed because it is not used.

The primary response is characterized by immunoglobulin type M (IgM) production with very little immunoglobulin type G (IgG) being produced (more about antibody types later). Rechallenging the animal with the antigen after the total elimination of virus infection and the decrease of antigen specific antibodies to very low levels will result in a secondary response to the antigen which has a number of important differences from the primary response. First, the response is much quicker than the primary response because there is now a pool of memory B cells which have been primed to respond to the antigen from the primary infection. Second, the amount of antibody produced is much higher-usually at least 10-fold. Third, the affinity of the antibodies produced against the antigen are higher in the secondary response (discussed later). Finally, the response comprises primarily IgG with very little IgM and small numbers of cells producing immunoglobulin types E and A (IgE and IgA). This phenomenon of changing the antibody class is called class switching (Bauer *et al.*, 1963; Uhr and Finkelstein, 1963).

To understand class switching it is necessary to know something about the genes coding for antibody molecules and makeup of the immunoglobulin molecule itself. There are two primary polypeptides found in every immunoglobulin molecule - a heavy chain (H) and a light chain (L). Each of these has an amino terminal variable (V) region followed by a constant (C) region. Together the variable regions of the two chains make up the antigen binding region of the antibody molecule. The C region of the heavy chain determines the type or subtype (additional diversification within the IgG type) which is selected, depending on the role the immunoglobulin is to play in immunity (such as secretion or cell surface expression of antibody molecules). In the mouse there are eight heavy chain constant (C_H) regions. The switching of antibody production from one class to another involves the rearrangement of the genes coding for the C_H regions, but no change occurs in the variable region so the antigen specificity of the immunoglobulin is not affected. This process is primarily an antigen-induced differentiation of mature B cells and involves an intrachromosomal recombination that brings the V_H gene in close proximity to a new C_H gene with the resulting deletion of all intervening C_H genes. This deletion means that it is not possible for an organism to regenerate a previously produced immunoglobulin type because the C_H gene coding for that immunoglobulin type is lost (Coffman and Cohn, 1977; Coffman *et al.*, 1993).

Antibody Molecular Structure

The basic structural unit of immunoglobulin molecules is a dimer of a heavy plus light chain as shown in Figure I-4 for IgG. The light chain is approximately 25 kDa and the H chain is 50-77 kDa and the chains are held together by both covalent and noncovalent bonds. The IgG molecule can be divided into two Fabs (antigen binding fragments) and the Fc (fragment crystallizable) based on the ability of papain to cleave

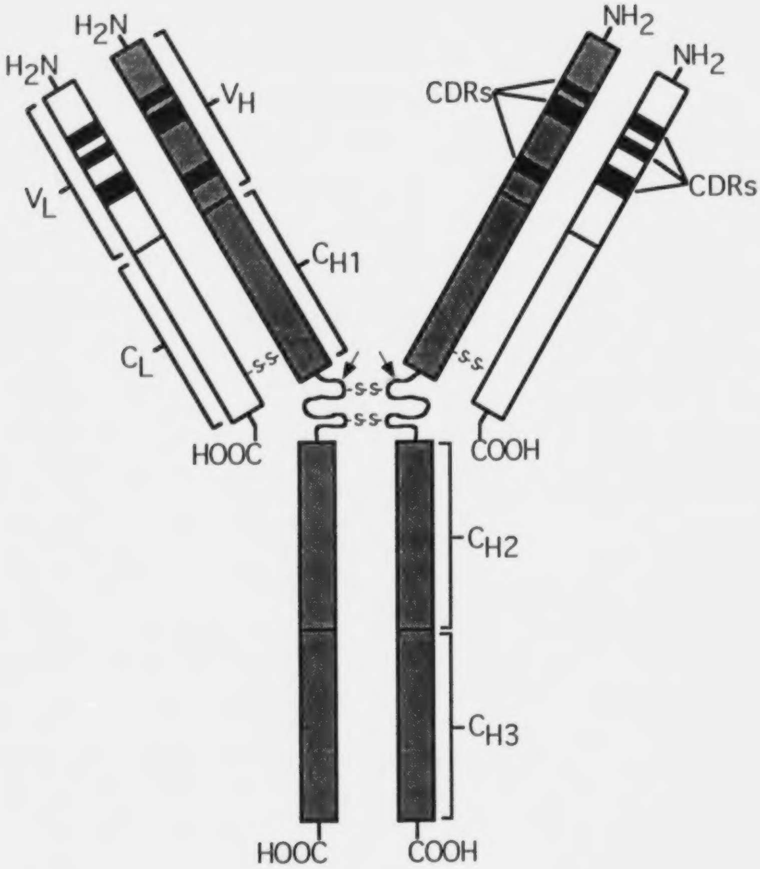

Figure I-4. Basic structure of an IgG molecule. The molecule is made up of two identical light chains (L) (white) and two identical heavy chains (H) (gray). Each is composed of an amino terminal variable region (V_L or V_H) and a carboxyl terminal constant region (C_L or C_H). The C_H region is composed of internal homology units C_H1, C_H2, C_H3. Within the V regions are the sequences which make up the antigen recognition domain, primarily in loops coded by the complementarity-determining regions (CDRs). Arrows (→) indicate the position of cleavage by papain within a flexible hinge region of the heavy chain to release one Fc and two Fab fragments.

the molecule into three pieces. The antigen binding sites are contained within the Fab fragments (reviewed in Davies and Padlan, 1990). Although each mature B cell will produce immunoglobulin molecules which specifically recognize only a single epitope on an antigen there is a large repertoire of B cells, each producing an antibody molecule with a different epitope specificity, so that the immune system is capable of recognizing an almost endless variety of foreign antigens. This diversity is the result a large number of genes which code for the variable regions of both the heavy and light chains. Through a mechanism of somatic recombination an exon coding for just one of the genes for the variable (V) region is connected to an exon coding for a joining (J) segment (in some instances there is more than one possible J gene) which is in turn connected to any one of the few genes coding for the constant (C) region. The variable region of the mature light gene is coded for by the combination of the V and J genes (Hozumi and Tonegawa, 1976; Tonegawa *et al.*, 1977).

In the case of the H chain an additional small gene called D for diversity is added between the V and J genes, and there are multiple copies of the D gene which can be used. During recombination there is one additional mechanism by which diversity is generated in the variable regions. The joining reaction is not fixed in position and can occur between different base pairs so that several different amino acids can be generated at the site of each recombination. As a result of these mechanisms of generating diversity it is estimated that at least one million different antibodies are possible and the actual number may in fact be one to two orders of magnitude higher (Tonegawa, 1983).

The IgM molecule is essentially a pentamer in a pinwheel shape of H and L chains of an IgG molecule arrangement (reviewed in Davis and Schulman, 1989). IgA can be either a monomer similar in structure to IgG or a dimer (reviewed in Mestecky and McGhee, 1987).

Nature of the Interaction Between Antibody and Antigen.

The binding region of an antibody molecule is made up of six hypervariable loops called complementarity determining regions (CDRs). Three loops come from each of the heavy and light chains and are connected to a network of β-sheet which varies little among different antibodies (Davies *et al.*, 1975). As discussed above, a large number of genes codes for the variable regions of the H and L chains and all the different combinations of those genes result in the generation of a very large number of immunoglobulin molecules, each with specificity for a different epitope. Antigen specificity is also enhanced by the selection of clones of a B cell having somatic mutations in the variable regions of the antibody molecules which increase the affinity of the antibody for the antigen. The selection is most pronounced during the period of rapid division of B cell in response to repeated exposure with antigen and is believed to occur through a mechanism of site-directed hypermutation confined to the genes coding for the variable regions of the immunoglobulin molecule (Rizzo *et al.*, 1992; Küppers *et al.*, 1993).

There are four intermolecular forces which contribute to the stable interaction between antibody and antigen:

1) hydrogen bonding;
2) electrostatic interactions between charged groups;
3) Van der Waals interactions due to the dipole moments between atoms in close proximity; and
4) hydrophobic interactions which rely on the association of hydrophobic groups to exclude water molecules from the site of interaction.

Hydrophobic forces may contribute as much as 50 percent to the overall strength of the antibody-antigen interaction. As well, the complementarity of the shape of antigen and antibody is essential to optimize the contacts for the greatest stabilization of the interaction (Berzofsky and Berkower, 1984; Sheriff *et al.*, 1987). Studies done with various antibody-antigen combinations have identified a number of properties which are important for efficient interaction. Epitopes must be accessible for interaction with the combining site of the antibody molecule. An antibody combining site will cover an area of between 680 and 880 $Å^2$ (Davies *et al.*, 1975; Davies and Padlan, 1990). As well, epitopes recognized by antibodies on native protein antigens are often discontinuous; this is because the antibodies recognize the surface of an intact antigen which is made up of residues from a variety of positions in the polypeptide chain. This means that any one continuous linear sequence of amino acid residues from such a site will not contain enough of the critical binding contacts for recognition. Continuous epitopes on the surface of viral antigens have also been well characterized; among these is an immunodominant loop on the surface VP1 of the capsid of foot-and-mouth disease virus (Logan *et al.*, 1993). In general, although many of the residues within the binding site contribute to the overall stabilization of binding, the specific interactions are dominated by a relatively small number of side chains.

One additional mechanism by which diversity can be created and interaction between antigen and antibody optimized is through conformational changes which can occur at the combining site. This induced-fit model applies to conformational changes within both the antibody and antigen but has been best characterized for the antibody (reviewed in Davies and Padlan, 1992; Rini *et al.*, 1992). Antibodies can be quite sensitive to the conformation of the antigen. Small conformational changes in the epitope of the antibody can lead to the loss of specific recognition of the antigen probably because of changes in the position of residues critical for the recognition of the site. Even the limited conformational changes which an antigen experiences when it is bound to and flattens against a solid substrate, such as is done in the binding of antigen to wells of an ELISA plate, can be sufficient to destroy the ability of some antibodies to bind to their epitopes (Schwab and Bosshard, 1992).

Mechanisms of Antibody Mediated Neutralization of Picornaviruses

There are a number of ways that an antibody could neutralize the infectivity of a picornavirus:

1) It could cause aggregation of virions by bivalent attachment to reduce the concentration of individual infectious particles. Nearly all antibodies will cause the aggregation of virions *in vitro* but this is often an artifact of the experimental procedure and not relevant to the true mechanism of neutralization *in vivo*. A few antibodies have been identified which do appear to neutralize virus solely by aggregation with no other effect on the virions. In such cases, the aggregates are mostly non-infectious and will release infectious virions if disrupted (Thomas *et al.*, 1986).

2) Attachment of antibody to virus could sterically hinder the attachment of the virion to its host cell receptor (Colonno *et al.*, 1989). This would require a large ratio of antibody to virus particles since all picornavirus capsids contain 60 equivalent receptor-binding sites.

3) Antibody attachment might cause a conformational change in the virion with an accompanying decrease in its isoelectric point and possibly loss of the RNA from the virions resulting in the formation of either a dissociated or a non-infectious empty capsid (Deleat *et al.*, 1992). The nature and significance of the isoelectric point as an indicator of conformational change is not well understood. The recent determination of the structure of human rhinovirus 14 complexed with an Fab fragment from a neutralizing antibody indicated that there were no gross conformational changes in virus structure accompanying antibody binding and the pI change. The pI change may simply be due to small changes in exposed surfaces on the virions as a result of binding of an Fab or whole antibody molecule (Smith *et al.*, 1993).

4) Bivalent attachment of antibody to virions could cross-link the pentameric subunits to prevent uncoating of virions so the RNA cannot be released (Wetz, 1993). Recently, evidence that bivalent attachment of antibody to virions can occur was obtained

from the determination of the structure of rhinovirus 14 bound to Fab fragments of a neutralizing antibody (Smith *et al.*, 1993).

5) Binding of an antibody may lock the conformation of the virion such that the conformational change to release the RNA which is normally initiated by receptor binding cannot occur.

Mechanisms of neutralization can be dependent on a number of factors including the antibody type, the concentration of antibody and antigen and how the virus-antibody complex interacts with the target cell (Kingsford *et al.*, 1991). It should also be noted that in a host animal a virus is exposed to a polyclonal population of cells producing antigen specific antibodies so no single mechanism of neutralization will account for the reduction in virus infectivity. In general complete neutralization of virus is achieved only through the net effect of the binding of several different antibodies which can each neutralize virus by a variety of mechanisms. The use of only a single monoclonal antibody to neutralize virus usually results in a small persistent population of virus which is not neutralized (Kingsford, 1984). As well the vertebrate immune system contains a large population of B cells producing antibodies which do not neutralize virus directly but play an important role in recognition of virions and clearance of virus by other components of the immune system. Macrophages and other phagocytes carry cell surface receptors for the Fc portion of IgG molecules. Antibodies enhance the removal of antigens from circulation by phagocytes by binding to the antigen. The Fc portion of the antibody is then recognized by the Fc receptor of the phagocytes and the antigen-antibody complex is removed from circulation; this process is termed opsonization (Paul, 1993; McCullough *et al.*, 1988).

T Lymphocytes

The recovery of a host animal from an acute virus infection involves the activity of virus specific immune T cells. These locate and destroy virus infected cells and secrete cytokines responsible for the stimulation of the activity of B cells and other lymphocytes against antigen infected cells and free circulating antigen. This is particularly true during the stage of infection which involves intracellular virus replication. To resolve the infection at this stage requires the interplay of all components of the immune system including interferon (IFN), virus specific antibodies and complement proteins. The key players of the T-lymphocyte response are the helper T (Th) and cytotoxic T (Tc) lymphocytes. The Th cell subset is distinguished by the presence of the CD (cluster of differentiation) 4 marker protein on the cell surface while Tc lymphocytes have CD8 molecules but no CD4 molecules on their surface.

Cytotoxic T Cells

Cytotoxic T-lymphocytes which recognize infected cells have been shown to provide the major defense against viral infection. These cells are able to recognize and lyse virus-infected cells (Raychaudhuri and Morrow, 1993). Detection of infected cells is mediated by a T cell receptor which specifically recognizes the combination of the major histocompatibility complex (MHC) class I α,β-heterodimer with particular peptide fragments of the viral proteins held in a groove on the surface of the MHC and displayed on the outer surface of the infected cell. Cells which display peptides using either the class I or II MHC molecules, whether the peptides are derived from foreign or host cell proteins, are termed antigen presenting cells (APCs). Class I MHC molecules almost exclusively present peptides derived from endogenously synthesized proteins, including viral proteins which are synthesized in infected cells. Experimental evidence suggests that the peptides which are presented by the class I MHC molecules are generated in low levels from the pool of proteins residing in the cytoplasm. The proteolytic activity of a multicatalytic proteinase termed the proteasome is believed to be responsible for the degradation of proteins in the cytosol as part of the house keeping functions of the cell. A heterodimeric complex composed of two polypeptides coded by the transporter of antigenic peptides-1 (TAP-1) and TAP-2 genes is believed to form a peptide transporter which carries the peptides into the lumen of the endoplasmic reticulum (Germain and Margulies, 1993; Van Kaer *et al.*, 1992). Peptides which meet specific sequence requirements coassemble with newly synthesized class I MHC molecules in the lumen of the ER and then the MHC molecules, stabilized by the interaction with the antigenic peptides, are transported to the cell surface. The MHC-peptide complex interacts with a Tc lymphocyte expressing a specific T-cell receptor complex on its surface capable of recognizing the peptide bound in the MHC molecule. The association of the Tc-lymphocyte with the APC results in the activation of the Tc lymphocyte which then mediates the lysis of the infected cell. The MHC molecule can present a wide variety of peptides derived from both self and foreign proteins. A particular T-cell receptor is capable of recognizing only one specific peptide-MHC complex, but because of the high degree of diversity of T-cell receptor genes there are T cells available which are capable of recognizing the other peptide-MHC complexes. Recognition of MHC molecules carrying self peptides, by T lymphocytes, generally does not occur because of the selection and elimination of cells bearing TCRs capable of doing so early in immune development (Marrack and Kappler, 1993).

Helper T Cells

The Th cell subpopulation of lymphocytes serves a number of important roles in mounting an effective immune response to viral infection which are distinct from the role of Tc cells. Th cells are activated by the association of their cell surface T cell receptor molecules with peptides derived primarily from exogenous antigens displayed on the surface of APCs in association with class II MHC molecules. Activated Th cells secrete cytokines which mediate the response of other cellular components of the immune system in response to foreign antigens. Different patterns of cytokine secretion within the Th cell population has made it possible to divide the Th cells into two subsets, Th1 and Th2. Macrophages act as APC cells for peptides derived from exogenous antigens and are believed to be particularly effective activators of Th1 cells. Th1 cells in turn activate macrophages by secretion of specific cytokines. Similarly Th2 cells respond particularly well to antigens presented by B cells and Th2 cells are important for the activation and increased production of eosinophils, mast cells and enhancing the production of antibody by B lymphocytes (Bass *et al.*, 1989; Rizzo *et al.*, 1992).

Briefly, the process of presentation of foreign viral peptides and the activation of Th cells occurs in the following sequence.

1) Lymphocytes, dendritic cells, macrophages and/or endothelial cells phagocytose foreign antigens (virus particles). This process can also be antigen specific (receptor-mediated endocytosis) as in the recognition of antigen by surface bound immunoglobulin molecules on B lymphocytes. The antigen is taken into endosomal compartments in the cells.

2) In the endosomes the antigens are processed into peptides about 13 to 25 residues in length by acid-optimal proteases (cathepsins) (Goldberg and Rock, 1992; reviewed in Brodsky and Guagliardi, 1991; Brodsky, 1992).

3) New MHC molecules produced in the rough ER enter the pathway via the Golgi apparatus to a storage vesicle which then fuses to the endosome where antigen processing is occurring. Each MHC complex acquires a single processed peptide. An MHC can bind peptides with a wide variety of sequences, ensuring many peptides from an antigen will be presented, but each peptide must meet specific minimal sequence requirements for recognition. The vesicle is then transported to the cell surface where the MHC-peptide complex is displayed on the exterior of the cell (Lanzavecchia, 1985; Reiss, 1993; Raychaudhuri and Morrow, 1993).

Among the wild-type population of all vertebrate species, the MHC genes are highly polymorphic. All class II MHC complexes are composed of two non-covalently associated α- and β-glycopolypeptides which are very similar in overall structure. Starting at the C terminal end of the protein there is a cytoplasmic region of variable length. This is linked to a transmembrane domain of about 25 amino acid residues. Following is an immunoglobulin-like region in both subunits containing an intrachain disulphide bond; this region is probably important for maintaining the non-covalent interactions between the subunits. At the amino end of each subunit is the peptide binding region formed by the interaction between the two subunits (Brodsky and Guagliardi, 1991). Determination of the structure of the human MHC class II heterodimer HLA-DR1 has shown that the peptide binding groove is composed of eight strands of antiparallel β-sheet which forms the bottom of a trough with two antiparallel helical regions making up the walls of the trough (Brown *et al.*, 1993). Peptides which bind in this pocket are 13 to 25 residues in length, held in an extended conformation and have anchor residues in critical positions to ensure stable binding in the pocket (Hammer *et al.*, 1993). The heterogeneity in peptide length is permitted because the ends of the peptide binding trough are open, allowing the N and C ends to extend beyond the binding cleft. This is in contrast to peptides bound to the class I MHC molecule which have the strict requirement of being eight or nine residues in length with critical anchor residues in specific positions relative to their N and C termini. Class I MHC complexed peptides bind in an extended conformation but the ends of the binding cleft are closed so peptides must be of specific length to be accommodated. The strict requirement for peptide structure in class I MHC molecules has made the identification of anchor residues possible by comparison of many peptides which bind the complex; however the size heterogeneity of class II MHC bound peptides has made the identification of such residues much more difficult (Hammer *et al.*, 1993). The requirement of only a few critical residues for binding is the reason that an MHC molecule can bind a large number of peptides of different sequence as long as the minimum recognition requirement is met.

4) The final step in the activation of Th cells is the recognition of the MHC-peptide complex by a T cell antigen receptor (TCR) molecule on the surface of a $CD4^+$ T cell. The TCR is also a highly polymorphic heterodimeric structure. The polymorphism is generated by recombination of V, D and J genetic elements, which are each present in various tandem repeats with small variations at each locus, in a mechanism of recombination of genetic elements similar to that discussed above for the genes coding for immunoglobulins. A given T cell will express only one TCR, with specific recognition properties, but within the T cell population many TCRs will be expressed to ensure recognition of many different peptide-MHC complexes. As with B cells the Th

cells which expresses a T cell receptor capable of recognizing a self antigen are deleted during immune development to avoid auto-immune disease (Marrack and Kappler, 1993).

The TCR recognizes peptide bound in the groove of the MHC molecule. This interaction of the T-cell and APC initiates the activation of the T cells. Secretion of cytokines by both the T cell and the APC stimulate the cells to proliferate so that T cells capable of recognizing specific antigenic fragments of the antigen will be produced in quantity.

B and Th Cell Interaction

B cells are initially activated by antigen which is presented to their cell surface immunoglobulin molecules by APCs such as macrophages. Activation also requires the presence of interleukin-1 (IL-1) produced by the macrophages and IL-4 produced by Th cells. These factors work together to stimulate the expression of additional cytokine receptors in B cells which have a cell surface immunoglobulin capable of recognizing the antigen. As mentioned B lymphocytes can act as APCs for Th cells through the process outlined above for activation of Th cells. This in turn stimulates the Th cells to secrete additional cytokines (IL-2, IL-4, IL-5, interferonγ), some of which promote the rapid division of the B cells which recognize the antigen. In this pool of dividing cells the cytokines also stimulate the differentiation of the cells to form either antibody-forming plasma cells (AFCs) which secrete antigen specific antibody or memory B cells (Bass *et al.*, 1989; Rizzo *et al.*, 1992).

REFERENCES

Andino, R., G.E. Rieckhof, P.L. Achacoso and D. Baltimore (1993). Poliovirus RNA synthesis utilizes and RNP complex formed around the 5'-end of viral RNA. *EMBO Journal* **12**, 3587-3598.

Bass, H., T. Mosmann and S. Strober (1989). Evidence for mouse Th1- and Th2-like helper T cells *in vivo.* Selective reduction of Th1-like cells after total lymphoid irradiation. *Journal of Experimental Medicine* **170**, 1495-1511.

Bauer, D.C., M.J. Mathies and A.B. Stavitsky (1963). Sequences of synthesis of γ-1 macroglobulin and γ-2 globulin antibodies during primary and secondary responses to proteins, salmonella antigens and phage. *Journal of Experimental Medicine* **117**, 889-907.

Berzofsky, J.A. and I.J. Berkower (1984). Antigen-antibody interaction. In *Fundamental Immunology* (ed W.E. Paul), pp 595-644. Raven Press, New York.

Brodsky, F.M. (1992). Antigen processing and presentation: close encounters in the endocytic pathway. *Trends in Cell Biology* **2**, 109-115.

Brodsky, F.M. and L.E. Guagliardi (1991). The cell biology of antigen processing and presentation. *Annual Review of Immunology* **9**, 707-744.

Brown, J.H., T.S. Jardetsky, J.C. Gorga, L.J. Stern, R.G. Urban, J.L. Strominger and D.C. Wiley (1993). 3-Dimensional structure of the human class II histocompatibility antigen HLA-DR1. *Nature* **364**, 33-39.

Burness, A.T.H. and I.U. Pardoe (1983). A sialoglycopeptide from human erythrocytes with receptor-like properties for encephalomyocarditis and influenza viruses. *Journal of General Virology.* **64**, 1137-1148.

Coffman, R.L., and M. Cohn (1977). The class of surface immunoglobulin on virgin and memory B lymphocytes. *Journal of Immunology* **118**, 1806-1815.

Coffman, R.L., D.A. Lebman and P. Rothman (1993). Mechanism and regulation of immunoglobulin isotype switching. *Advances in Immunology* **54**, 229-270.

Colonno, R.J., P.L. Callahan, D.M. Leippe, R.R. Rueckert and J.E. Tomassini (1989). Inhibition of rhinovirus attachment by neutralizing antibodies and their Fab fragments. *Journal of Virology* **63**, 36-42.

Davies, D.R., E.A. Padlan and D.M. Segal (1975). Three-dimensional structure of immunoglobulins. *Annual Review of Biochemistry* **44**, 639-667.

Davies, D.R. and E.A. Padlan (1990). Antibody-antigen complexes. *Annual Review of Biochemistry* **59**, 439-473.

Davies, D.R. and E.A. Padlan (1992). Twisting into shape. *Current Biology* **2**, 254-256.

Davis, D.R. and M.J. Schulman (1989). IgM-molecular requirements for its assembly and function. *Immunology Today* **10**, 118-128.

Dea, S. R, Bilodeau, R. Sauvageau and G.P. Martineau (1991). Outbreaks in Quebec pig farms of respiratory and reproductive problems associated with encephalomyocarditis virus. *Journal of Veterinary Diagnosis and Investigation* **3**, 275-282.

Deleat, I., R. Vrijsen and A. Boeyé (1992). Antigenic N to H conversion of poliovirus by a monoclonal antibody at low ionic strength. *Virology* **188**, 93-101.

Duke, G.M., A.C. Palmenberg (1989). Cloning and synthesis of infectious cardiovirus RNAs containing short discrete poly(C) tracts. *Journal of Virology* **63**, 1822-1826.

Duke, G.M., J.E. Osorio and A.C. Palmenberg (1990). Attenuation of Mengo virus through genetic engineering of the 5' noncoding poly(C) tract. *Nature* **343**, 474-476.

Flanegan, J.B., G.J. Tobin, M.S. Oberste, B.J. Morasco, D.C. Young and P.S. Collis (1990). *In* New Aspects of Positive-Strand RNA Viruses (M.A. Brinton and F.X. Heinz, Eds), pp. 55-60. American Society for Microbiology, Washington, D.C.

Francki, R.I.B., C.M. Fauquet, D.L. Knudson and F. Brown (1991). Classification and nomenclature of viruses. Fifth Report of the International Committee on Taxomony of Viruses. *Archives of Virology. Supplementum* **2**: 320-326.

Fricks, C.E. and J.M. Hogle (1990). The cell-induced conformational change of poliovirus: externalization of the amino terminus of VP1 is responsible for liposome binding. *Journal of Virology* **97**, 1934-1945.

Germain, R.N. and D.H. Margulies (1993). The biochemistry and cell biology of antigen processing and presentation. *Annual Review of Immunology* **11**, 403-450.

Goldberg, A.L. and K.L. Rock (1992). Proteolysis, proteasomes and antigen presentation. *Nature* **357**, 375-379.

Hammer, J., P. Valsasnini, K. Tolba, D. Bolin, J. Higelin, B. Takacs and R. Sinigaglia (1993). Promiscuous and allele-specific anchors in HLA-DR-binding-peptides. *Cell* **74**, 197-203.

Hozumi, N. and S. Tonegawa (1976). Evidence for somatic rearrangement of immunoglobulin genes coding for variable and constant regions. *Proceedings of the National Academy of Science. USA* **73**, 3628-3632.

Huber S.A. (1994). VCAM-1 is a receptor for encephalomyocarditis virus on murine vascular endothelial cells. *Journal of Virology* **68**, 3453-3458.

Hubbard, G.B., K.F. Soike, T.M. Butler, K.D. Carey, H. Davis, W.I. Butcher and C.J. Gauntt (1992). An encephalomyocarditis virus epizootic in a baboon colony. *Laboratory Animal Science* **42**, 233-239.

Hunt, S.L., A. Kaminski, and R.J. Jackson (1993). The influence of viral coding sequences on the efficiency of internal initiation of translation of cardiovirus RNAs. *Virology* **197**, 801-807.

Jang, S.K. and E. Wimmer (1990). Cap-independent translation of encephalomyocarditis virus RNA: structural elements of the internal ribosomal entry site and involvement of a cellular 57-kD RNA-binding protein. *Genes and Development* **4**, 1560-1572.

Jin. L., B.M. Fendly and J.A. Wells (1992). High resolution analysis of antibody-antigen interactions. *Journal of Molecular Biology* **226**, 851-865.

Kim, S., U. Boege, S. Krishnaswamy, I. Minor, T.J. Smith, M. Luo, D.G. Scraba and M.G. Rossmann (1990). Conformational variability of a picornavirus capsid: pH dependent structural changes of Mengo virus related to its host receptor attachment site and disassembly. *Virology* **175** , 176-190.

Kingsford, L. (1984). Enhanced neutralization of La Crosse virus by the binding of specific pairs of monoclonal antibodies to the G1 glycoprotein. *Virology* **136**, 265-273.

Kingsford, L., K.H. Boucquey and T.P. Cardoso (1991). Effects of specific mononclonal antibodies on La Crosse virus neutraization: aggregation, inactivation by Fab fragments, and inhibition of attachment to baby hamster kidney cells. *Virology* **180**, 591-601.

Koonin, E.V. and V.V. Dolja (1993). Evolution and Taxonomy of Positive-Strand RNA Viruses: Implications of Comparative Analysis of Amino Acid Sequences. *Critical Reviews in Biochemistry and Molecular Biology* **28**, 375-430.

Krishnaswamy, S. and M.G. Rossmann (1990). Structural refinement and analysis of Mengo virus. *Journal of Molecular Biology* **211** , 803-844.

Küppers, R., M. Zhao, M-L.Hansmann and K. Rajewsky (1993). Tracing B-cell development in human germinal centres by molecular analysis of single cells picked from histological sections. *EMBO Journal* **12**, 4955-4967.

Lanzavecchia, A. (1985). Antigen-specific interaction between T and B cells. *Nature* **314**, 537-539.

Logan, D., R. Abu-Ghazaleh, W. Blakemore, S. Curry, T. Jackson, A. King, S. Lea, R. Lewis, J. Newman, N. Parry, D. Rowlands, D. Stuart and E. Fry (1993). Structure of a major immunogenic site on foot-and-mouth disease virus. *Nature* **362**, 566-568.

Luo, M., G. Vriend, G. Kamer, I. Minor, E. Arnold, M.G. Rossmann, U. Boege, D.G. Scraba, G.M. Duke and A.C. Palmenberg (1987). The atomic structure of Mengo virus at 3.0 Å resolution. *Science* **235** , 182-191.

Madshus, I.H., S. Olsnes and K. Sandvig (1984). Different pH requirements for entry of two picornaviruses, human rhinovirus 2 and murine encephalomyocarditis virus. *Virology* **139**, 346-357.

Mak, T.W., J.S. Colter and D.G. Scraba (1974). Structure of the Mengo virion. II. Physiochemical and electron microscopic analysis of degraded virus. *Virology* **57**, 543-553.

Marc, D., G. Masson, M. Girard and S. van der Werf (1990). Lack of myristoylation of poliovirus capsid polypeptide VP0 prevents the formation of virions or results in the assembly of noninfectious virus particles. *Journal of Virology* **64**, 4099-4107.

Marrack, P. and J.W. Kappler (1993). How the immune system recognizes the body. *Scientific American* **269**, 81-89.

McCullough, K.C., D. Parkinson and J.R. Crowther (1988). Opsonization-enhanced phagocytosis of foot-and-mouth disease virus. *Immunology* **65**, 187-191.

Mestecky J. and J.R. McGhee (1987). Immunoglobulin A (IgA): Molecular and Cellular Interactions Involved in IgA Biosynthesis and Immune Response. *Advances in Immunology* **40**, 153-245.

Mian, S., A.R. Bradwell and A.J. Olson (1991). Structure, function and properties of antibody binding sites. *Journal of Molecular Biology* **217**, 133-151.

Mirzayan, C. and E. Wimmer (1994). Polioviruses: molecular biology. *In* Encyclopedia of Virology (R.G. Webster amd A. Granoff, Eds.), pp.1119-1132. Academic Press Inc., San Diego, CA.

Moore, N.F., B. Reavy and L.A. King (1985). General characteristics, gene organization and expression of small RNA viruses of insects. *Journal of General Virology* **66**, 647-659.

Morishima, T., P.R. McClintock, G.S. Aulakh, L.C. Billups, A.L. Notkins (1982). Genomic and receptor attachment differences between Mengovirus and encephalomyocarditis virus. *Virology* **122**, 461-465.

Olson, N.H., P.R. Kolatkar. M.A. Oliveira, R.H. Cheng, J.M. Greve, A. McClelland, T.S. Baker and M.G. Rossmann (1993). Structure of a human rhinovirus complexed with its receptor molecule. *Proceedings of the National Academy of Science. USA* **90**, 507-511.

Palmenberg, A.C. (1989). Sequence alignments of picornaviral capsid proteins. *In* Molecular Aspects of Picornavirus Infection and Detection (B.L. Semler and E. Ehrenfeld, Eds.), pp. 211-241. American Society of Microbiology, Washington, D.C.

Palmenberg, A.C. (1990). Proteolytic processing of picornaviral polyprotein. *Annual Review of Microbiology* **44**, 603-623.

Paul, W.E. (1993). Infectious diseases and the immune system. *Scientific American* **269**, 91-97.

Pelletier, J. and N. Sonenberg (1988). Internal initiation of translation of eukaryotic mRNA directed by a sequence derived from poliovirus RNA. *Nature* **334**, 320-325.

Pevear, D.C., J. Borkowski, M. Calenoff, C.K. Oh, B. Ostrowski, and H.L. Lipton (1988). Insights into Theiler's virus neurovirulence based on a genomic comparison of the neurovirulent GDVII and less virulent BeAn strains. *Virology* **165**, 1-12.

Porter, A.G. (1993). Picornavirus nonstructural proteins: emerging roles in virus replication and inhibition of host cell functions. *Journal of Virology* **67**, 6917-6921.

Porterfield, J.S. (1989). Picornaviridae. *In* Andrewes' Viruses of Vertebrates, 5th ed., pp. 120-145, Baillière Tindall, London.

Raychaudhuri, S. and W.J.W. Morrow (1993). Can soluble antigens induce $CD8^+$ cytotoxic T-cell responses? A paradox revisited. *Immunology Today* **14**, 344-348.

Reiss, C.S. (1993). Antigen processing and presentation of vesicular stomatitis virus glycoprotein. *Seminars in Virology* **4**, 101-107.

Reuer, Q., R.J. Kuhn and E. Wimmer (1990). Characterization of poliovirus clones containing lethal and nonlethal mutations in the genome-linked protein VPg. *Journal of Virology* **64**, 2967-2975.

Rini, J.M., U. Schulze-Gahmen and I.A. Wilson (1992). Structural evidence for induced fit as a mechanism for antibody-antigen recognition. *Science* **255**, 959-965.

Rizzo, L.V., R.H. Dekruyff and D.T. Umetsu (1992). Generation of B cell memory and affinity maturation. Induction with Th1 and Th2 T cell clones. *Journal of Immunology* **148**, 3733-3739.

Roivainen, M., L. Piirainen, T. Rysa, A. Narvanen and T. Hovi (1993). An immunodominant N-terminal region of the VP1 protein of poliovirion that is buried in the crytal structure can be exposed in solution. *Virology* **195**, 762-765.

Rossmann, M.G. (1989). The canyon hypothesis. *Journal of Biological Chemistry* **264**, 14587-14590.

Rossmann, M.G. and J.E. Johnson (1989). Icosahedral RNA virus structure. *Annual Review of Biochemistry* **58**, 533-573.

Rossmann, M.G., E. Arnold, J.W. Erickson, E.A. Frankenberger, J.P Griffith, H. Hecht, J.E. Johnson, G. Kamer, M. Luo, A.G. Mosser, R.R. Rueckert, B. Sherry and G. Vriend (1985). Structure of a human common cold virus and functional relationship to other picornaviruses. *Nature* **317**, 145-153.

Rotbart, H.A. and K. Kirkegaard (1992). Picornavirus pathogenesis: viral access, attachment and entry into susceptible cells. *Seminars in Virology* **3**, 483-499.

Rueckert R.R. (1990) Picornaviridae and their replication. *In* Fields Virology, 2nd ed. (B.N. Fields and D.M. Knipe, Eds.), pp. 507-548. Raven Press, New York, N.Y.

Schwab, C. and H.R. Bosshard (1992). Caveats for the use of surface-adsorbed protein antigen to test the specificity of antibodies. *Journal of Immunological Methods* **147**, 125-134.

Scraba, D.G. (1990). Functional aspects of the capsid structure of Mengo virus. *Journal of Structural Biology* **104**, 52-62.

Scraba, D.G. (1994). Cardioviruses. *In* Encyclopedia of Virology (R.G. Webster and A. Granoff, Eds.), pp. 255-260. Academic Press Inc., San Diego, CA.

Sheriff, S., E.W. Silverton, E.A. Padlan, G.H. Cohen, S.J. Smith-Gill, B.C. Finzel and D.R. Davies (1987). Three-dimensional structure of an antibody-antigen complex. *Proceedings of the National Academy of Science. USA* **84**, 8075-8079.

Smith, T.J., N.H. Olson, R.H. Cheng, H. Liu, E.S. Chase, W.M. Lee, D.M. Leippe, A.G. Mosser, R.R. Rueckert and T.S Baker (1993). Structure of human rhinovirus complexed with Fab fragments from a neutralizing antibody. *Journal of Virology* **67**, 1148-1158.

Thomas, A.A.M., R. Vrijsen and A. Boeyé (1986). Relationship between poliovirus neutralization and aggregation. *Journal of Virology* **59**, 479-485.

Tonegawa, S., N. Hozumi, G. Matthyssens and R. Schuller (1977). Somatic changes in the content and context of immunoglobulin genes. *Cold Spring Harbor Symposium on Quantitative Biology* **41**, 877-889.

Tonegawa, S. (1983). Somatic generation of antibody diversity. *Nature* **302**, 575-581.

Uhr, J.W. and M.S. Finkelstein (1963). Antibody formation. IV. Formation of rapidly and slowly sedimenting antibodies and immunological memory to bacteriophage ϕX 174. *Journal of Experimental Medicine* **117**, 457-.

Van Kaer, L., P.G. Ashton-Rickardt, H.L. Ploegh and S. Tonegawa (1992). TAP1 mutant mice are deficient in antigen presentation, surface class I molecules, and $CD4^{-}8^{+}$ T cells. *Cell* **71**, 1205-1214.

Wang, G., C. Porta, Z. Chen, T.S. Baker and J.E. Johnson (1992). Identification of a Fab interaction footprint site on an icosahedral virus by cryoelectron microscopy and x-ray crystallography. *Nature* **355**, 275-278.

Wetz, K. (1993). Attachment of neutralizing antibodies stabilizes the capsid of poliovirus against uncoating. *Virology* **192**, 465-472.

Wimmer, E. (1982). Genome-linked proteins of viruses. *Cell* **28**, 199-201.

CHAPTER II

CHARACTERIZATION OF MENGO VIRUS NEUTRALIZATION EPITOPES*

INTRODUCTION

Neutralization of viral infectivity by antibodies produced by the animal host is a complex and, as yet, poorly understood phenomenon. The advent of monoclonal antibodies, however, has made it possible to study the first step in the neutralization process, namely the recognition of a specific epitope on a virus particle by an antibody molecule. The experimental approach to define epitopes is to select mutant viruses which are able to escape neutralization by a particular monoclonal antibody and to identify those amino acid residues which were altered in the escape mutants. This protocol was first applied by Laver *et al.* (1979) to study the antigenicity of the influenza A virus hemagglutinin. Three monoclonal antibodies were used to select a total of ten non-neutralizable mutants which were characterized by peptide mapping and partial amino acid sequencing. When the three dimensional structure of the hemagglutinin was determined by X-ray crystallography (Wilson *et al.*, 1981) the amino acid changes in the escape mutants could be located precisely. This information was combined with that obtained from naturally-occurring antigenic variants to define four neutralization sites on the influenza A virus hemagglutinin (Wiley *et al.*, 1981).

Similar methodology has been used to identify the neutralization antigenic determinants of picornaviruses, whose simple icosahedral capsids are assembled from four different protein molecules (60 copies of each). Amino acid alterations in picornavirus escape mutants have been identified by direct sequencing of the capsid protein coding regions of their RNA genomes. Antigenic determinants for members of all five picornavirus genera have now been identified: poliovirus (genus *Enterovirus*; Diamond *et al.*, 1985; Blondel *et al.*, 1986; Minor *et al.*, 1986; Page *et al.*, 1988; Wiegers *et al.*, 1990; Roivainen *et al.*, 1991; Reynolds *et al.*, 1991; Patel *et al.*, 1993), Coxsackie B virus (genus *Enterovirus*, Haarmann *et al.*, 1994), bovine enterovirus (genus *Enterovirus*, Smyth *et al.*, 1990), human rhinoviruses 2 and 14 (genus *Rhinovirus*; Rossmann *et al.*, 1985; Sherry *et al.*, 1986; Appleyard *et al.*, 1990; Speller *et al.*, 1993), foot-and-mouth disease virus (FMDV; genus *Aphthovirus*; Xie *et al.*, 1987; Stave *et al.*, 1988; Thomas *et al.*, 1988; Barnett *et al.*, 1989; Baxt *et al.*, 1989; Parry *et al.*, 1989; Kitson *et al.*, 1990; Saiz *et al.*,

---

*A version of this chapter has been published. Boege *et al.*, 1991, *Virology* **181**:1-13.

1991; Crowther *et al.*, 1993), human hepatitis A virus (genus *Hepatovirus*, Ping and Lemon; 1992) and Theiler's encephalomyelitis virus (genus *Cardiovirus*, Nitayaphan *et al.*, 1985; Ohara *et al.*, 1988; Kim *et al.*, 1992; Roos and Casteel, 1992). When neutralization-escape mutations were located on the three dimensional structures of rhinovirus 14 (Rossmann *et al.*, 1985) and poliovirus types 1 and 3 (Page *et al.*, 1988; Filman *et al.*, 1989; Hogle and Filman, 1989), it became apparent that the antigenic determinants recognized by neutralizing antibodies are usually discontinuous, three-dimensional entities composed of spatially contiguous amino acid residues which are distant in the primary sequence of a particular protein, or even contributed by different capsid proteins. Three independent neutralization sites have been mapped on the surfaces of rhinovirus 14 and poliovirus types 1 and 3. These are located around the 5-fold and 3-fold icoasahedral axes of the virion and away from the "canyons", the surface depressions which contain the binding sites for cellular receptors (Rossmann, 1989).

Since the surface topography of Mengo virus, whose three dimensional structure has also been determined to 3 Å resolution (Luo *et al.*, 1987), is noticeably different from those of rhino- and polioviruses (Rossmann *et al.*, 1985; Hogle *et al.*, 1985), it is worthwhile to characterize its antigenic sites and to compare the results. We have investigated the amino acid changes in 20 escape mutants selected with a set of four neutralizing monoclonal antibodies. Our results indicate the existence of two independent neutralization sites on the surface of the Mengo virion.

METHODS

Monoclonal antibodies

Hybridoma cell lines secreting monoclonal antibodies which neutralized Mengo virus were a generous gift from Drs. J. H. Bowen and J. S. Colter (University of Alberta, Edmonton). These had been obtained using standard procedures of fusing spleen cells from 6 non-sibling female BALB/c mice immunized with Mengo virus subviral 13.4S pentamers with SP2/0 myeloma cells. From 2 separate fusions, 6 monoclonal antibody-producing cell lines were obtained. Four of these produced antibodies which neutralized virus infectivity (Bowen, 1985). The cell lines producing neutralizing monoclonal antibodies (numbered 1, 4, 5 and 6) were grown in Dulbecco's modified Eagle's medium (DME) containing 10% fetal calf serum (FCS). Supernatants of cell cultures maintained at ~ 10^6 cells per ml were collected, cleared from cell debris by centrifugation and stored at -70°.

Mutant selection

Mengo virus (M plaque variant; Ellem and Colter, 1961) was propagated at low multiplicity of infection (0.1 plaque forming units, PFU, per cell) in confluent mouse L-929 cell monolayers in roller bottles and purified as described previously (Ziola and Scraba, 1974; Boege *et al.*, 1986). The virus was mixed at 10^4 PFU per ml in phosphate buffered saline (PBS), containing 0.1% bovine serum albumin (BSA), with an equal volume of hybridoma supernatant. For the isolation of neutralization escape mutants a standard plaque test procedure was employed. 200 µl of the undiluted mixture as well as of 1:10 and 1:100 dilutions were plated on L-cell monolayers, allowed to attach for 45 min at room temperature and overlaid with 0.8% agar in a 1:1 (v:v) mixture of DME and the particular hybridoma supernatant. After 48 h at 37° the wells were overlaid with a second agar layer containing hybridoma supernatant ("feeder layer"). Vital staining with neutral red was performed six days after infection. Mutant plaques were picked and frozen-thawed twice in 1 ml DME without FCS. All variants were purified by replaquing them at least three times in the presence of the particular antibody. The mutant virions were propagated in L-cell monolayers in 150 cm^2 tissue culture flasks and subsequently in roller bottles. They were isolated from the culture fluid by methanol precipitation followed by chymotrypsin treatment and centrifugation in 15-30% sucrose gradients in 100 mM sodium phosphate buffer (pH 7.3) for 16 h at 36000 rpm (Beckman SW27 rotor). The 150 S peak was localized by centrifuging ^{3}H-leucine labeled Mengo virus in a parallel gradient. The virus peaks were pooled and the virions pelleted by centrifugation at 100,000 g for 2 h.

Radiolabeled virus preparations

Confluent L-cell monolayers in 150 cm^2 tissue culture flasks were infected with mutant plaque isolates in Eagle's basal medium (BME) containing 1% FCS. After 15 h the culture medium was replaced with amino acid deficient Eagle's minimum essential medium (MEM), containing 1% FCS and 250 µl per flask ^{35}S-methionine (10 mCi/ml, >800 Ci/mmol). Cell lysis occurred at 35 to 40 h postinfection. Virions were recovered from the supernatant by methanol precipitation and partially purified by centrifugation at 4° in 15-30% sucrose gradients in 100 mM phosphate (pH 7.3) for 1 h 35 min at 36,000 rpm (Beckman SW 41 rotor).

RNA isolation

Pellets of mutant virus obtained from 6 x 10^8 infected cells were resuspended in 2.25 ml "RNA buffer" (100 mM KCl, 10 mM Tris, 1 mM EDTA, pH 7.2, containing 1%

SDS) and extracted three times with equal volumes buffer-saturated phenol:chloroform, (4:1). After three washes of the aqueous phase with buffer-saturated ether and removal of residual ether by N_2, 200 µl of 2 M sodium acetate (pH 5.0) were added and the RNA precipitated with three volumes of cold (-25°) absolute ethanol. The pellet was recovered by centrifugation, dried under vacuum, resuspended in 50 µl water, and stored at -25°.

RNA sequence determinations

The region of the Mengo virus genome coding for the capsid proteins was sequenced directly by a modification of the dideoxy chain termination method (Sanger *et al.*, 1977) using 12 different primers and reverse transcriptase. Primers were synthesized using Applied Biosystems DNA synthesizers at the University of Wisconsin and at the University of Alberta. Appendix A contains a complete list of all the primers used for sequencing. They were 5' end-labeled for 30 min at 37° with γ-^{32}P-ATP (10 mCi/ml, 5000 Ci/mmol) and T4 polynucleotide kinase (BRL, Burlington, Ontario) in 70 mM Tris (pH 7.6), 10 mM $MgCl_2$, 5 mM DTT, at a concentration of 12 µg/ml primer, 770 U/ml kinase, and 77 µCi/ml γ-^{32}P-ATP. The total reaction volume was 13 µl, which subsequently was diluted to 20 µl with water. After inactivation of the kinase by heating to 100° for 5 min, 1 µl of labeled primer was added to the RNA for 3 min at 70° in 10 mM Tris (pH 8.3), 240 mM KCl to melt out secondary RNA structure. The mixture was then cooled to 40° hybridize the primer to the RNA. The concentrations of RNA and primer were approximately 125 µg and 1 µg per ml, respectively, in a total volume of 12 µl. For polynucleotide chain extension, one volume (2 µl) of the annealed RNA primer was incubated with 2.15 volumes (4.3 µl) of the reaction mixture consisting of 24 mM Tris (pH 8.3), 16 mM $MgCl_2$, 8 mM DTT, 0.4 mM dATP, dCTP, and dTTP, 0.8 mM dGTP, as well as 0.3 mM ddATP, ddCTP, ddGTP or 0.6 mM ddTTP. Reverse transcriptase from avian myelobastosis virus (Life Sciences, St. Petersburg, Florida) was present at a concentration of 2000 U per ml. After incubation at 50° for 45 min, the reactions were stopped by addition of FDE (90% formamide, 20 mM EDTA, 0.1% bromophenol blue, 0.1% xylene cyanol), boiled for 5 min, and loaded onto 6% polyacrylamide sequencing gels containing 8.3 M urea. Electrophoresis was performed at 45 watts in 45 mM Tris-borate (pH 8.3), 14 mM EDTA.

The amount of RNA used for each sequencing reaction was that obtained from the virus produced by 3×10^7 infected cells.

These experiments were done in collaboration with Dr. U. Boege.

Cross neutralization

The resistance of each mutant virus isolate to each of the neutralizing monoclonal antibodies was tested in a microtiter neutralization test. 50 µl of undiluted hybridoma supernatant were incubated with 50 µl mutant isolate at 100-fold 50% tissue culture infective dose for 1 h at 37°, then 5 x 10^4 L-cells in 100 µl BME were added. After 48 h at 37°, the plates were stained with 0.1% crystal violet in 20% ethanol.

These experiments were done in collaboration with Dr. U. Boege.

Isoelectric focusing

Isoelectric focusing was carried out in 1.5 mm horizontal polyacrylamide gels using an LKB Multiphor unit. The gel mixture consisted of 3.78% acrylamide, 0.22% bisacrylamide, 8 M urea, 2% NP40, 0.75% pH 2.5-4.5 ampholines, 2.0% pH 3.5-9.5 ampholines, 3.0% pH 5-8 ampholines, 0.01% N, N, N', N' - tetramethylethylenediamine (TEMED) and 0.03% ammonium persulfate.

^{35}S-methionine labeled mutant Mengo viruses were applied in 8 M urea, 2% NP40, ampholines as above, and 5% 2-mercaptoethanol. The electrode buffers were 1 M NaOH and 1 M H_3PO_4. Focusing was performed at 250 V for 14h, followed by 500 V for 1 h and 700 V for 30 min. The temperature was kept constant at 21° by a circulating waterbath. The gels were fixed in 20% methanol, 10% trichloroacetic acid and 5% sulfosalicylic acid and washed with 30% methanol, 10% acetic acid. After treatment with En^{3}Hance (NEN, Dupont Canada, Markham, Ontario) and washing with water, the gels were dried and subjected to autoradiography.

These experiments were done by Dr. S. Onodera.

Nomenclature

The VP1 through VP4 nomenclature is used for the capsid proteins of Mengo virus in this communication. To compare with the older Greek letter cardiovirus nomenclature and the systematic nomenclature proposed by Rueckert and Wimmer (1984), VP1 = α = 1D; VP2 = β = 1B; VP3 = γ = 1C; VP4 = δ = 1A. Amino acid residues are identified by their position in the polypeptide sequence preceded by 1, 2, 3 or 4, depending on the respective capsid protein. Thus 2144 indicates amino acid residue 144 of protein VP2.

RESULTS

To identify the Mengo virus neutralization epitopes, we followed the strategy of selecting mutants which had become resistant to neutralizing monoclonal antibodies. Since Mengo is a murine virus we have the advantage of producing the monoclonal antibodies in the natural host. However, wild type Mengo virus is highly pathogenic for mice; therefore the immunogen was not intact virus but 13S pentamer subunits. These were obtained by exposing Mengo virus to 0.15 M chloride at pH 6.0 (Mak *et al.*, 1974). Several monoclonal antibody secreting hybridoma cell lines were obtained; four of these (designated 1, 4, 5 and 6) were found to neutralize intact (native) Mengo virus. Antibodies 1 and 6 belong to IgG class 2a, while antibodies 4 and 5 are class 1 IgG molecules (Bowen, 1985). These antibodies were used to select "escape" mutants of Mengo virus from a wild type virus stock which had been propagated at low multiplicity of infection (0.1 PFU/cell) and purified (Ziola and Scraba, 1974; Boege *et al.*, 1986). Mutants were found at frequencies between 3 x 10^{-3} and 5 x 10^{-5} per PFU of wild type Mengo virus (Table II-1). It was noted that the dilutions of neutralized virus did not produce corresponding decreases in the number of plaques. This observation underscores the fact that neutralization of virus infectivity by antibodies is a complex phenomenon, and that estimating mutation frequency from plaque reduction assays is probably not very reliable.

Cross neutralization tests using the panel of four monoclonal antibodies indicated two independent neutralization sites (Figure II-1). For example, all mutants selected for their resistance to antibody 1 were still neutralized by antibodies 4, 5 and 6; as well all mutants selected for their resistance to antibody 4, or 5, or 6 were neutralized by antibody 1. Also, the mutants 5/01-S, M and L were able to escape neutralization by antibodies 4 and 6 as well as by antibody 5. Considering monoclonal antibodies 4, 5 and 6, it is clear from Figure II-1 that each recognizes a distinct epitope within the neutralization site. For example, antibody 4 neutralizes all of the antibody 1 escape mutants as well as mutants 5/04, 5/11-S, 5/11-L and 6/18; antibody 5 neutralizes all of the other escape mutants; antibody 6 neutralizes the antibody 1 escape mutants as well as 5/04, 5/11-S and 5/11-L. Based on the cross neutralization data it is clear that the epitopes recognized by antibodies 4, 5 and 6 overlap extensively and constitute one antigenic determinant while antibody 1 defines a second independent antigenic determinant.

For the characterization of the mutant viruses in terms of amino acid charge changes in their capsid proteins, these viruses were replicated in cultured L-cells in the presence of ^{35}S-methionine and their proteins separated by isoelectric focusing. Charge changes were observed predominantly in protein VP2 (Figure II-2). Only three of the twenty-one mutants had a charge alteration in VP1, and two of those had an additional charge change in VP2. No charge change in VP3 was observed in any of the mutants. These results were

TABLE II-1

Frequency of Escape Mutations

Monoclonal antibody	Frequency of mutation per PFU of wild type virus[a]
1	1.8×10^{-5}
4	2.7×10^{-3}
5	4.8×10^{-5}
6	1.7×10^{-4}

[a] Frequencies were calculated from plaque reduction assays performed as described under Mutant selection (see Methods).

CROSS NEUTRALIZATION DATA

	Monoclonal Antibody Number			
Virus Mutant	1	4	5	6
1/01	□	■	■	■
1/02	□	■	■	■
1/03	□	■	■	■
1/04	□	■	■	■
1/06	□	■	■	■
1/11	□	■	■	■
4/01	■	□	■	□
4/02	■	□	■	□
4/04	■	□	■	□
4/08	■	□	■	□
4/09	■	□	■	□
4/12	■	□	■	□
5/01-S	■	□	□	□
5/01-M	■	□	□	□
5/01-L	■	□	□	□
5/04	■	■	□	■
5/11-S	■	■	□	■
5/11-L	■	■	□	■
6/16	■	□	■	□
6/18	■	■	■	□

Figure II-1. Cross neutralization pattern of neutralization escape mutants of Mengo virus. Mutants selected with one of the four neutralizing antibodies were tested for resistance to the other antibodies in microtiter plates on mouse L-929 cell monolayers. □, cell lysis; ■, no cell lysis (virus neutralized).

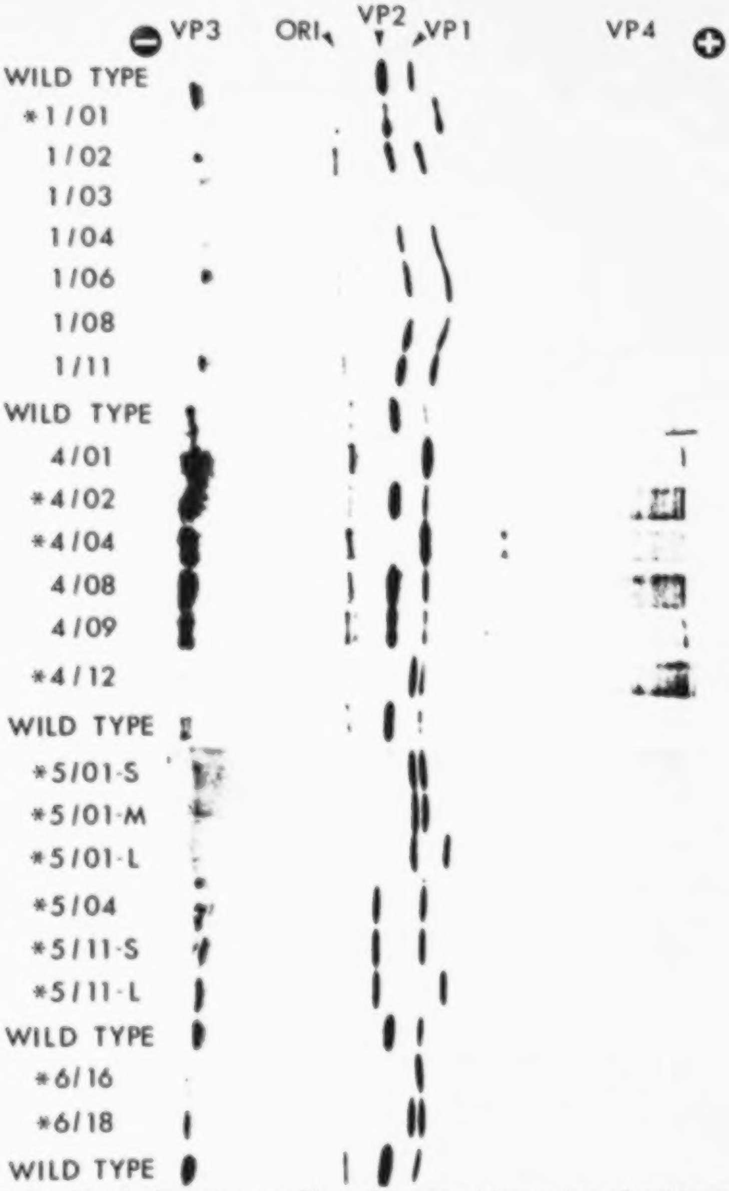

Figure II-2. Isoelectric focusing profiles of the capsid proteins of wild type Mengo virus and neutralization escape mutants. The mutants are listed on the left, with the number before the slash indicating the selecting antibody, and the number(s) after the slash indicating the plaque isolate. S, M and L refer to small-, medium- and large-size plaques, respectively. Virions were labeled with ^{35}S-methionine *in vivo*, and the proteins separated and focused in polyacrylamide/urea gels containing ampholites to form a pH-gradient (see Methods for details). Considering the proteins of wild type Mengo virus, VP3 has a net positive charge, while VP2, 1 and 4 have increasingly negative charges. In order to identify the proteins in the focusing gels, individual bands were eluted and electrophoresed in SDS-polyacrylamide gels together with Mengo marker proteins. Mutants exhibiting an isoelectric change in one or more of the capsid polypeptides are denoted with an asterix (see Table II-2).

initially intended to be used as a guide for sequence determination, with the expectation that the location of an amino acid change causing an isoelectric change would preclude the necessity of further RNA sequencing. However, eight mutant viruses exhibited no isoelectric changes in VP1, 2 or 3. Also, as sequencing progressed, we discovered that several of the mutations causing isoelectric changes were, in fact, second-site mutations which were not the cause of the neutralization-escape phenotype.

In order to locate the mutations in the Mengo genome, mutant viruses were grown in L-cells, partially purified and their RNA's isolated and subjected to nucleotide sequence analysis by the primer extension procedure. Twelve different synthetic oligonucleotide primers were chosen to cover the capsid protein coding region; these were end-labeled, annealed in turn to viral RNA and extended with reverse transcriptase. The extent to which each mutant genome was sequenced is indicated in Figure II-3. There is a sequencing gap for most of the mutants which corresponds to nucleotides coding for the βI strand of VP2; however this is an element of the β-barrel shell-forming domain which is located on the interior surface of the capsid, and would be unlikely to harbor a mutation capable of causing the neutralization-escape phenotype. For the same reason sequence analyses were not extended into the VP4 coding region. Mutant 1/08 was found to have reverted to wild-type during its replication prior to RNA isolation: no differences in sequence from wild-type RNA were found and the replicated virus behaved like wild-type when added to cell monolayers in the presence of antibody 1. Thus we were left with 20 authentic neutralization-escape mutants of Mengo virus.

Figure II-3 also shows the locations of mutations causing amino acid changes in capsid proteins. Most of the mutants exhibit a single change; in these cases the interpretation is unambiguous. In mutants with more than one amino acid change, one of these corresponds to the neutralization-escape mutation of other mutants in its group. The additional mutation(s) is therefore likely to be a second-site mutation resulting in an amino acid change which has no deleterious effect on capsid structure or function and which is unrelated to the neutralization-escape phenotype. This argument is strengthened when the mutations are located on the ribbon diagrams of the Mengo capsid proteins (Figure II-4). The second-site mutations are not located in physical proximity to those responsible for neutralization-escape.

Table II-2 summarizes the nucleotide changes, amino acid changes and isoelectric changes for the 20 authentic escape mutants. Isoelectric changes were detected in a total of 14 capsid proteins (12 mutants); of these, 8 changes were as a result of the mutation which conferred resistance to neutralization while the other 6 were second-site mutations. These

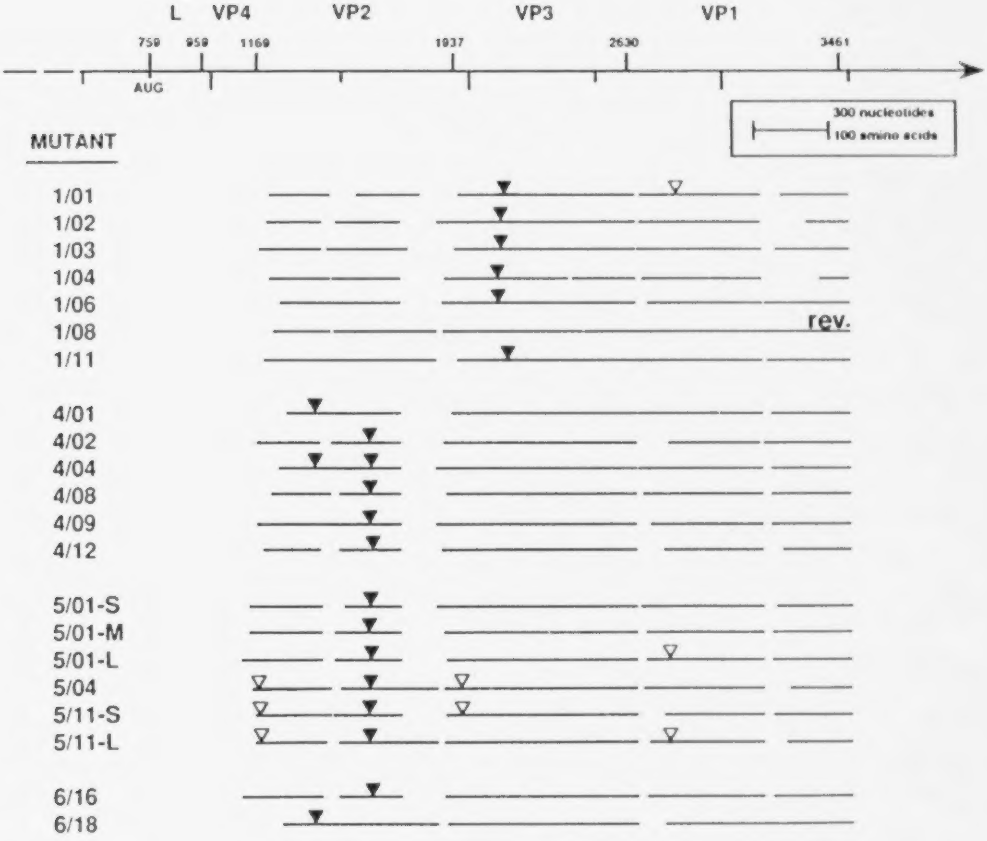

Figure II-3. Mutant virus sequence information. Data shown for 21 Mengo virus neutralization escape mutants selected with monoclonal antibodies 1, 4, 5 and 6, as listed on the left. The genome organization of the capsid region is shown at the top. Sequences obtained for the individual mutants are shown as horizontal bars. Base changes leading to an amino acid alteration are indicated by arrowheads. The black arrowheads indicate the mutations conferring resistance to neutralization, while the outlined arrowheads indicate second-site mutations. The original mutant 1/08 reverted to wild-type during its production in quantity for RNA sequencing.

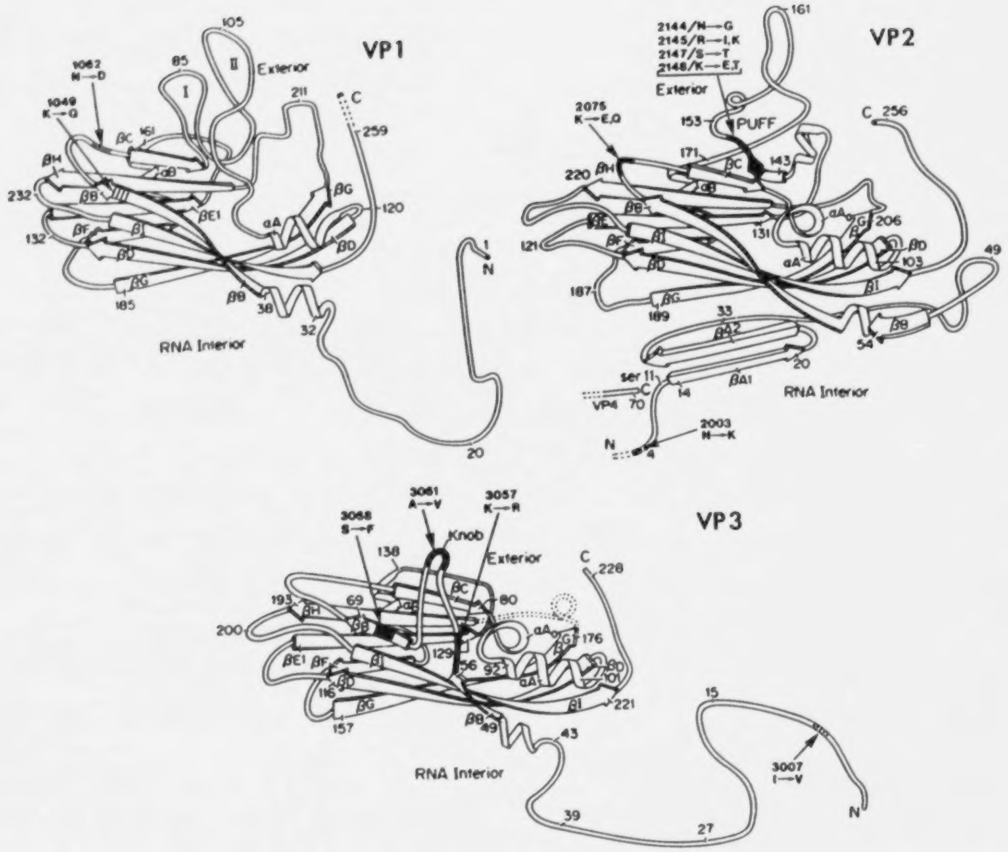

Figure II-4. Position of mutations in neutralization escape mutants. Ribbon diagrams of the Mengo virus capsid proteins displaying the eight-stranded, antiparallel β-barrel motif common to the structural proteins of picornaviruses. Sites of amino acid changes in the neutralization escape mutants fall within the black regions. The striped regions indicate the locations of second-site mutations.

[a] The nucleotide numbers refer to the position in the Mengo virus genome, beginning with nucleotide 1 at the 5'-end [the complete poly(C) tract is included].

[b] The amino acid residues are identified according to the "Rossmann system", with the first digit representing viral capsid protein 1, 2, or 3, and the next three digits indicating position from the N-terminal.

[c] Isoelectric changes are expressed in terms of the mutant capsid protein having a more basic (+) or more acidic (-) isoelectric point than the corresponding wild-type protein; no change in isoelectric point is indicated by 0.

[d] Denotes a second-site mutation. These are not involved with resistance to neutralization.

TABLE II-2

Changes in Nucleotide Sequence, Amino Acid Sequence and Isoelectric points for the External Capsid Proteins of Mengo Virus Escape Mutants

		Amino acid changes[b] in			Isoelectric changes[c] in		
Mutant virus	Nucleotide change[a]	VP1	VP2	VP3	VP1	VP2	VP3
1/01	2814 A→G	1062 N→D[d]			—	0	0
	2140 C→U			3068 S→F			
1/02	2119 C→U			3061 A→V	0	0	0
1/03	2119 C→U			3061 A→V	0	0	0
1/04	2107 A→G			3057 K→R	0	0	0
1/06	2107 A→G			3057 K→R	0	0	0
1/11	2140 C→U			3068 S→F	0	0	0
4/01	1392 A→G		2075 K→E		0	—	0
4/02	1603 G→A		2145 R→K		0	0	0
4/04	1392 A→G		2075 K→E		0	—	0
	1608 U→A		2147 S→T				
4/08	1603 G→A		2145 R→K		0	0	0
4/09	1603 G→A		2145 R→K		0	0	0
4/12	1612 A→C		2148 K→T		0	—	0
5/01-S	1603 G→U		2145 R→I		0	—	0
5/01-M	1603 G→U		2145 R→I		0	—	0
	1956 A→G			3007 I→V[d]			
5/01-L	2775 A→C	1049 K→Q[d]			—	—	0
	1603 G→U		2145 R→I				
5/04	$\frac{1599}{1600}$ AA→GG		2144 N→G		0	+	0
	1956 A→G			3007 I→V[d]			
	1178 U→G		2003 N→K[d]				
5/11-S	$\frac{1599}{1600}$ AA→GG		2144 N→G		0	+	0
	1956 A→G			3007 I→V[d]			
	1178 U→G		2003 N→K[d]				
5/11-L	2775 A→C	1049 K→Q[d]			—	+	0
	$\frac{1599}{1600}$ AA→GG		2144 N→G				
	1178 U→G		2003 N→K[d]				
6/16	1611 A→G		2148 K→E		0	—	0
6/18	1392 A→C		2075 K→Q		0	—	0

results underscore our naiveté in thinking that isoelectric focusing could be useful as a guide and to limit sequencing. The identification of all of the mutations responsible for isoelectric changes, on the other hand, provides assurance that all of the changes in nucleotide sequence of the capsid coding region for the escape mutants have been identified. There were a number of nucleotide changes discovered which did not lead to an amino acid substitution. These are listed in Table II-3. One of the silent mutations, at nucleotide 1544, was observed 13 times. It is conceivable that this nucleotide change might be necessary to compensate for the escape mutations in maintaining nucleic acid secondary structure, which in turn guarantees efficient replication and thus viability. More likely, however, natural heterogeneity is present in the genomes of the wild type population at this position. In fact, sequence analysis of wild-type RNA demonstrated the concomitant appearance of U and C at nucleotide 1544.

Considering the amino acid alterations which resulted in escape from neutralization by antibody 1, all of these occurred in VP3 and none produced a charge change. The alterations were at amino acid residues 3057, 3061 and 3068, and are associated with the surface proturbance called the "knob" (Figure II-4). These alterations did not affect the neutralization of mutants 1/01, 1/02, 1/04, 1/06 or 1/11 by antibodies 4, 5 or 6. The antibody 4-escape mutants were characterized by amino acid changes in VP2 at either of two positions in the primary sequence. One of these was at Lys2075 in the βB-βC loop, and the other was from residues 2145-2148 in part of the VP2 tertiary structure called the "puff". These two regions are very close to one another on the surface of the virion (see Figs. II-4 and II-5). Mutants resistant to neutralization by antibody 5 had either an Asn→Gly change at residue 2144 or an Arg→Ile change at residue 2145. The latter mutants were resistant to neutralization by antibodies 4 and 6 as well as by antibody 5 (Fig. II-1). In comparison, the mutants selected by resistance to antibody 4 which had an Arg→Lys change at residue 2145 were still neutralized by antibody 5. These observations suggest that a positive charge at 2145 is required for recognition by antibody 5, and that the epitopes for antibodies 4, 5 and 6 overlap at Arg2145. Mutant 6/16 has an alteration of the same amino acid residue as mutant 4/12 (Lys2148) and exhibits the same cross-neutralization pattern, *i.e.* both mutants are neutralized only by antibody 5. In mutant 6/18, the change is from Lys2075→Gln, and this mutant is neutralized by antibody 4 or antibody 5 (Fig. II-1). Recognition by antibody 4 is apparently abolished if residue 2075 changes charge from positive to negative (mutants 4/01 or 4/04), but not from positive to neutral (mutant 6/18).

All of the Mengo virus mutations conferring resistance to neutralization by one or

TABLE II-3

Silent Mutations Found in Mengo Escape Mutants

Nucleotide position	Codon change	Amino acid	Occurrence
2675	GCA→GCC	Ala1015	1 x
2946	CUA→UUA	Leu1106	1 x
1244	AAC→AAU	Asn2025	1 x
1544	AGU→AGC	Ser2125	13 x
1772	GCC→GCU	Ala2201	1 x
1790	ACA→ACU	Thr2207	4 x
1838	ACC→ACU	Thr2223	1 x

more of the four monoclonal antibodies are located in loops which connect β-strand elements of the shell-forming β-barrel domains of the capsid polypeptides (the one exception is the Ser→Thr change at 3068; this residue forms part of the interrupted βB strand in VP3), and all are exposed on the external surface of the capsid see Fig. II-4). The second (and third)-site mutations which were found in mutants 1/01, 5/01-L, 5/04, 5/11-S and 5/11-L fall into two groups. The Asn2003→Lys and Ile3007→Val mutations are located on the interior surface of the capsid in "random-coil" regions near the ends of polypeptide chains. In contrast, the Lys1049→Gln and Asn1062→Asp mutations are on the exterior surface in the loop connecting βB and βC in VP1 (strictly speaking, residue 1049 is in βB, at its carboxyl end). These mutations play no role in resistance to antibodies 1 or 5, yet they are the only mutations which were found in VP1, and they do correspond with neutralization site 1 in poliovirus types 1 and 3 and NIm-IA of human rhinovirus type 14 (see Table II-4). Thus, while mutations in the VP1 βB-βC loop can be tolerated in terms of the structural and functional requirements of the Mengo virus capsid, these are not recognized by the group of monoclonal antibodies at our disposal. It is conceivable that this site in VP1 is immunogenic in mice if intact virions would have been used as immunogen; this has been confirmed (see Chapter III). The conditions used to dissociate virions into 13.4S pentamers (0.14 M NaCl, 0.01 M Na-phosphate, pH 6.2), which were used to immunize mice, may have destroyed the immunogenicity of the βB-βC VP1 surface loop.

DISCUSSION

Since Mengo virus causes a systemic and lethal infection in its natural host (Duke *et al.*, 1990), pentameric capsid subunits were used to immunize mice and prepare hybridoma cell lines. Four of such lines were found to secrete monoclonal antibodies which were capable of neutralizing intact virus. The four monoclonal antibodies in turn were employed to select 20 neutralization mutants of Mengo virus, and capsid amino acid residues which were altered in the mutants were determined by direct RNA sequencing of the capsid-coding regions of their genomes. Amino acid alterations were located in the three-dimensional structure of Mengo virus, which has been determined to 3 Å resolution (Luo *et al.*, 1987; Krishnaswamy and Rossmann, 1990). The results are summarized in Table II-2 and Figures II-4 and II-5.

The mutations conferring resistance to neutralization by the four monoclonal antibodies are all located on the external surface of the capsid, as one might expect. No

[a] Amino acid sequence alignments for picornavirus proteins have been tabulated by Palmenberg (1989). The designation for β-strands (β) and α-helical sequences (α) is according to the original proposals of Rossmann *et al.* (1985) and Hogle *et al.* (1985); refer to the ribbon diagrams of Figure II-4. Antigenic epitopes, as a general rule, occur in flexible surface loops which link the eight antiparallel β-strands comprising the "shell" domain of each capsid polypeptide.

[b] Data taken from Diamond *et al.* (1985), Blondel *et al.* (1986), Page *et al.* (1988), Wiegers *et al.* (1989) and Wiegers *et al.* (1990). Sites 2 and 3 are immunodominant for type 1 poliovirus.

[c] Data from Minor *et al.* (1985), Minor *et al.* (1986), Filman *et al.* (1989) and Hogle and Filman (1989). Site 1 is immunodominant for type 3 poliovirus.

[d] Data from Rossmann *et al.* (1985) and Sherry *et al.* (1986). HRV-2 has neutralization sites which likely correspond to NIm-IA and NIm-II of HRV-14, and a third site involving residues 2236 and 2238 near the icosahedral 3-fold axes (Skern *et al.*, 1987; Appleyard *et al.*, 1990); however, the 3-dimensional structure of HRV-2 has not yet been determined.

[e] The 3-dimensional structure for FMDV serotype O_1 has been determined by Acharya *et al.* (1989). Based upon this structure, neutralization sites for serotypes O_1 (Xie *et al.*, 1987; Stave *et al.*, 1988; Parry *et al.*, 1989), A_{10} (Thomas *et al.*, 1988), A_{12} (Baxt *et al.*, 1989) and C (Mateu *et al.*, 1989) have been correlated with structure elements. The immunodominant site for each of the serotypes is contained within the highly flexible loop in VP1 connecting the βG and βH strands (the corresponding segment in HRV-14 and Mengo viruses has been called the "FMDV loop"; see Fig. II-4). Studies with synthetic peptides have shown that a composite of the FMDV O_1 loop (1141-1158) and the VP1 C-terminal (1200-1213) has enhanced ability to elicit the formation of neutralizing antibodies and to protect cattle against subsequent challenge with live virus (DiMarchi *et al.*, 1986). These two elements, the FMDV loop and the C-terminal 14 residues of a VP1 molecule from the protomer to the right, are located together in a region near the icosahedral 3-fold axis (Acharya *et al.*, 1989).

TABLE II-4

A Comparison of the Locations of Neutralization Epitopes in Picornaviruses

Location[a]	Poliovirus-1[b]	Poliovirus-3[c]	Rhinovirus-14[d]	FMDV[e]	Mengo
	Site 1		*NIm-I*		
VP1 βB-βC	1097-1101	1089-1100	1091, 1095 (IA)		
VP1 βD-βE	1144		1083 – 1085 1138, 1139 (B)	1083	
VP1 βE-αA		1166			
VP1 βH-βI		1253		1169, 1173	
	Site 2		*NIm-II*	*Groups 1, 2*	
VP1 βG-βH	1221-1226		1210	1138-1157 (1)	
VP1 C-term.				1200-1213 (2)	*Site 1*
VP2 βE-αB ("Puff")	2164 – 2170 2142	2164-2172	2158 – 2162 2136	2132 (1)	2144-2148
VP2 C-term.	2270				
	Site 3		*NIm-III*	*Group 3*	
VP1 C-term.		1286-1290	1287		
VP2 βB-βC	2072 (3B)				2075
VP2 βC-αA				2080	
VP2 βH-βI				2196	*Site 2*
VP3 βB ("knob")	3058 – 3060 (3A)	3058, 3059			3057, 3061
VP3 βB	3071, 3073	3070, 3071			3068
VP3 βB-βC	3076 (3B)	3077, 3079	3072-3078	3069, 3070	
VP3 βE-αB				3136, 3139	
VP3 βG-βH				3175, 3178	
VP3 βH-βI			3203	3195	

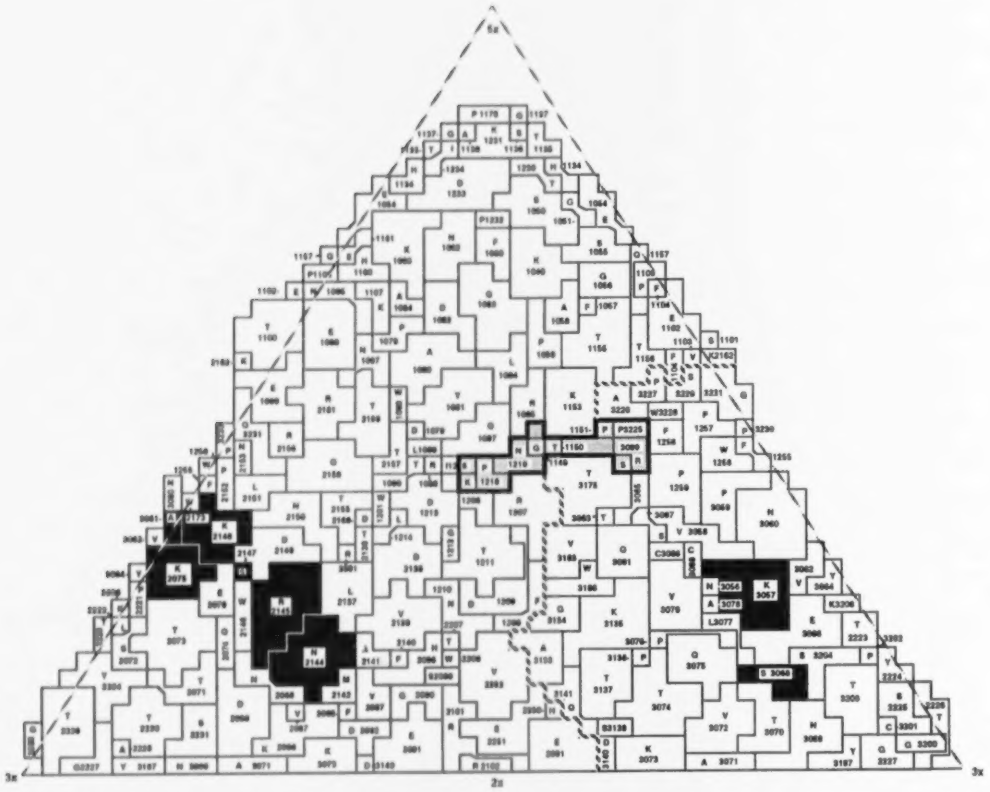

Figure II-5. Surface map of one crystallographic asymmetric unit of the Mengo virus capsid (redrawn from Rossmann and Palmenberg, 1988; redefined pit dimensions provided by A.C. Palmenberg and J.-Y. Sgro, Institute for Molecular Virology, Madison, WI). The icosahedral 5-, 3- and 2-fold symmetry axes are marked. The section shown is at a radius of 144 Å from the center of the virion and it has been divided into 2 Å squares. Amino acid residues are identified by the single letter code, and the surface areas occupied by each are indicated. The numbers indicate the polypeptide (first digit: 1=VP1, 2=VP2, 3=VP3) and position in the sequence from the N-terminal (last 3 digits). The pit area is shaded in grey; this surface depression is approximately 30 Å in diameter and 20 Å in depth. The striped line (extended through the pit area) indicates that the lower right third of the crystallographic subunit is occupied by a VP3 molecule from the biological (assembly) protomer to the right. Thus, the amino acid residues (shown in black) which are changed in the neutralization-escape mutants form two independent antigenic determinants within one biological protomer (see Figure II-6).

mutations were discovered which might alter the β-barrel domain (the shell-forming motif) of the capsid proteins VP1, VP2 or VP3, and there was no suggestion of a mutation at an interior position promoting a distant conformational change which could disrupt antibody binding. All of the neutralization-escape mutations were located on surface loops of VP2 and VP3, and these define two separate antigenic determinants within a biological protomer (Figure II-6). Cross-neutralization experiments (Figure II-1) confirmed that each of the four monoclonal antibodies recognizes a distinct set of epitopes within the antigenic determinants, including antibodies 4, 5 and 6 which bind to distinct but overlapping epitopes on VP2.

Table II-4 provides a comparison of the location of the Mengo virus neutralization epitopes with those of other picornaviruses whose 3-dimensional structures have been determined at atomic resolution. Polioviruses serotypes 1 and 3 and human rhinovirus type 14 (HRV-14) are similar in that there are three major antigenic determinants on each; these are located near the three vertices of the crystallographic protomer (such as that shown for Mengo in Figure II-5) and flank the deep groove or canyon, which in all likelihood contains the recognition elements for a cellular receptor (Rossmann, 1989). In terms of the tertiary structure of the capsid protein molecules the Mengo virus neutralization epitopes comprising part of site 1 (2144-2148; the VP2 ridge) correspond to site 2 in the polioviruses and NIm-II in HRV-14. Residue 2075 from site 1 in Mengo aligns with site 3B in poliovirus type 1. Site 2 in Mengo (3057, 3061, 3068; the VP3 "knob") corresponds to site 3A in poliovirus and NIm-III in HRV-14. Foot-and-mouth disease virus (FMDV; Acharya *et al.*, 1989) differs markedly in surface design from poliovirus, rhinovirus and Mengo, and it also differs in the location of antigenic regions. The major antigenic/immunogenic determinant in FMDV is contained with the βG-βH loop of VP1 (Parry *et al.*, 1989) which extends from the capsid surface and is flexible (it cannot be seen in the X-ray diffraction electron density map). In close proximity, also protruding from the capsid surface and contributing to the determinant is the carboxyl-terminal 13 residues of VP1 (Di Marchi *et al.*, 1986) from an adjacent protomer. Again in contrast to other picornaviruses, the VP1 βG-βH loop of FMDV carries the receptor binding site which includes an R-G-D sequence (Fox *et al.*, 1989).

None of our four monoclonal antibodies was directed against sites involving surface residues of VP1 which are clustered around the 5-fold axes of the virion (*i.e.* in the upper third of the crystallographic protomer shown in Figure II-5). Mutations were observed at residues 1049 and 1062, but these were not involved with the neutralization-

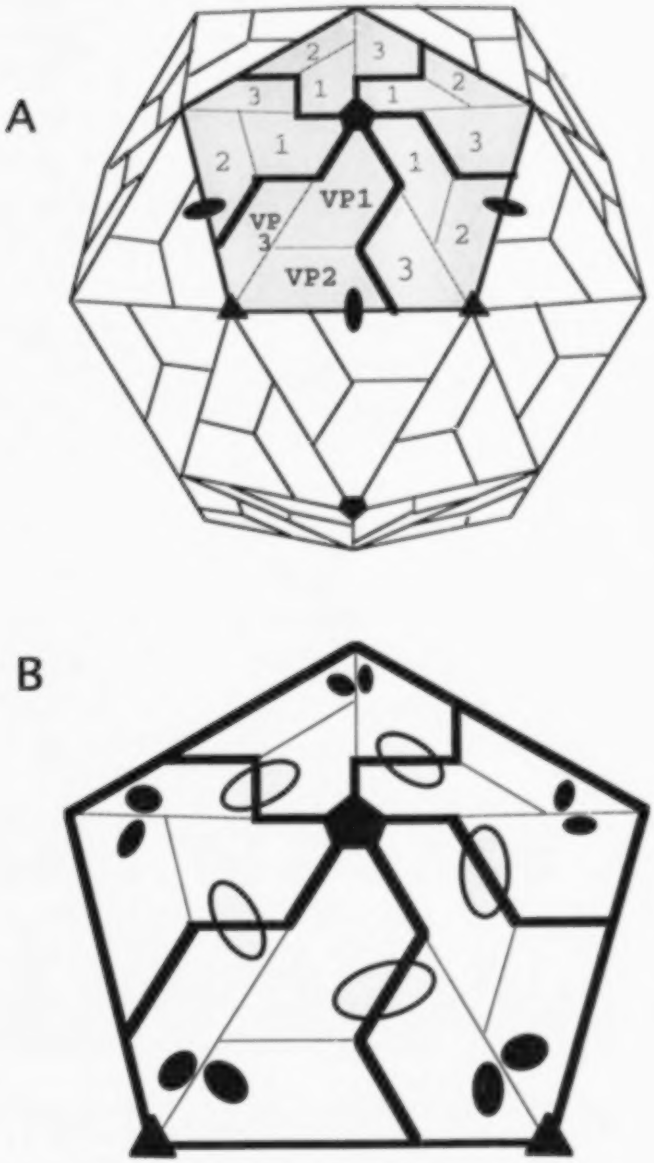

Figure II-6. (A) Diagrammatic representation of the Mengo virus capsid (redrawn from Luo *et al.*, 1987). The biological protomer or asymmetric assembly unit comprises one molecule each of VP1, VP2 and VP3, and is outlined by thicker lines. The crystallographic protomer depicted in Figure 5 is defined by a 5-fold and two 3-fold axes; it comprises VP1 and VP2 from one biological protomer and VP3 from a second biological protomer to the right. (B) Enlarged view of the pentameric capsid subunit outlined in A. The deepest parts of the surface depression ("pits") are indicated schematically by the gray ovals. The neutralization epitopes identified in this communication are located within the black, crescent-shaped regions and comprise VP2 and VP3.

escape phenotype. Considering the disposition of antigenic determinants in poliovirus or rhinovirus, one might expect that some of the VP1 surface loops in Mengo (*e.g.* βB-βC, βC-αA, βD-βE, βH-βI; see Figure 4) would also be immunogenic and antigenic. These may not have been discovered to date because of the small number of monoclonal antibodies which have been employed as selecting agents, and/or because there has been some distortion in these loops which accompanied the preparation of the 13.4S pentamers used as immunogens in mice. To address these potential deficiencies in our analyses, we have used an attenuated strain of Mengo virus (Duke *et al.*, 1990) as immunogen and generated a second set of mouse monoclonal antibodies. The results of these experiments are presented in Chapter III.

Likewise no mutations were detected in the carboxy-terminus of Mengo virus VP1, although this part of the molecule emerges near the right hand edge of the pit and extends in the general direction of the icosahedral 2-fold symmetry axis (Krishnaswamy and Rossmann, 1990; the last residue clearly identifiable and shown in Figure II-4 is Pro1259, the next 9 residues have been identified on the basis of weak electron density and the final 6-9 are invisible - *i.e.* they are in a flexible conformation). Maturation of the Mengo virion involves trimming of 3 residues (Glu1277, Leu1276 and Met1274) from a majority of the VP1 polypeptides, and this post-assembly processing has been correlated with the dissociability of the virion (Boege and Scraba, 1989). Theiler's murine encephalomyelitis virus, which is closely related to Mengo and the other cardioviruses (Palmenberg, 1989), has a neutralization escape mutation at Val1268 (Ohara *et al.*, 1988). It will be interesting to see if monoclonal antibodies directed against "native" Mengo virions recognize a site which includes residues from the VP1 C-terminal.

To reiterate, one antigenic determinant on the Mengo virion (Figure II-6) includes residues 3068, 3057, 3061 and a second determinant is composed of residues 2075, 2144, 2145, 2147, 2148. For bovine enterovirus (BEV), a picornavirus whose 3-dimensional structure has not yet been determined, it has been shown that synthetic peptides corresponding to BEV residues 2152-2161 and 3054-3063 can elicit neutralizing antibodies in BALB/c mice (Smyth *et al.*, 1990). The correspondence may be fortuitous, or the BEV and Mengo capsids may be similarly organized with respect to polypeptide conformations and antigenic determinants.

REFERENCES

Acharya, R., E. Fry, D. Stuart, G. Fox, D. Rowlands and F. Brown (1989). The three-dimensional structure of foot-and-mouth disease virus at 2.9 Å resolution. *Nature* **327**, 709-716.

Appleyard, G., S.M. Russell, B.E. Clarke, S.A. Speller, M. Trowbridge and J. Vadolas (1990). Neutralization epitopes of human rhinovirus type 2. *Journal of General Virology* **71**, 1275-1282.

Barnett, P.V., E.J. Ouldridge, D.J. Rowlands, F. Brown and N.R. Parry (1989). Neutralizing epitopes of type O foot-and-mouth disease virus. I. Identification and characterization of three functionally independent, conformational sites. *Journal of General Virology* **70**, 1483-1491.

Baxt, B., V. Vakharia, D.M. Moore, A.J. Franke and D.O. Morgan (1989). Analysis of neutralizing antigenic sites on the surface of type A_{12} foot-and-mouth disease virus. *Journal ofVirology* **63**, 2143-2151.

Blondel, B., R. Crainic, O. Fichot, G. Dufraisse, A. Candrea, D. Diamond, M. Girard and F. Horaud (1986). Mutations conferring resistance to neutralization with monoclonal antibodies in Type 1 poliovirus can be located outside or inside the antibody-binding site. *Journal of Virology* **57**, 81-90.

Boege, U. and D.G. Scraba (1989). Mengo virus maturation is accompanied by C-terminal modification of capsid protein VP1. *Virology* **168**, 409-412.

Boege, U., D.S.-W. Ko and D.G. Scraba (1986). Toward an *in vitro* system for picornavirus assembly, purification of Mengovirus 14S capsid precursor particles. *Journal of Virology* **57**, 275-284.

Bowen, J. H. (1985). The use of monoclonal antibodies in studies of the capsid proteins and the poly(U) polymerase of Mengo virus. Ph.D. thesis, University of Alberta, Edmonton, Canada.

Crowther, J. R., S. Farias, W.C. Carpenter and A.R. Samuel (1993). Identification of a fifth neutralizable site on type O foot-and-mouth disease virus following characterization of single and quintuple monoclonal antibody escape mutants. *Journal of General Virology* **74**, 1547-1553.

Davies, D. R., E.A. Padlan and S. Sheriff (1990). Antibody-antigen complexes. *Annual Review of Biochemistry* **59**, 439-473.

Diamond, D. C., B.A. Jameson, J. Bonin, M. Kohara, S. Abe, H. Itoh, T. Komatsu, M. Arita, S. Kuge, A. Nomoto, A.D.M.E. Osterhaus, R. Crainic and E. Wimmer (1985). Antigenic variation and resistance to neutralization in poliovirus type 1. *Science* **229**, 1090-1093.

Di Marchi, R., G. Brooke, C. Gale, V. Cracknell, T. Doel and N. Mowat (1986). Protection of cattle against foot-and-mouth disease by a synthetic peptide. *Science* **232**, 639-641.

Duke, G. M., J.E. Osorio and A.C. Palmenberg (1990). Attenuation of the Mengo virus through genetic engineering of the 5' noncoding poly(C) tract. *Nature* **343**, 474-476.

Ellem, K.A.O. and J.S. Colter (1961). The isolation of three variants of Mengo virus differing in plaque morphology and hemagglutinating characteristics. *Virology* **15**, 340-347.

Filman, D. J., R. Syed, M. Chow, A.J. Macadam, P.D. Minor and J.M. Hogle (1989). Structural factors that control conformation transitions and serotype specificity in type 3 poliovirus. *EMBO Journal* **8**, 1567-1579.

Fox, G., N.R. Parry, P.V. Barnett, B. McGinn, D.J. Rowlands and F. Brown (1989). The cell attachment site on foot-and-mouth disease virus includes the amino acid sequence RGD (arginine-glycine-aspartic acid). *Journal of General Virology* **70**, 625-637.

Haarmann, C. M., P.L. Schwimmbeck, T. Mertens, H.-P. Schultheiss and B.E. Strauer (1994). Identification of serotype-specific and nonserotype-specific B-cell epitopes of coxsackie B virus using synthetic peptides. *Virology* **200**, 381-389.

Hogle, J. M., M. Chow and D.J. Filman (1985). Three-dimensional structure of poliovirus at 2.9 Å resolution. *Science* **229**, 1358-1365.

Hogle, J. M. and D.J. Filman (1989). The antigenic structure of poliovirus. *Philosophical Transactions of the Royal Society (London), Series* B **323**, 467-478.

Laver, W. G., G.M. Air, R.G. Webster, W. Gerhard, C.W. Ward and T.A.A Dopheide

(1979). Antigenic drift in type A influenza virus. Sequence differences in the hemagglutinin of Hong Kong (H3N2) variants selected with monoclonal hybridoma antibodies. *Virology* **98**, 226-237.

Luo, M., G. Vriend, G. Kamer, I. Minor, E.A. Arnold, M.G. Rossmann, U. Boege, D.G. Scraba, G.M. Duke and A.C. Palmenberg (1987). The atomic structure of Mengo virus at 3.0 Å resolution. *Science* **235**, 182-191.

Kim, B. S., Y.-K. Choe, M.A. Crane and R.J. Colleen (1992). Identification and localization of a limited number of predominant conformation-independent antibody epitopes of Theiler's murine encephalomyelitis virus. *Immunological Letters* **31**, 199-206.

Kitson, J. D. A., D. McCahon and G. J. Belsham. (1990). Sequence analysis of monoclonal antibody resistant mutants of type O foot-and-mouth disease virus: evidence for the involvement of the three surface exposed capsid proteins in four antigenic sites. *Virology* **179**, 26-34.

Krishnaswamy, S. and M.G. Rossmann 1990). Structural refinement and analysis of Mengo virus. *Journal of Molecular Biology* **211**, 803-844.

Mak, T. W., J.S. Colter and D.G Scraba (1974). Structure of the Mengo virion. II. Physicochemical and electron microscopic analysis of degraded virus. *Virology* **57**, 543-553.

Mateu, M. G., M.A. Martinez, E. Rocha, D. Andreu, J. Parejo, E. Giralt, F. Sobrino and E. Domingo (1989). Implication of a quasispecies genome structure, effect of frequent, naturally-occurring amino acid substitutions on the antigenicity of foot-and-mouth disease virus. *Proceedings of the National Academy of Science (U.S.A.)* **86**, 5883-5887.

Minor, P. D., D.M. Evans, M. Ferguson, G.C. Schild, G. Westrop and J.W. Almond (1985). Principal and subsidiary antigenic sites of VP1 involved in the neutralization of poliovirus type 3. *Journal of General Virology* **66**, 1159-1165.

Minor, P. D., M. Ferguson, D.M.A. Evans, Almond and J.P. Icenogle (1986). Antigenic structure of polioviruses of serotypes 1, 2 and 3. *Journal of General Virology* **67**, 1283-1291.

Nitayaphan, S., M.M. Toth and R.P. Roos (1985). Neutralizing monoclonal antibodies to Theiler's murine encephalomyelitis viruses. *Journal of Virology* **53**, 651-657.

Nicholas, J. A., M.A. Mitchell, M.E. Levely, K.L. Rubino, J.H. Kinner, N.K. Harn and C.W. Smith (1988). Mapping an antibody-binding site and a T-cell-stimulating site on the 1A protein of respiratory syncytial virus. *Journal of Virology* **62**, 4465-4473.

Ohara, Y., A. Senkowski, J. Fu, L. Klaman, J. Goodall, M. Toth and R.P. Roos (1988). Trypsin-sensitive neutralization site on VP1 of Theiler's murine encephalomyelitis viruses. *Journal of Virology* **62**, 3527-3529.

Page, G. S., A.G. Mosser, J.M. Hogle, D.J. Filman, R.R. Rueckert and M.Chow (1988). Three-dimensional structure of poliovirus serotype 1 neutralizing determinants. *Journal of Virology* **62**, 1781-1794.

Palmenberg, A. C. (1989). Sequence alignments of picornaviral capsid proteins. *In* "Molecular Aspects of Picornavirus Infection and Detection" (B.L. Semler and E. Ehrenfeld, Eds.), pp. 211-241. American Society for Microbiology, Washington, D.C.

Parry, N. R., P.V. Barnett, E.J. Ouldridge, D.J. Rowlands and F. Brown (1989). Neutralizing epitopes of type O foot-and-mouth disease virus. II. Mapping three conformation sites with synthetic peptide reagents. *Journal of General Virology* **70**, 1493-1503.

Patel, V., M. Ferguson and P.D. Minor (1993). Antigenic sites on type 2 poliovirus. *Virology* **192**, 361-364.

Ping, L. and S. Lemon (1992). Antigenic structure of human hepatitis A virus defined by analysis of escape mutants selected against murine monoclonal antibodies. *Journal of Virology* **66**, 2208-2216.

Reynolds, C., G. Page, H. Zhou and M. Chow (1991). Identification of residues in VP2 that contribute to poliovirus neutralization antigenic site 3B. *Virology* **184**, 391-396.

Roivainen, M., A. Närvänen, M. Korkolainen, M. Huhtala and T. Hovi (1991). Antigenic regions of poliovirus type 3/Sabin capsid proteins recognized by human sera in the peptide scanning technique. *Virology* **180**, 99-107.

Roos, R. P. and N. Casteel (1992). Determinants of neurological disease induced by Theiler's murine encephalomyelitis virus. *In* Molecular Neurovirology (R.P. Roos, Ed.), pp. 283-318. Humana Press Inc., Totowa, N.J.

Rossmann, M. G., and Palmenberg, A. C. (1988). Conservation of the putative receptor attachment site in picornaviruses. *Virology* **164**, 373-382.

Rossmann, M. G., E. Arnold, J.W. Erickson, E.A. Frankenberger, J.P. Griffith, H.J. Hecht, J.E. Johnson, G. Kamer, M. Luo, A.G. Mosser, R.R. Rueckert, B. Sherry and G. Vriend (1985). Structure of a human common cold virus and functional relationship to other picornaviruses. *Nature* **317**, 145-153.

Rossmann, M. G. (1989). The canyon hypothesis. *Journal of Biological Chemistry* **264**, 14587-14590.

Rueckert, R. R. and E. Wimmer (1984). Systematic nomenclature of picornavirus proteins. *Journal of Virology* **50**, 957-959.

Saiz, J. C., M.J. Gonzalez, M.V. Borca, F. Sobrino and D.M. Moore (1991). Identification of neutralizing antigenic sites on VP1 and VP2 of type A5 foot-and-mouth disease virus, defined by neutralization-resistant variants. *Journal of Virology* **65**, 2518-2524.

Sanger, F., S. Nicklen and A.R. Coulson (1977). DNA sequencing with chain-terminating inhibitors. *Proceedings of the National Academy of Sciences (U.S.A.)* **74**, 5463-5467.

Sherry, B., A.G. Mosser, R.J. Colonno and R.R. Rueckert (1986). Use of monoclonal antibodies to identify four neutralization immunogens on a common cold picornavirus, human rhinovirus 14. *Journal of Virology* **57**, 246-257.

Skern, T., C. Neubauer, L. Frasel, P. Gründler, W. Sommergruber, M. Zorn, E. Kuechler and D. Blaas (1987). A neutralizing epitope on human rhinovirus type 2 includes residues between 153 and 164 of virus capsid protein VP2. *Journal of General Virology* **68**, 315-323.

Smyth, M. S., E.M. Hoey, A. Trudgett, S.J. Martin and F. Brown (1990). Chemically synthesized peptides elicit neutralizing antibody to bovine enterovirus. *Journal of General Virology* **71**, 231-234.

Speller, S. A., D.V. Sangar, B.E. Clarke and D.J. Rowlands (1993). The nature and spatial distribution of amino acid substitutions conferring resistance to neutralizing monoclonal antibodies in human rhinovirus type 2. *Journal of General Virology* **74**, 193-200.

Stave, J. W., J.L. Card, D.O. Morgan and V.N. Vakharia (1988). Neutralization sites of type 0 foot-and-mouth disease virus defined by monoclonal antibodies and neutralization-escape virus variants. *Virology* **162**, 21-29.

Thomas, A. A. M., R.J. Woortmeijer, W. Puijk and S.J. Barteling (1988). Antigenic sites on foot-and-mouth disease virus type A10. *Journal of Virology* **62**, 2782-2789.

Wiegers, K., H. Uhlig and R. Dernick (1989). N-AgIB of poliovirus type 1: a discontinuous epitope formed by two loops of VP1 containing residues 96-104 and 141-152. *Virology* **170**, 583-586.

Wiegers, K. J., K. Wetz and R. Dernick (1990). Molecular basis for linkage of a continuous and discontinuous neutralization epitope on the structural polypeptide VP2 of poliovirus type 1. *Journal of Virology* **64**, 1283-1289.

Wiley, D. C., I.A. Wilson and J.J. Skehel (1981). Structural identification of the antibody-binding sites of Hong Kong influenza haemagglutinin and their involvement in antigenic variation. *Nature* **289**, 373-378.

Wilson, I. A., J.J. Skehel and D.C. Wiley (1981). Structure of the haemagglutinin membrane glycoprotein of influenza virus at 3 Å resolution. *Nature* **289**, 366-373.

Xie, Q.-C., D. McCahon, J. R. Crowther, G.J. Belsham and K.C. McCullough (1987). Neutralization of foot-and-mouth disease virus can be mediated through any of at least three separate antigenic sites. *Journal of General Virology* **68**, 1637-1647.

Ziola, B. R. and D.G. Scraba (1974). Structure of the Mengo virion. I. Polypeptide and ribonucleate components of the virus particle. *Virology* **57**, 531-542.

CHAPTER III

FURTHER CHARACTERIZATION OF MENGO VIRUS NEUTRALIZATION EPITOPES

INTRODUCTION

Monoclonal antibodies generated against subviral pentameric particles (Chapter II) have proven useful in characterizing some of the capsid surface elements which constitute neutralization epitopes. With the development of an attenuated strain of Mengo virus (Duke *et al.*, 1990) having the same capsid structure as the wild-type virus, it became possible to examine the authentic antibody response of a natural host to a picornaviral infection. It was of interest to examine the epitopes which are recognized in response to immunization with the intact virus because there is a possibility that when whole virions were dissociated into pentamers for immunization conformational changes could have occurred which altered the antigenic characteristics of the capsid. The attenuated virus was derived from wild-type by cDNA cloning, and the attenuating alteration is a truncation of the poly(C) tract in the 5'-noncoding region of the viral RNA. Presumably this alteration adversely affects viral RNA replication *in vivo*, allowing the immune response of the infected mouse to control the spread of the virus.

The study of the B cell response to a live virus infection is also relevant because much of the work which has been done to characterize the epitopes of neutralizing monoclonal antibodies to other picornaviruses has been done in mice. Many of these picornaviruses, such as rhinovirus and poliovirus, do not replicate in mice. The immune response produced in mice may not be indicative of the protective response which the natural host must generate to protect itself from infection. In addition the B cell response generated in mice against rhinovirus or poliovirus may not be relevant to humans.

The fact that rodents, in particular mice, are the natural carriers of Mengo virus is particularly advantageous for the examination of the epitopes of neutralizing monoclonal antibodies since mice and rats are currently the only species for which suitable myeloma cells for the production of hybridomas of B cells through cell fusion are available. To continue our analysis of the neutralization epitopes of Mengo virus, five monoclonal hybridoma cell lines which secrete neutralizing anti-Mengo virus antibodies were generated from mice immunized with live attenuated Mengo virus. The epitopes on the Mengo virion recognized by four of the five antibodies were mapped by the selection and sequencing of neutralization resistant mutants. The epitope of the fifth neutralizing antibody was mapped indirectly using an antibody competition binding assay.

METHODS

Hybridoma Production for Anti-Mengo Virus Monoclonal Antibodies

Mice were immunized according to the following schedule. Each mouse was initially injected, by the intraperitoneal (IP) route, with 5×10^6 PFUs of attenuated Mengo virus #3 (the poly (C) tract in this virus is $C_{13}UC_{10}$; in the wild-type it is $C_{50}UC_{10}$) in 200 µl complete PBS. The initial seed stock of the attenuated virus #3 was generously provided by A.C. Palmenberg. After 30 days, sufficient time for the primary response to disappear, the mice were given an IP booster injection of 7.5 µg of wild-type Mengo virus or attenuated Mengo virus #3. Second and subsequent IP booster injections of 20 µg of wild-type or attenuated Mengo virus #3 were spaced at intervals of 30 days. Mice were selected for the fusion of isolated spleen cells to SP2/0 myeloma cells after the third or fourth booster injection. Two days after the final boost the serum antibody levels of each mouse were tested to ensure a sufficiently strong response to warrant proceeding with the fusion (positive ELISA response greater than 1:1000 dilution of the serum). Fusions were performed three days after the final booster injection.

At the time of final immunization a stock of SP2/0 cells was grown in RPMI 1640 (HyClone Laboratories) containing 10% FCS. The cells were required to be at least 95% viable, growing rapidly, and about 10^8 cells was required per fusion (*i.e.* per spleen). On the day of the fusion the required number of cells were resuspended in serum-free RPMI at a density of 10^7 cells/mL. The spleen was removed from the sacrificed mouse and the cells from the spleen were dissected into 5 mL of serum-free RPMI. The cells were suspended by drawing them through a 21G needle followed by a 25G needle (to break up cellular aggregates) and collected by centrifugation at 500xg (IEC Centra-7R centrifuge) for 5 minutes. The cell pellet was washed by resuspending it in 20 mL of serum-free RPMI and recentrifuging. This step was repeated twice. The spleen cells were counted using a hemacytometer (cell count was usually in the range of 8×10^7 to 1.2×10^8 cells). These cells were combined with SP2/0 cells at a ratio of 8:1 spleen:SP2/0 cells and pelleted together by centrifugation. The supernatant was removed and the cell pellet was loosened into a dense fluid suspension of cells by gently tapping the tube. At this point the cells were ready for fusion. First, 0.5 mL of PEG 3350 (Sigma #P-2906, 2.0 g PEG in 2.0 mL distilled water, autoclaved 15 min on liquid cycle) at 37° was added dropwise during a one minute interval with gentle agitation. Agitation was continued, just enough to keep cell suspension moving, for an additional 90 seconds, then 8.5 mL of serum-free RPMI (37°) was added dropwise, with continued gentle agitation, over a period of 5 to 8 minutes. The mixture was incubated at 37° in a water bath for at least 20 min, then an additional 10 mL of warm, serum-free RPMI was added slowly to the suspension. The hybridomas were centrifuged (500xg, IEC Centra-7R) for 5 min and gently resuspended in 45 mL of hybridoma medium. The cells were plated at 10^5 cells/well (100 µl/well) in 96 well tissue culture plates and incubated at 37°, 5% CO_2. In addition to the hybridoma medium, each well also contained 40 µl of SP2/0 conditioned medium to provide additional factors required by the hybridoma cells when growing at very low density.

The hybridoma medium used consisted of the following components:

310 mL RPMI 1640 (HyClone Laboratories Inc.)
0.8 mL Penicillin (200 units/mL)/Streptomycin (100 µg/mL) stock
150 mg L-glutamine (Sigma, #G-5763)
50 mL FCS-heat inactivated at 56° for 30 min (HyClone Laboratories Inc.)
10 mL 50X OPI media supplement (Sigma #O-5003)
2.5 g glucose (Sigma #G-7021)
50 mL NCTC-109 medium (Gibco #320-1340)
5 mL hypoxanthine-thymidine 100X stock (Gibco #320-1067)
2 mL aminopterin (1.8 mg/100mL) (Gibco #670-4010)
2 mL 24 mM 2-mercaptoethanol stock (Sigma #M-7522)

The cells were maintained by the replacement of the hybridoma medium, usually at weekly intervals (100-200 µl/well), although this varied depending on the density of fused cells. This was monitored daily by microscopic observation. Once the clones were large enough to see by the unaided eye (usually about 200 cells) they were considered to be ready for testing and cloning and were maintained with RPMI 1640 containing 10% FCS.

Plates were screened for anti-Mengo virus antibodies by standard direct ELISA and/or micro-neutralization assays.

Hybridoma cell line JEL 370 was generated in collaboration with Dr. J. S. Lee at the University of Saskatchewan.

Preparation of SP2/O Conditioned Medium

Hybridoma cells grown at very low density, such as during cloning or thawing of frozen aliquots of cells, required the addition of growth factors secreted by cells which are normally present in sufficient amounts when cells are cultured at moderate density. This can be accomplished by the addition of feeder cells, such as a spleen cell suspension, to the culture or by the use of media which has already been used to sustain a population of cells (conditioned medium). Conditioned medium was prepared by the culturing of SP2/0 cells in RPMI 1640 containing 10% FCS until the medium was nearly depleted of nutrients and the cells began to die. The medium was then collected, the cells and cell debris removed by centrifugation and the medium was filtered through a 0.22 µm filter unit (Millipore Sterifil D-GS). The medium was stored at 4°.

Cloning Cells Secreting Anti-Mengo Virus Antibodies

Positive hybridomas were cloned as soon as they were identified to avoid overgrowth by nonproducing cells. Positives were routinely expanded by growing in 25 cm^2 tissue culture flasks and were frozen in two aliquots to insure against loss of the hybridoma.

For cloning, 3 to 5 96-well tissue culture plates (Costar) were seeded with 0.05 cells/well in 100 µl RPMI 1640 containing 10% FCS and supplemented with 30 µl/well of conditioned RPMI. This was done to ensure that most wells of the plate would not contain a cell and no well should receive more than one cell (care was taken to ensure that cells were completely suspended and not clumped). Plates were fed with RPMI containing 10% FCS after about one week of growth. It was necessary to check the wells prior to addition of medium by microscopy for individual clones because once medium was added the cells become dispersed in the well and it is not possible to distinguish single from multiple clones. Plates were usually ready to be tested by ELISA or micro-neutralization assay after two to three weeks. All monoclonal cell lines selected after one cycle of cloning were recloned at least once to ensure they were monoclonal.

Freezing and Thawing Aliquots of Hybridoma Cells

In preparation for freezing, the cells were fed with fresh RPMI containing 10% FCS so that they were healthy and dividing rapidly. The cells were counted and then pelleted by centrifugation at 500xg (IEC Centra-7R) for 5 min at 4°. The cell pellet was gently resuspended in a mixture of sterile 8% DMSO (BDH Chemicals) and 92% FCS at 4° so that the final concentration of cells was between 5×10^6 and 5×10^7 cells/mL. The cell suspension was aliquoted into cryotubes (1 mL/aliquot; Nunc Cryotubes #377267), placed in an insulated box and slowly cooled to -70°. For long term storage the aliquots were transferred to liquid nitrogen after about one week at -70°.

To thaw an aliquot of cells, it was removed from -70° freezer or liquid nitrogen storage and thawed quickly with gentle agitation in a 37° water bath. To dilute the

DMSO, the aliquot was pipetted into 5 mL of serum-free RPMI at 37° and then centrifuged at 500xg for 5 minutes. The cell pellet was gently resuspended in warm RPMI containing 10% FCS and transferred to a 25 cm^2 tissue culture flask. Freshly thawed aliquots of cells were cultured in 20 mL RPMI 1640 containing 10% FCS and supplemented with approximately 30% SP2/0 conditioned medium.

Enzyme-Linked Immunosorbant Assays (ELISA)

A. Direct ELISA

This procedure was used to examine the ability of an antibody to bind to Mengo virus which had been adsorbed to a solid substrate. High protein affinity polystyrene ELISA plates were used (Immulon 2,"U" plates, Dynatech Laboratories, Inc.; supplied by Fisher). Each well of the plate was coated with Mengo virus at 3 µg/ml, 100 µl/well overnight at 4° in either complete PBS (nondenaturing) or ELISA-coating buffer (13.5 mM Na_2CO_3, 34.9 mM $NaHCO_3$, pH 9.6 - partially denaturing). Plates were washed twice with PBS-Tween (0.5 ml Tween 20/1L PBS). To prevent non-specific binding of reagents, each well was coated with 200 µl of 1% BSA (Sigma, fraction V, #A-4503) in PBS for one hour at 20° and the plates were again washed twice. 100 µl of either undiluted hybridoma supernatant or ascites fluid diluted in PBS-Tween was added to each well. This step may be repeated to increase the amount of bound antibody in the wells if the concentration in the source was low. Plates were incubated for 2 hr at 20° and then washed twice. A second antibody to detect antibody bound to the antigen was added next: this was goat anti-mouse IgA-, IgG- or IgM-specific antibody conjugated to alkaline phosphatase (Cedarlane Laboratories, Hornby, Ontario). Each well was incubated for 1.5 hr with a 1:1500 dilution (100 µl/well) of the conjugated antibody in PBS-Tween. Plates were washed five times to ensure the removal of any unbound alkaline phosphatase-conjugated antibody. 100 µl of substrate (one tablet of p-nitrophenyl phosphate [Sigma #104-105] in 5 ml 10% diethanolamine, pH 9.8) was added per well. Positive results were indicated by the development of yellow color which was quantitated at 410 nm with ELISA plate reader (MR600 Micro Plate Reader, Dynatech Laboratories Inc.).

B. Direct Peptide ELISA

This was a modification of the standard direct ELISA used to detect anti-Mengo virus antibodies. Wells were coated with selected peptides (2.0 µg/ml, 100 µl/well) in ELISA-coating buffer and then incubated overnight at 20°. Appendix B contains a complete list of all the peptides covering the capsid proteins. The ability of antibodies to bind to the peptides was tested as described in the procedure for standard direct ELISA.

C. Peptide Competition ELISA

This assay was used to measure the ability of a peptide, which contains at least part of the epitope of a monoclonal antibody, to compete for recognition by the antibody with its epitope on the native antigen. Using the standard direct ELISA with Mengo virus as antigen, the dilution of monoclonal antibody required to give 75% of the maximum absorbance was determined; this antibody dilution was incubated with 200 nmol/ml peptide at for 2 hr at 20°. The monoclonal antibody-peptide mixtures were then tested using the standard ELISA protocol on plates coated with Mengo virus to determine which peptides inhibit the binding of the monoclonal antibody to virus.

D. Determination of Monoclonal Antibody Isotype

ELISA plate wells were coated with Mengo virus as in the direct ELISA. The sequence of steps was the same as in the direct assay with the usual requirement of washes with PBS-Tween (2-5X) between each step. Each monoclonal hybridoma supernatant to be tested was screened with rabbit anti-mouse anti-sera specific to mouse IgG_1, IgG_{2a}, IgG_{2b}, IgG_3, IgM or IgA as well as with antisera to the κ or λ light chains of mouse antibodies (Biorad #172-2055). The rabbit antibodies were then detected with a goat anti-rabbit IgG conjugated to horseradish peroxidase (Biorad #170-6513). The presence of bound conjugated antibody was detected by the addition of a freshly prepared solution of equal parts of 2,2'-azino-di(3-ethyl-benzthiazoline sulfonate) and hydrogen peroxide (Biorad #172-1064), 100 µl/well. Positive results were indicated by the development of blue color. The reaction could be stopped by the addition of 100 µl/well 2% oxalic acid. Results were quantitated by measuring the absorbance at 414 nm.

E. Antibody Competition ELISA

This assay was used to examine whether the binding of one antibody to Mengo virus could block the binding of a second antibody. The results obtained can be used to infer an approximate site of binding of an antibody for which there is no other information available about its epitope. The procedure used was a modification of the one used to determine the isotype of each antibody. Competitor antibody was first bound to Mengo virus, then the binding of the second antibody was determined using the isotype specific panel of antisera described for the isotyping of antibodies. It is not possible to do the assays using two antibodies of the same isotype since in this case the binding of one antibody cannot be distinguished from the binding of the other. In all cases hybridoma supernatants or dilutions of supernatant in PBS-Tween were used.

Micro-Neutralization Assays

Micro-neutralization assays were used to screen supernatants from hybridoma cell lines for the presence of neutralizing anti-Mengo virus antibodies. The procedure used was identical to that outlined in Chapter II, page 35 for cross-neutralization assays with wild-type Mengo virus used as the antigen.

Western Blots

Mengo virus capsid proteins were separated on a 1 mm thick, 7.5% polyacrylamide Laemmli gel (Laemmli, 1990). Generally 10-20 µl virus stock were used per lane (virus stock contained approximately 500 µg/ml). The proteins were transferred to nitrocellulose by wet electrophoretic transfer. One sheet of nitrocellulose (Biorad #162-0115) was cut to cover the entire gel. The nitrocellulose was carefully placed on top of a 5% methanol solution and allowed to wet by capillary action. The nitrocellulose was then soaked in transfer buffer (10 mM CAPS [3-(cyclohexylamino)-1-propanesulfonic acid], 10% methanol, pH 11.0). The Biorad Trans-Blot cell was used for the electrophoretic transfer according to the instructions provided. Transfers were done overnight (15-18 hr) at 60V and a temperature of 4°. Transfer was checked by staining the blot with 0.1% coomassie brilliant blue in 50% methanol and destaining with 50% methanol, 10% acetic acid. The blot was washed several times with PBS, then it was blocked to avoid non-specific binding of reagents with 3% BSA in PBS for 2 hr at 20° with agitation. The blot was washed twice for 5 min in PBS and monoclonal antibody in hybridoma supernatant was added. To test multiple monoclonal antibodies the blot was cut into strips and each strip was incubated separately with hybridoma supernatant in a test tube for at least 2 hr. The blot was then washed four times in PBS. To detect bound antibody, a 1:1500 dilution of goat anti-mouse IgG, IgA or IgM alkaline phosphatase-conjugated antibody in blocking buffer was incubated with the blot strips for one hour at 20°. The blot was washed with four changes of 150 mM NaCl, 50 mM Tris (pH 7.5). The final step was the detection of the bound alkaline phosphatase conjugated antibodies using bromochloroindolyl phosphate/nitroblue tetrazolium (BCIP/NBT), which forms a purple precipitate in the presence of alkaline phosphatase. The substrate solution used was 66µl NBT stock (5% NBT in 70% dimethylformamide) plus 33µl BCIP stock (5% BCIP in 100% dimethylformamide) in 10 ml alkaline phosphatase buffer (100 mM NaCl, 5 mM $MgCl_2$, 100 mM Tris, pH 9.5). The blot was developed until the bands appear and the reaction was stopped by replacing the substrate with PBS containing 20 mM EDTA.

Selection of Mutant Mengo Virions Which Escape Neutralization

The procedure used for the selection of mutants with antibodies JEL 370, 9B and 352 has been described in Chapter II, page 33. Mutants which escape neutralization by antibody 3A were selected, using the same procedure outlined in Chapter II, from a stock of mutant virus designated 4/12 which had been selected using the anti-pentamer monoclonal antibody MCP4 (see Chapter II).

Attempts were made to select mutants which escape neutralization by antibody 6A from stocks of wild-type Mengo virus, all mutants which had been selected with the other monoclonal antibodies, and encephalomyocarditis virus (EMCV). Again the same procedure was used as outlined in Chapter 1. The EMCV clone (obtained from Dr. A. C. Palmenberg, University of Wisconsin) was termed $_vEC_4$ and contained a truncated poly (C) tract of C_4 (wild type is $C_{115}UCUC_3UC_{10}$). $_vEC_4$ has the identical capsid structure to that of wild-type EMCV, and has 97% identity with that of Mengo virus.

Preparation of Mutant Mengo Virus for RNA Extraction

The procedure has been described in Chapter II, page 33 (*Mutant selection).*

RNA Isolation

The procedure has been described in Chapter II, page 33.

RNA Sequence Determination

The procedure has been described in Chapter II, page 34.

Cross Neutralization Assays

The procedure has been described in Chapter II, page 35. It was necessary to concentrate the antibody in tissue culture hybridoma supernatants from monoclonal cell lines MCP1 and 9B to provide a sufficiently high concentration of antibody for efficient neutralization of virus. Supernatants were concentrated in sterile Centriprep 30 concentrators (Amicon) at 2000xg according to the provided instructions.

Ribbon Diagrams

The ribbon diagrams of Mengo capsid proteins VP1, VP2 and VP3 used in this chapter were generated from the crystallographic coordinates for the virus (Brookhaven Protein Data Bank) using the graphics program MOLSCRIPT (Kraulis, 1991).

RESULTS

Over 100 hybridoma cell lines producing anti-Mengo virus antibodies were generated in 13 separate fusions with spleen cells from mice which had been immunized with live attenuated Mengo virus and boosted at least twice with either live attenuated or wild-type Mengo virus. All of these cell lines were initially identified using direct ELISA to screen for the presence of virus-specific secreted antibody . The supernatants containing anti-Mengo virus antibodies were then screened in micro-neutralization assays to identify which antibody producing cell lines secreted antibodies capable of neutralizing Mengo virus. Only five were found to produce antibodies which neutralized Mengo virus. These cell lines were cloned and the antibody type produced by each was determined by an ELISA typing assay. Table III-1 lists the monoclonal cell lines and the antibody type which each produced. Most of these cell lines, as well as most of the cell lines which produced non neutralizing anti-Mengo virus antibodies, produced IgM antibodies. Cell line 6A produces antibody of type IgG_{2a} while 3A secretes the relatively rare antibody type IgA.

It is difficult to understand the lack of success experienced in isolating cell lines which produced neutralizing antibodies, particularly considering that the polyclonal serum taken from each mouse prior to the fusions had a high level of virus-neutralizing activity and that the mice were protected from exposure to the large amounts of virus administered in booster injections. In the last three fusions 242 cell lines which secreted anti-Mengo virus antibodies were detected using ELISA. Of these only one, designated monoclonal cell line 352, continuously produced usable quantities of neutralizing antibodies. Because of the poor success at selecting cell lines which secreted neutralizing antibodies from cell lines which were initially identified by ELISA, the cell lines produced in the last three fusions were also screened by micro-neutralization assay. A total of 269 cell lines were identified which secreted antibody capable of neutralizing Mengo virus. Interestingly, with the exception of cell line 352, most of these cell lines produced neutralizing antibodies which were not detectable using a direct ELISA. Unfortunately most of the antibody producing cell lines identified by either procedure

TABLE III-1

Monoclonal Hybridoma Cell Lines
Generated Against Live Attenuated Mengo Virus

Cell line	Antibody type
JEL 370	IgM
3A	IgA
6A	IgG_{2a}
9B	IgM
352	IgM

stopped producing antibody in usable quantity within three weeks, as indicated by the loss of ELISA or neutralization activity. Although these fusions did not yield the number of cell lines which produced neutralizing antibodies that was hoped for they did provide the interesting observation that a very large proportion of the cell lines producing neutralizing antibodies secrete antibodies which cannot be detected in direct ELISA assays.

Selection of Mengo virus mutants which escaped neutralization by each of monoclonal antibodies was attempted. Mixtures of hybridoma supernatant and virus were plated onto confluent monolayers of mouse fibroblast cells, and plaques which grew in the presence of the antibody were selected. Mutant selection with monoclonal antibody from cell lines JEL 370, 9B and 352 was straightforward and several mutants were selected with each. All mutants were picked and replaqued at least twice in the presence of selecting antibody to ensure that they were true neutralization-escape mutants. In the course of these experiments it was observed that many of the mutant viruses grew considerably slower in the presence of antibody than in control wells which did not contain antibody indicating some interaction between the antibody and some of the mutants. Large quantities of each mutant were produced in roller bottles of mouse fibroblast cells and the RNA genome of each was isolated for sequencing of the capsid coding region.

No neutralization escape mutants could be isolated from wild-type Mengo virus in the presence of monoclonal antibodies from cell lines 6A or 3A despite repeated attempts using different concentrations of antibody and virus. Repeated cloning of both cell lines ensured that both were monoclonal and that neither cell line was contaminated with a second cell line producing antibodies capable of neutralizing Mengo virus. This conclusion is supported by the antibody typing experiments which indicated that 3A produces IgA and it is extremely unlikely that this clone contains another cell line also producing neutralizing IgA antibodies. The same can be said of cell line 6A which produces IgG_{2a}. Based on the results of cross-neutralization assays (discussed later) it was observed that mutants selected with monoclonal antibody MCP4, as well as mutant 6/16 selected with MCP6 (see Chapter II), demonstrated a very limited ability to grow in the presence of antibody 3A. Four mutants capable of escaping neutralization by antibody 3A were selected from the stock of mutant virus 4/12. Unlike the original mutant virus 4/12, these mutants grew as well in the presence or absence of a 1:5 dilution of 3A hybridoma supernatant, even though this dilution of the antibody is capable of neutralizing 100% of wild type Mengo virus (see Figure III-1). The neutralization escape

Figure III-1. Plaque assay of 3A mutants. Each mutant selected with antibody 3A and 10^5 PFU/mL wild-type Mengo virus was plated with and without a 1:5 dilution of 3A hybridoma supernatant. Wells containing wild-type virus are shown one day after plating; 3A mutants are shown five days after plating.

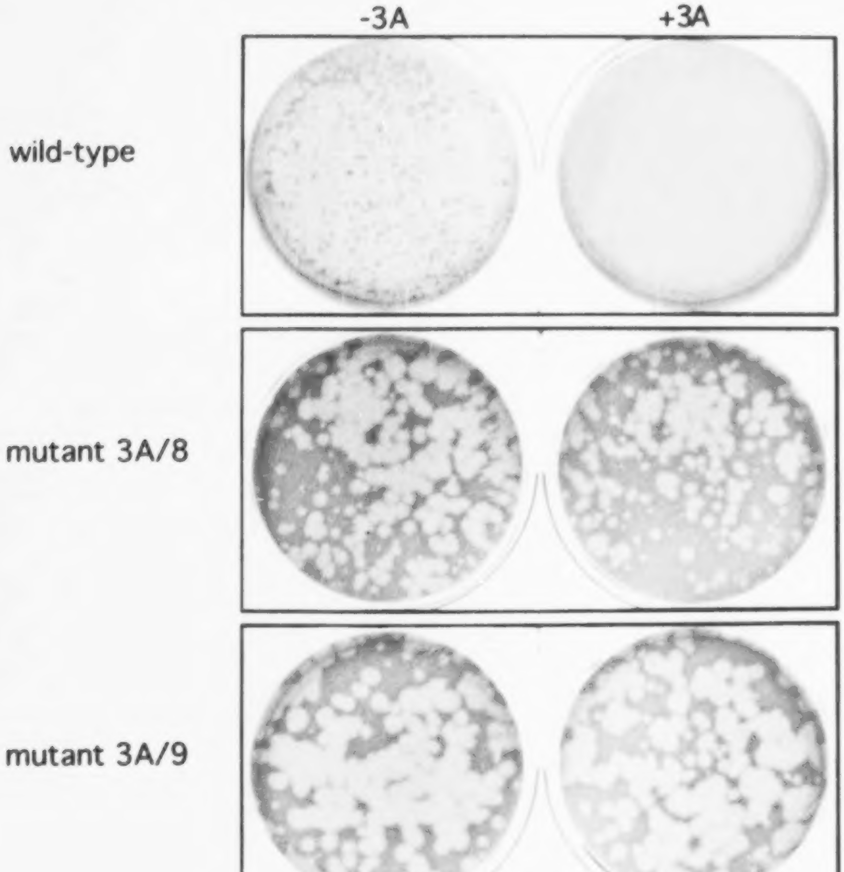
-3A
+3A
wild-type
mutant 3A/8
mutant 3A/9
mutant 3A/10
mutant 3A/11

mutants selected from 4/12 virus with antibody 3A grew at least 50% slower than wild type virus in plaque assays. Attempts to culture sufficient mutant virus to isolate enough RNA for sequencing was not successful because none of the mutants efficiently infected monolayers of L-cells: even four days post infection there was no cell lysis.

In cross-neutralization assays none of the mutants selected with any of the other monoclonal antibodies were capable of even limited growth in the presence of antibody 6A so it was necessary to attempt other procedures to map the epitope recognized by antibody 6A (discussed later).

The RNA genomes of mutants which escaped neutralization were sequenced directly using 12 different synthetic oligonucleotide primers designed to cover the region of the genome coding for capsid proteins VP1, VP2 and VP3. This region was completely sequenced for all the mutants selected with monoclonal antibodies JEL 370, 9B and 352. To do this ^{32}P end labeled primers were annealed to the RNA and extended, in reaction mixtures containing a mixture of deoxy nucleotides and one per reaction mix of each of the dideoxy nucleotides ddATP, ddCTP, ddGTP or ddTTP, using AMV reverse transcriptase. In some cases it was necessary to incubate the extension reactions at 56° rather than 50° to eliminate nonspecific termination of cDNA synthesis caused by secondary structures in the RNA. Table III-2 indicates the location of the nucleotide mutation(s) found for each mutant and the resulting amino acid changes in the capsid proteins. The mutants selected with JEL 370, designated 370/1-L, 2-L, 5, and 8-L, all have a mutation at residue 1100 in VP1. The 9B mutants (9B/2, 3, 4, 9) all have a mutation resulting in a change in either residue 1049 or 1062 in VP1, and mutant 9B/4 has an additional mutation at residue 2016 in VP2. The mutants selected with antibody 352 (352/1, 5, 6, 7) have mutations at residues 3073, 3074 or 3075 of VP3, or in residue 2144 in VP2. Mutant 352/1 has an additional mutation at residue 1049 in VP1. The amino acid change(s) in the 3A mutants remains unidentified, although at least part of the binding site of the IgA antibody must lie in the regions of residue 2148 of VP2 since this is the site of the mutation in mutant virus 4/12 from which the 3A mutants were selected.

Cross neutralization assays (Table III-3) were used to examine the ability of mutants selected with each of the monoclonal antibodies to escape neutralization by the other available monoclonal antibodies; these assays included the mutants and antibodies described in Chapter II. Although no neutralization-escape mutants could be selected with antibody 6A, this antibody was tested for its ability to neutralize the mutants selected with the antibodies.

TABLE III-2

Changes in Nucleotide Sequence and Amino Acid Sequence of Mengo Virus Escape Mutants

Mutant virus	Nucleotide change[a]	Amino acid change[b]
370S/1-L	2928 A→G	1100 Thr→Ala
370S/2	2929 C→U	1100 Thr→Ile
370S/5-L	2929 C→U	1100 Thr→Ile
370S/8-L	2929 C→U	1100 Thr→Ile
9B/2	2814 A→G	1062 Asn→Asp
9B/3	2775 A→C	1049 Lys→Gln
9B/4	1217 A→C	2016 Gln→His
	2814 A→C	1062 Asn→His
9B/9	2814 A→G	1062 Asn→Asp
352/1	2775 A→C	1049 Lys→Gln
	2154 A→C	3073 Lys→Gln
352/5	2160 C→G	3075 Gln→Glu
352/6	2158 C→U	3074 Thr→Ile
352/7	1600 A→G	2144 Asn→Ser

[a] The nucleotide numbers refer to the position in the Mengo virus genome, beginning with nucleotide 1 at the 5'-end [the complete poly (C) tract is included].

[b] The amino acid residues are identified according to the "Rossmann system", with the first digit representing viral capsid protein 1, 2 or 3, and the next three digits indicating position from the N-terminal.

TABLE III-3

CROSS NEUTRALIZATION DATA[a]

	Monoclonal Antibody								
Virus Mutant	MCP1	MCP4	MCP5	MCP6	JEL 370	3A	6A	9B	352
1/01	□	■	■	■	■	■	■	□	■
1/02	□	■	■	■	■	■	■	■	■
1/03	□	■	■	■	■	■	■	■	■
1/04	□	■	■	■	■	■	■	■	■
1/06	□	■	■	■	■	■	■	■	■
1/11	□	■	■	■	■	■	■	■	■
4/01	■	□	■	□	■	▨	■	■	■
4/02	■	□	■	□	■	▨	■	■	■
4/04	■	□	■	□	■	▨	■	■	■
4/08	■	□	■	□	■	▨	■	■	■
4/09	■	□	■	□	■	▨	■	■	■
4/12	■	□	■	□	■	▨	■	■	■
5/01-S	■	□	□	□	■	■	■	■	■
5/01-M	■	□	□	□	■	■	■	■	■
5/01-L	■	□	□	□	■	■	■	□	■
5/04	■	■	□	■	■	■	■	■	■
5/11-S	■	■	□	■	■	■	■	■	■
5/11-L	■	■	□	■	■	■	■	□	■
6/16	■	□	■	□	■	▨	■	■	■
6/18	■	■	■	□	■	■	■	■	■
370/1-L	■	■	■	■	□	■	■	■	■
370/2	■	■	■	■	□	■	■	■	■
370/5-L	■	■	■	■	□	■	■	■	■
370/8-L	■	■	■	■	□	■	■	■	■
3A/8	■	□	□	□	■	□	■	■	■
3A/9	■	□	□	□	■	□	■	■	■
3A/10	■	□	□	□	■	□	■	■	■
3A/11	■	□	□	□	■	□	■	■	■
9B/2	■	■	■	■	■	■	■	□	■
9B/3	■	■	■	■	■	■	■	□	■
9B/4	■	■	■	■	■	■	■	□	■
9B/9	■	■	■	■	■	■	■	□	■
352/1	■	■	■	■	■	■	■	■	□
352/5	■	■	■	■	■	■	■	■	□
352/6	■	■	■	■	■	■	■	■	□
352/7	■	■	■	■	■	■	■	■	□

[a] The pattern of cross neutralization with escape mutants of Mengo virus and the anti-Mengo antibodies is shown. □ - indicates mutants which escape neutralization; ■ - indicates neutralization of the mutant; ▨ - indicates mutants which partially escape neutralization.

In addition to neutralizing the mutants selected with the other anti-pentamer antibodies (Chapter II), antibody MCP1 is capable of neutralizing all the mutants selected with antibodies JEL 370, 3A, 9B and 352. Antibody MCP4 therefore neutralizes all mutant viruses except 5/01-S, 5/01-M, 5/01-L, 6/16 and the mutants selected with antibody 3A. MCP5 neutralizes all mutants except those selected with antibody 3A. MCP6 does not neutralize the mutants selected with antibodies MCP4 and 3A nor mutants 5/01-S, 5/01-M and 5/01-L.

Antibody JEL 370 neutralized all the mutants selected with the other antibodies and none of the mutants selected JEL 370 were neutralized by any other antibody. Similarly antibody 9B neutralized all the mutants selected with other antibodies with the exception of mutants 1/01, 5/01-L and 5/11-L which have second site mutations in the epitope of 9B at residues 1049 and 1062 of VP1. Antibody 352 also neutralized all the mutants selected with the other antibodies.

Antibody 3A completely neutralized all the mutants selected with all antibodies except the MCP4 mutants and mutant 6/16. The observed escape from neutralization of these mutants was limited, *i.e.* they grew very slowly.

The three major capsid proteins of Mengo virus (VP1-VP3) were separated by gel electrophoresis and blotted onto a PVDF membrane by wet electrophoretic transfer. The blot was then cut into strips and each strip was probed separately with hybridoma supernatants from monoclonal antibodies JEL 370, 3A, 6A, 9B and 352 to determine if any were capable of recognizing any capsid protein in a denatured state (Figure III-2). Only antibody 6A is capable of binding to any of the denatured capsid proteins and it interacts specifically with VP2.

The ability of antibody 6A to recognize VP2 in western blots suggested that it could recognize a linear antigenic determinant and that it might be possible to map the epitope of 6A using a panel of overlapping peptides representing VP2. The peptide panel was the same as that used in the T-cell assays and will be discussed in more detail in Chapter IV. The synthetic peptides were 10-18 residues in length, overlapping in sequence five residues at either end, and covered the entire sequence of VP2. Two approaches were used for peptide mapping of the 6A epitope.

In the first approach, individual VP2 peptides were adsorbed to ELISA plates. Antibody 6A was then tested for its ability to bind to each of the immobilized peptides. 6A antibody did not recognize any of the VP2 peptides. In this assay the peptides were

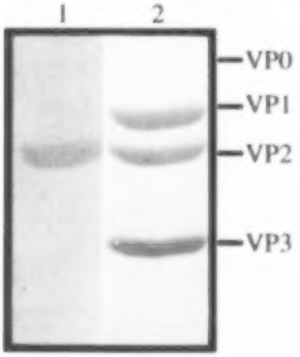

Figure III-2. Western blot analysis of antibody 6A from tissue culture hybridoma supernatant (lane 1). Lane 2 contains the major capsid proteins also blotted onto nitrocellulose and stained for protein content.

conformationally constrained by being bound to a solid support; this could have precluded recognition by antibody 6A. Therefore, an assay was set up to test the interaction between the VP2 peptides and antibody 6A in solution. Antibody 6A was incubated separately with each peptide, then the peptide-antibody mixtures were assayed by standard ELISA for the ability of any one of the peptides to inhibit the binding of the antibody to immobilized Mengo virus. None of the peptides inhibited the binding of antibody 6A to the virus.

The final approach used to try to obtain some information about the region of the capsid to which antibody 6A binds involved examining the ability of each of the other monoclonal antibodies to inhibit the binding of antibody 6A to Mengo virus. Only antibodies 3A and MCP4 were able to inhibit binding of antibody 6A (Figure III-3), indicating that there may be overlap between the epitopes of these three antibodies. It was already known that the epitopes of 3A and MCP4 must overlap because the 3A mutants were selected from a mutant selected with MCP4. These data would tentatively place the epitope of antibody 6A primarily within VP2 and probably including residues 2075 and 2144-2148, although this requires confirmation.

The antibodies generated against live attenuated Mengo virus bind to three distinct sites on the capsid of Mengo virus. One of these sites overlaps antigenic Sites 1 and 2 characterized with the antipentamer antibodies described in Chapter II, while the other two sites have not been previously characterized and define two new antigenic determinants, Sites 3 and 4. The third site is defined by the epitope recognized by antibody JEL 370 and the fourth is recognized by antibody 9B. Thus, combined with the results presented in Chapter II, we can now define four separate antigenic determinants on the surface of the Mengo virion. Site 1 includes residue 2075 in the βB-βC loop of VP2, and residues 2144, 2145, 2147 and 2148 in the βE-αB loop of VP2. Site 2 includes residues 3057 and 3061 in βB_1-βB_2 loop ("knob") of VP3; and 3068, 3073, 3074 and 3075 in the βB_2-βC loop of VP3. Site 3 includes residue 1100 in Loop II between the βC strand and αA helix of VP1. Site 4 contains residues 1049 and 1062 located in the βB-βC loop of VP1. All of these residues are exposed on the surface of the virion and, as expected, none are in or very close to the "pit" region, the predicted receptor binding site (Luo *et al.*, 1987).

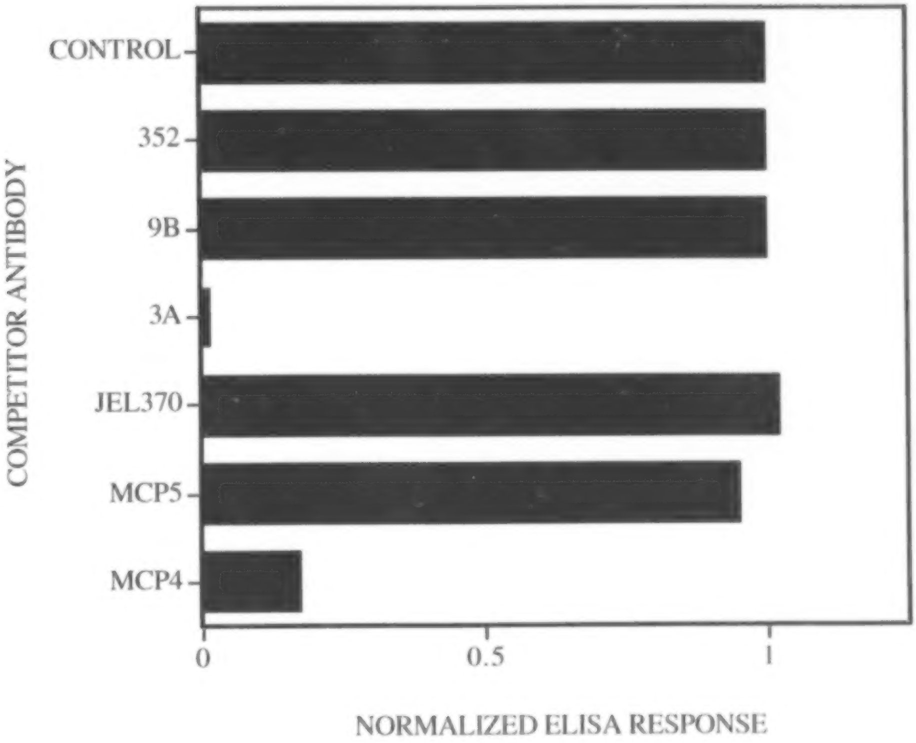

Figure III-3. Antibody competition analysis. The ability of antibody 6A to bind to virions previously saturated with monoclonal antibodies MCP4, MCP5, JEL 370, 9B and 352 is shown. All results were normalized to control response with antibody 6A.

DISCUSSION

The procedure for immortalization of normal antibody-forming plasma cells by their fusion to plasmacytoma cells developed by Kohler and Milstein (1975) has been used routinely for the generation of cell lines producing high affinity antibodies, generally of isotype IgG. Based on knowledge of the maturation of the immune response of an animal to an antigen a typical immunization protocol would involve initial immunization and a series of booster injections to ensure the development of mature antibody producing cells for *in vitro* fusions (Harlow and Lane, 1988). The primary antibody response to antigen in mice is mostly IgM and peaks at about 7-10 days post-immunization. If no further antigen is presented to the immune system the response declines as the plasma cells die; however the memory helper T and B cells remain and are available for rapid response to the re-introduction of antigen. This secondary response from the memory cells is characterized by the presence of larger amounts of higher affinity IgG, rather than IgM antibodies (Coffman *et al.*, 1993). The immunization protocol used in this study allowed one month between the initial injection and all subsequent challenges with Mengo virus. Despite this schedule, most of the hybridoma cell lines generated from mice immunized with live attenuated virus were IgM producers. The most probable explanation for this result is that the plasma B cells producing antibodies in response to Mengo virus were not completely removed from circulation after one month, perhaps as a result of a low level persistent infection, so that the subsequent injections restimulated the production of IgM antibodies from circulating plasma cells rather than stimulating the production of IgG antibodies from memory B cells.

Another interesting feature of the *in vivo* antibody response to Mengo virus is that the majority of antibody producing cell lines which were selected from the fusions by ELISA recognized but did not neutralize the virus. The presence of a large number of cell lines producing non-neutralizing antibodies suggests a role for antibodies in controlling a virus infection in addition to the neutralization of virus. It is known that the binding of antibody to antigen promotes opsonization, or the ingestion of antigen by phagocytes as a means of clearing circulating antigen. This has been demonstrated for FMDV with monoclonal antibodies under non-neutralizing conditions (McCullough *et al.*, 1988), and is likely to occur with Mengo virus.

Because experience had shown that a very large number of cell lines producing anti-Mengo virus antibodies must be screened to find a small number producing neutralizing antibodies, screening the final three fusions of hybridoma cell by neutralization assay was attempted. It was found that these fusions did generate a large number of cell lines which produce neutralizing antibodies, but most of these antibodies did not recognize Mengo virus in a standard ELISA assay. This suggests that many hybridoma cell lines produce antibodies capable of binding to and neutralizing Mengo virus free in solution, but that these antibodies do not recognize virions bound to a solid support. A similar finding has been reported for a number of protein antigens, including viruses (Ouldridge *et al.*, 1984; Wang *et al.*, 1992; Schwab and Bosshard, 1992). The recognition specificity of an antibody for an antigen can be dramatically altered or even destroyed by small conformational changes induced in the antigen when it is bound and flattens slightly against the solid support in an ELISA. In retrospect, our results suggest that it would have been much more efficient to select cell lines directly by neutralization assay.

To identify the sites on the capsid which are recognized by the various monoclonal antibodies, the capsid coding region of neutralization-resistant mutants was sequenced. While this approach was not successful with antibody 6A and only partially successful with antibody 3A, it did provide useful information concerning the identity of the epitopes recognized by the other antibodies. The mutants selected with antibody JEL 370 all have amino acid changes at residue 1100 of VP1 which is located in a prominent and exposed loop of the capsid protein (Figure III-4). JEL 370 appears to bind to a unique site on the virion based on the unique pattern of cross-neutralization observed with and the mutants selected with this antibody (Table III-3): a mutation at residue 1100 of VP1 does not confer neutralization resistance to any of the other antibodies, and none of the other mutants selected with the other monoclonal antibodies are capable of escaping neutralization by JEL 370.

The epitope recognized by antibody 9B would be predicted to also be unique based on the physical separation between the mutations found in neutralization resistant mutants selected with antibody 9B at residues 1049 and 1062 in a surface loop of VP1 and the sites of binding determined for the other antibodies (Figures III-4 and 5). JEL 370 is the only antibody which might be able to overlap the binding site of antibody 9B, but the cross-neutralization data indicate that the 9B epitope is independent. Interestingly, the two residues identified in the 9B mutants are residues which have been associated with second-site mutations in mutants 1/01, 5/01-L and 5/11-L (Chapter II,

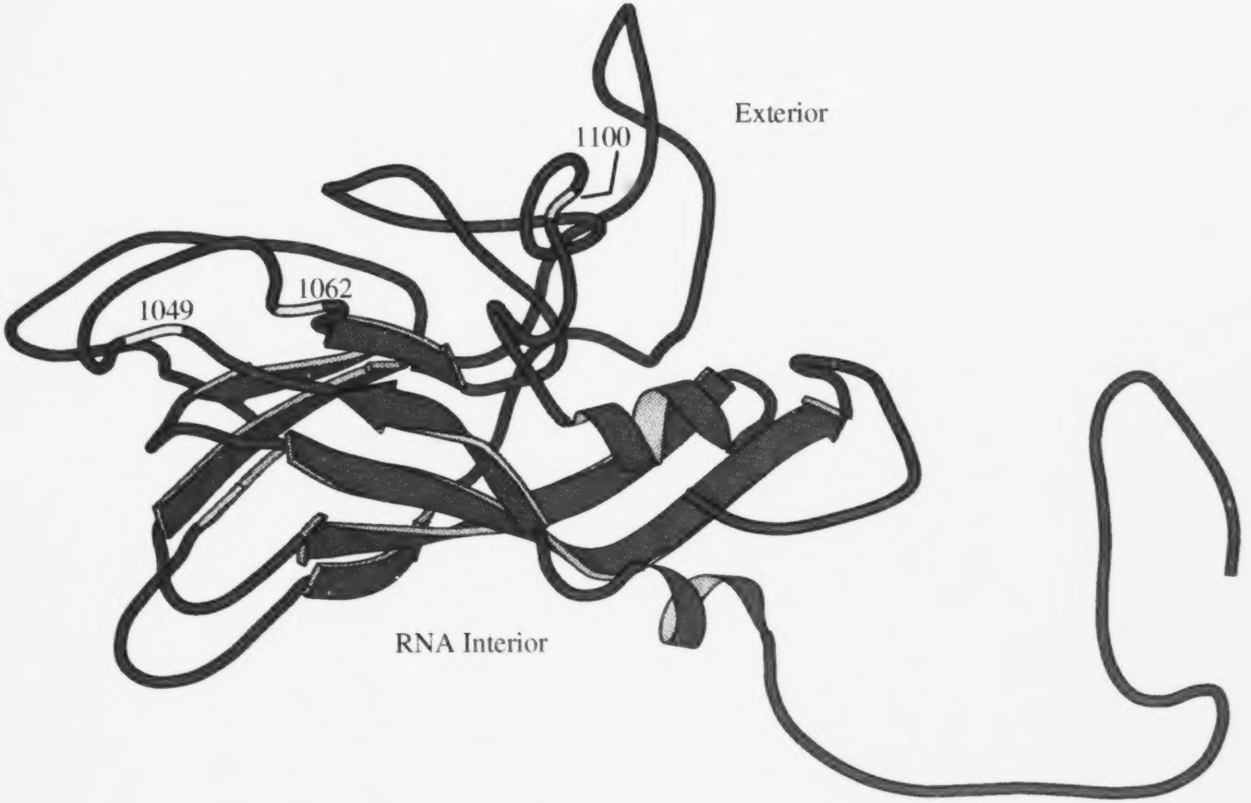

Figure III-4. Ribbon diagram representation of Mengo capsid protein VP1. Indicated are the positions of amino acid changes in neutralization escape mutants selected with antibodies JEL 370 and 9B.

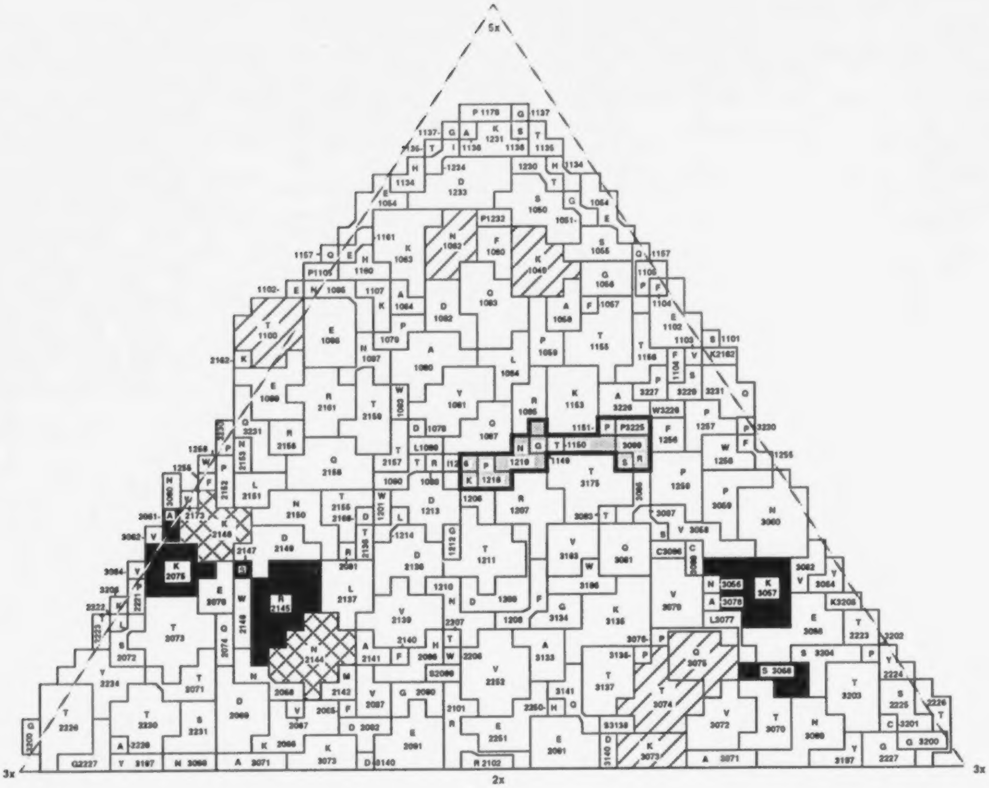

Figure III-5. Surface map of one crystallographic asymmetric unit of the Mengo virus capsid (revised from Chapter II, Figure II-5). The icosahedral 5-, 3- and 2-fold symmetry axes are marked. The pit area is shaded in grey. Mutations resulting in neutralization escape previously identified in mutants selected with anti-pentamer antibodies are shaded in black (Chapter II). Mutations identified in neutralization resistant mutants selected with anti-attenuated virus antibodies are indicated with diagonal hatching. Residues 2144 and 2148, common to both sets of mutants are indicated by cross-hatching.

page 43) and mutant 352/1 (Table III-2). In fact, mutants 9B/2 and 9B/9 have the same Asn→Asp change at residue 1062 which occurs as a second-site mutation in mutant 1/01, and 9B/3 has the same Gln→His change at residue 1049 as mutants 5/01-L and 5/11-L. As expected the double mutants are able to escape neutralization by antibody 9B while the other single mutants selected with MCP1 do not (Table III-3). Mutant 9B/4 has a unique Asp→His mutation at residue 1062. 9B/4 is also different from the other 9B mutants in that it has a second mutation resulting in a Gln→His change at residue 2016 in VP2. This change is probably a second site mutation, not related to the neutralization escape phenotype of mutant 9B/4, both because 9B/4 is the only mutant escaping antibody 9B with a change at that site and because VP2 residue 2016 is buried in the interior of the capsid. Since amino acid changes at 1049 and 1062 have been seen before as second site mutations, not related to neutralization escape, there was some question about these being the authentic mutations resulting in neutralization escape from antibody 9B. However, no other mutations at the surface of the capsid in any of the 9B mutants and the presence of a mutation at either residue 1049 or 1062 in all the 9B mutants confirmed that these are within the 9B binding site. The occurrence of these mutations in some of the other mutants indicates that changes which occur in the βB-βC surface loop of VP1 arise at random and are tolerated because they have no adverse effect on capsid structure or function.

The epitope recognized by antibody 352 was mapped to a site overlapping VP3 and VP2 including residues 3073, 3074 and 3075 of VP3 and 2144 of VP2 (see Figures III-5, 6 and 7). The closest approach of these residues would be between the VP3 residues of one pentamer and the VP2 residue 2144 from an adjacent pentamer across the two fold axis of rotation. The distance between these residues on the surface of a single biological or crystallographic protomer would approach the 30Å limit of an antibody footprint (Davies *et al.*, 1990). Thus, the epitope recognized by antibody 352 most likely comprises surface residues from two adjacent pentamers. The epitope recognized by antibody 352 also overlaps Site 1 in VP2 (residues 2075, 2144, 2145, 2147 and 2148) recognized by antibodies MCP4, MCP5 and MCP6 and Site 2 in VP3 (residues 3057, 3061 and 3068) recognized by MCP1 (Figure III-5). This would link the two sites previously described as being independent into a single large composite antigenic determinant. Cross-neutralization data do not indicate the overlap of the epitope of antibody 352 with that of any other antibody and suggests that care must be taken in assigning antibody epitopes and the overlap between epitopes based on such data. Clearly there must be some overlap between the binding sites of antibodies MCP1 and

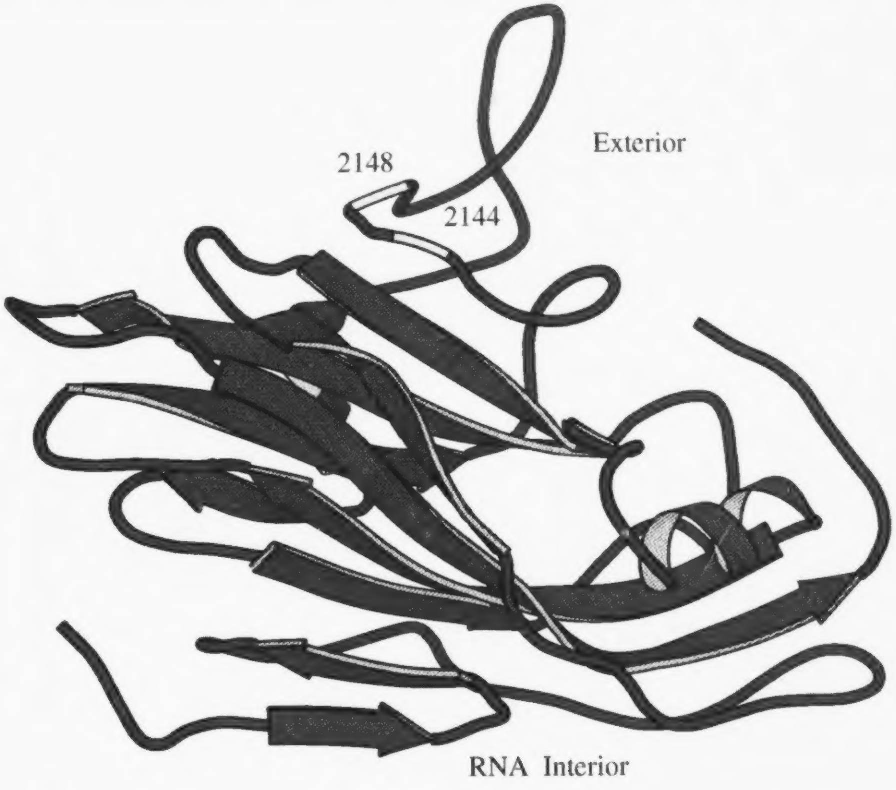

Figure III-6. Ribbon diagram representation of Mengo capsid protein VP2 indicating the positions of amino acid changes in neutralization escape mutants selected with antibody 3A and mutant 352/7 selected with antibody 352.

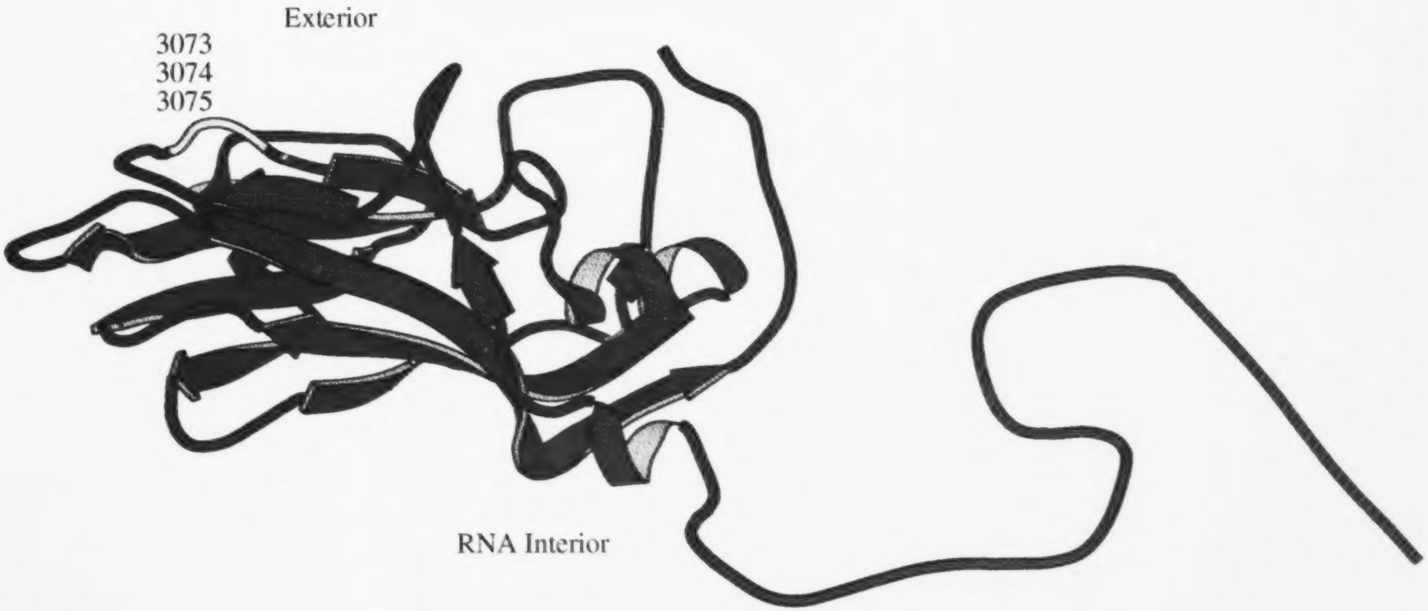

Figure III-7. Ribbon diagram representation of Mengo capsid protein VP3 indicating the positions of amino acid changes in neutralization escape mutants 352/1, 352/5 and 352/6 selected with antibody 352.

antibody 352 based on the position mutations in neutralization escape mutants selected with each, but the MCP1 mutants do not escape neutralization by antibody 352 nor do neutralization resistant mutants selected with antibody 352 escape neutralization by antibody MCP1. It is possible that each antibody is able to tolerate the amino acid changes in the mutants selected with the other antibody because they are in residues which are not critical for the recognition of the epitope by the first antibody. Mutants 5/04, 5/11-S and 5/11-L all have an Asn→Gly mutation at residue 2144 conferring neutralization resistance to antibody MCP5 but not antibody 352. MCP5 is still able to neutralize mutant 352/7 which has an asparagine to serine change at residue 2144 but this amino acid substitution now confers neutralization resistance to antibody 352. Residue 2144 is a shared recognition element, but a specific mutation results in resistance to neutralization by a specific antibody.

All the mutations mapped in neutralization escape mutants selected with antibodies generated against live attenuated Mengo virus or subviral pentamers are located on the surface of the capsid proteins. Figure III-8 shows a summary of the sites mapped using neutralization escape mutants on the surface of a ribbon diagram representation of a biological protomer. The location of the mutations suggests that the mutant viruses avoid the neutralizing activity of the antibody by directly altering the binding site of the antibody rather than through transmitted conformational changes. There is evidence that mutations in poliovirus at sites not directly accessible to antibody binding can confer neutralization resistance by the disruption of hydrogen bonds or salt bridges which causes a local disturbance in the conformation of an antigenic loop; however, mutations causing conformational disruption of an epitope at a distant site from the epitope have not been observed (Page *et al.*, 1988). Variants of foot-and-mouth disease virus (FMDV) have also been characterized which contain mutations at positions not directly involved in antibody binding. The mutations induce conformational changes in the orientation of the immunodominant βG-βH loop, which lies over the sites of mutations, with the result that antibodies directed against the loop no longer recognize their binding site (Parry *et al.*, 1990; Krebs *et al.*, 1993). Presumably long range conformational changes are unlikely to occur because they would alter capsid stability and/or the infectivity of the virion by altering critical contacts between subunits or changing the conformation of residues lining the pit so that receptor recognition is affected.

Analysis of the binding of the monoclonal antibodies by western blotting indicated that only antibody 6A was capable of recognizing any of the capsid proteins in

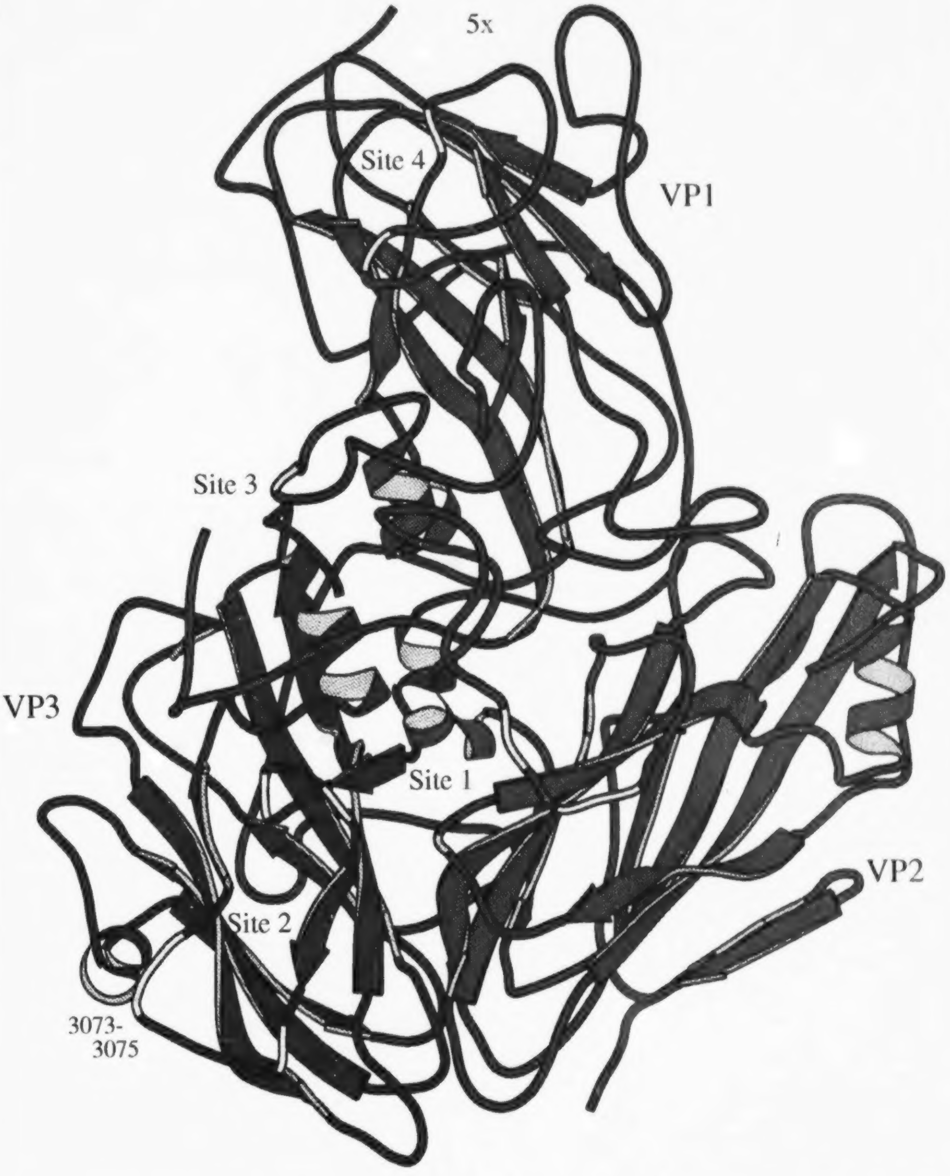

Figure III-8. Ribbon diagram representation of a biological protomer indicating the positions of the immunogenic determinants of the Mengo virion. The positions of the mutations in the neutralization resistant mutants selected with the anti-pentamer and anti-attenuated virus antibodies are highlighted. The position of the five-fold axis of rotation (5x) is also indicated. The diagram illustrates the spatial relationship of residues which contribute to each of the immunogenic determinants. Residues 3073-3075 represent part of the epitope of antibody 352 which bridges Sites 1 and 2.

a denatured state. This is not unusual considering that many antibodies generated against native protein bind to conformational or discontinuous epitopes rather than to linear or continuous epitopes. In a discontinuous epitope residues critical for antibody recognition which are distant in the linear sequence are brought together in the tertiary structure of the protein. Removal of residues critical for antibody recognition by denaturation of the protein usually removes enough of the epitope of the antibody that specific recognition of separate parts of the epitope is not possible. This is true for the recognition of a single polypeptide in its native conformation as well as the recognition of a discontinuous epitope made up of residues from two or more polypeptide chains. A notable exception among the picornaviruses for the specific recognition of a continuous epitope is the immunodominant epitope from FMDV (residues 1140-1160) which is in the βG-βH loop of VP1. This linear sequence is capable of eliciting the production of neutralizing antibodies to FMDV when presented to the immune system of pigs or guinea pigs as isolated VP1 polypeptide or as peptides covering this sequence (Kitson *et al.*, 1990; Logan *et al.*, 1993). This region represents an inserted sequence element not found in Mengo virus based on protein sequence alignments of structural elements of the capsid proteins (Acharya *et al.*, 1989).

The identification of the epitopes recognized by antibodies 3A and 6A presented particular difficulties. Selection of mutants, using a wide variety of antibody to virus ratios was not possible with either antibody because they are extremely efficient at neutralizing virus. A 1:2 dilution of 6A hybridoma tissue culture supernatant or a 1:5 dilution of 3A supernatant was capable of neutralizing 100% of wild-type Mengo virus at a concentration of 10^5 PFU/ml. The antibody concentration in hybridoma tissue culture supernatants is typically 10-50 μg/mL. None of the other antibodies was capable of neutralizing more than 95% of virus at a concentration of 10^3 PFU/mL regardless of the antibody concentration used (data not shown). Very efficient neutralization of virus is generally observed only when different neutralizing antibodies act synergistically (Kingsford, 1984). In such a case the probability of selecting a mutant capable of escaping neutralization would be unlikely because it would require the selection of a mutant containing simultaneously occurring mutations in each of the antibody binding sites. The possibility that cell lines 3A and 6A were not monoclonal and that each contained at least two different cell lines secreting neutralizing antibodies was addressed. Both cell lines were cloned extensively but antibody typing experiments and mutant selection attempts with cell lines derived from successive stages of cloning indicated that these two cell lines were monoclonal.

Cell lines 3A and 6A appear to be derived from mature B cells producing antibodies with very high affinity for virions. This is probably the result of the selection of the highest affinity antibodies during the maturation of the immune response. Generation of high affinity antibodies occurs through somatic mutations in the antibody combining region during the period of rapid expansion of B cells which respond to the antigen and is enhanced by repeated exposure of the immune system to the antigen. Both the opportunity and requirement for this response would be much greater in a live infection than in the response to noninfectious protein because of the presence of large amounts of replicating virus present against which the immune system must respond. The selection of B cells producing the highest affinity antibodies is not well understood but it is most likely related to the greater efficiency of these cells to bind to antigen and act as antigen presenting cells compared to B cells producing low affinity antibody. T cells, which respond to the presence of the antigen presented by the B cells, activate the B cells to mature and secrete antibody or produce memory B cells through the production of specific cytokines (Tonegawa, 1983; Rizzo *et al.*, 1992: Küppers *et al.*, 1993). This idea is supported by the procedure which was eventually used to select neutralization escape mutants with antibody 3A. Mutants which escaped neutralization by antibody 3A were selected from a stock of mutant 4/12, which has a Lys→Thr change at residue 2148. It appears that residue 2148 must lie within the epitope recognized by antibody 3A and that mutants containing a second mutation in the antibody epitope are being selected. Therefore, a single mutation within the binding site of antibody 3A is not sufficient to confer resistance to neutralization. The mutant selection procedure with antibody 3A provides the only information currently available concerning the identity of the 3A epitope. It must overlap residue 2148 as well as residues 2075, 2145 and 2147 of VP2, since these are altered in the other MCP4 and MCP6 mutants which contain subpopulation of double mutant virions capable of limited growth in the presence of antibody 3A. Even though mutants 5/01-S, 5/01-M, 5/01-L and 6/18 have amino acid changes in the same VP2 residues as mutants 4/01 and 4/02, they apparently do not contain subpopulations of doubly-mutated virions with the ability to grow in the presence of antibody 3A. Again, this indicates that antibodies can tolerate certain amino acid changes in residues which are important for binding to the epitope.

Although no neutralization mutants could be selected with antibody 6A some information about the location of the epitope has been obtained from indirect methods. Antibody 6A is the only antibody generated in this study which is capable of binding to a denatured capsid protein in a western blot: it binds to VP2. The other piece of information concerning the binding site for antibody 6A is that antibodies 3A and MCP4, if already bound to virions, are capable of inhibiting the binding of antibody 6A. This may indicate that the binding site of antibody 6A overlaps with those of antibodies 3A and MCP4. Even though antibodies MCP5 and MCP6 select mutants with changes in the same area of VP2 as antibody MCP4 they do not block 6A binding, so the former antibodies must be oriented such that 6A can still bind to the virion. This analysis of the binding of antibody 6A to Mengo virus does not eliminate the possibility 6A binds to an epitope in VP2 distinct from that of antibodies 3A and MCP4 and that these antibodies block the 6A binding simply by steric interference. Selection of mutants from stocks of all available neutralization escape mutants selected with other antibodies was tried but 6A neutralized these as efficiently as wild type Mengo virus. Selection of mutants from a stock of encephalomyocarditis virus (EMCV) was attempted (EMCV capsid proteins have 97% sequence identity with those of Mengo virus). The rationale behind the mutant selection attempt was that it was possible antibody 6A might still bind to EMCV but because of differences in its epitope compared to Mengo virus it might not be as efficient at neutralizing the virus and it would be possible to select mutants. Unfortunately antibody 6A neutralized EMCV as efficiently as it neutralized Mengo virus. The final attempt to map the epitope of 6A was made using peptides covering the sequence of VP2. This was a reasonable experiment because antibody 6A can bind to denatured VP2 in a western blot. However, neither binding 6A directly to immobilized VP2 peptides nor using peptides in solution to compete for 6A binding to Mengo virus with VP2 peptides was informative. It is possible that the peptides used were not of sufficient length to provide enough of the binding site for specific recognition of the epitope. Based on the available information it is possible to say only that the epitope of antibody 6A is located primarily in VP2 perhaps in the region that is recognized by antibodies MCP4 and 3A.

It has already been suggested that antibody 6A may be very efficient at neutralizing virus because it has a very high binding affinity. If this is true, a virion may require multiple mutations in the antibody epitope to reduce the affinity of the antibody such that it could escape neutralization. It is also very unlikely that multiple mutations within an epitope would occur spontaneously to generate mutants which escape the antibody. It should be noted that in our studies, most mutants selected with a particular antibody had mutations of just one residue, which conferred resistance to neutralization by the selecting antibody. Functional studies have suggested that epitopes may contain fewer amino acid residues which are necessary for epitope recognition (defines the functional epitope of the antibody) than the total number of residues which are in the contact region of the epitope (Geysen *et al.*, 1984; Getzoff *et al.*, 1987; Jin *et al.*, 1992). It is also possible that only one mutation in a single critical residue may confer neutralization resistance to antibody 6A but that this residue is located in such a position that any mutation which would allow a virion to escape neutralization also results in a defective viral capsid so the resulting virion is not viable.

One very interesting feature of the immune response to both pentameric subunits and to live attenuated virus is that the response to Site 1 located in VP2 is clearly immunodominant. Three of the four antibodies characterized in Chapter 1 and three of five antibodies characterized in this chapter interacted specifically with VP2 residues, primarily residues 2075, 2144, 2145, 2147 and 2148. Of the anti-pentamer antibodies only MCP1 recognized an epitope in VP3. Of the anti-virion antibodies 352 specifically interacted with residues in VP3, and its epitope overlaps with the immunodominant VP2 residues. These results are in contrast those reported by Lund *et al.* (1977) which indicated that only capsid polypeptide α (VP1) is capable of eliciting the production of neutralizing polyclonal antiserum injected into a rabbit as purified pentamers or isolated (denatured) polypeptide. Perhaps the discrepancy points out the species specificity of the immunizing antibody response to a particular antigen/virus.

The neutralization epitopes of Mengo virus have also been analyzed by Muir *et al.* (1991) who tested the ability of antisera, raised in mice against each of 140 overlapping synthetic peptides covering all of the sequences of the four capsid proteins, to neutralize Mengo virus. Only one of these peptides, corresponding to residues 1259-1277 of the external and flexible carboxyl end of VP1, induced high levels of polyclonal neutralizing antibodies. This epitope was not identified in our experiments using either subviral pentamers or live attenuated virus as immunogen. Muir *et al.* (1991) also reported that three other peptides in VP1 (residues 1041-1050, 1081-1090 and 1163-1172) induced a very weak neutralizing response against Mengo virus. One of these peptides contains residue 1049 which is part of the epitope recognized by antibody 9B. None of the other peptides covering the immunodominant site which we found in VP2 induced a protective response. This probably reflects the requirement of antibodies which neutralize the virus to interact specifically with other residues present on the capsid surface adjacent to the region containing the immunizing peptide sequence. In addition, antibodies selected by the immune system for their ability to recognize a peptide may not recognize it in the conformation that it exhibits in the native virion.

Based on the three-dimensional structure of the Mengo capsid, a number of linear amino acid sequences were predicted to be candidates for immunogenic epitopes because of their surface exposure and accessibility to antibodies (Luo *et al.*, 1987). These sites include the two loops between βB and αA in VP1 (residues 1078 to 1083 and 1093 to 1105) and the prominent βE-αA loop or "puff" in VP2 (residues 2154 to 2165). Of these sites, only the loop in VP1 formed by residues 1093 to 1105 was found to be involved in a neutralizing immunogenic epitope (recognized by antibody JEL 370). While it may be that a sufficient number of antibodies has not been examined to identify these other sites, it is clear from the current results that antibodies preferentially recognize regions of the capsid that are exposed on the surface but are not necessarily prominent protrusions. Although the protruding loop in VP2 (residues 2154 to 2165) is not recognized by any of the antibodies generated in our studies, residues at the base of the loop (residues 2144 to 2148) are mutated in a number of neutralization escape mutants. One could propose a number of reasons why (with the possible exception of the epitope recognized by antibody JEL 370) the identified epitopes are not located in the most prominent loops of the capsid. First, more residues within the antibody binding site are important for stable binding of the antibody to the antigen than are critical for the recognition of the epitope (Jin *et al.*, 1992) and an extended loop on a protein will have all the residues required for recognition of the epitope but may not provide as many surface contacts as are required for very stable binding. Antibody combining sites on proteins are most commonly observed to be flat or concave (reviewed in Davies *et al.*, 1990). It is not unreasonable to speculate that antibodies are directed against all parts of the surface of the virus, including the highly accessible loops, but binding to these loops on Mengo virus does not provide the required antibody to antigen position or interaction to allow the antibody to effect one or more of the potential mechanisms by which antibodies neutralize virus infectivity.

Comparison of the immune response to subviral pentamers with that produced against live attenuated Mengo virus did not indicate any dramatic differences in the epitopes which were recognized. One interesting feature of the murine immune response to live virus infection, not observed in mice immunized with non-infectious pentamers, was the generation of very high efficiency neutralizing antibodies (*i.e.* antibodies 3A and 6A). Some anti-viral antibodies recognized regions of the virus capsid not previously determined to be antigenic with anti-pentamer antibodies; *e.g.* the epitopes recognized by antibodies JEL 370 and 9B and residues recognized by antibody 352. However, it cannot be said whether this represents a significant difference in immune recognition of epitopes in response to a live infection versus noninfectious protein because of the relatively small number of antibodies which were surveyed.

REFERENCES

Acharya, R., E. Fry, D. Stuart, G. Fox, D. Rowlands and F. Brown (1989). The three dimensional structure of foot-and-mouth diesease virus at 2.9 Å resolution. *Nature* **327**, 709-716.

Coffman, R.L., D.A. Lebman and P. Rothman (1993). Mechanism and regulation of immunoglobulin isotype switching. *Advances in Immunology* **54**, 229-270.

Davies, D.R., E.A. Padlan and S. Sheriff (1990). Antibody-antigien complexes. *Annual Review of Biochemistry* **59**, 439-473.

Duke, G.M., J.E. Osorio and A.C. Palmenberg (1990). Attenuation of Mengo virus through genetic engineering of the 5' noncoding poly(C) tract. *Nature* **343**, 474-476.

Getzoff, E.D., H.M. Geysen, J.R. Stuart, H. Alexander, J.A. Tainer and R.A. Lerner (1987). Mechanisms of antibody binding to a protein. *Science* **235**, 1191-1196.

Geysen, H.M., R.H. Meloen and S.J. Barteling (1984). Use of peptide synthesis to probe viral antigens for epitopes to a resolution of a single amino acid. *Proceedings of the National Academy of Sciences, U.S.A.* **81**, 3998-4002.

Harlow, E. and D. Lane (1988). Antibodies: a laboratory manual. Cold Spring Harbor Laboratory, USA.

Jin, L., B.M. Fendly and J.A. Wells (1992). High resolution functional analysis of antibody-antigen interactions. *Journal of Molecular Biology* **226**, 851-865.

Kingsford, L. (1984). Enhanced neutralization of La Crosse virus by the binding of specific pairs of monoclonal antibodies to the G1 glycoprotein. *Virology* **136**, 265-273.

Kitson, D.A., D. McCahon and G.J. Belsham (1990). Sequence analysis of monoclonal antibody resistant mutants of type O foot and mouth diesease virus: Evidence for the involvement of the three surface exposed capsid proteins in four antigenic sites. *Virology* **179**, 26-34.

Kohler, G. and C. Milstein (1975). Continuous cultures of fused cells producing antibodies of predefined specificity *Nature* **256**, 495-497.

Kraulis, P.J. (1991). MOLSCRIPT: a program to produce both detailed and schematic plots of protein structures. *Journal of Applied Crystallography* **24**, 946-950.

Krebs, O. R. Ahl, O.C. Straub and O. Marquardt (1993). Amino acid changes outside the G-H loop of capsid protein VP1 of type O foot-and-mouth disease virus confer resistance to neutralization by antipeptide G-H serum. *Vaccine* **11**, 359-362.

Küppers, R., M. Zhao, M-L.Hansmann and K. Rajewsky (1993). Tracing B-cell development in human germinal centres by molecular analysis of single cells picked from histological sections. *EMBO Journal* **12**, 4955-4967.

Logan, D., R. Abu-Ghazaleh, W. Blakemore, S. Curry, T. Jackson, A. King, S. Lea, R. Lewis, J. Newman, N. Parry, D. Rowlands, D. Stuart and E. Fry (1993). Structure of a major immunogenic site on foot-and-mouth disease virus. *Nature* **362**, 566-568.

Lund, G.A., B.R. Ziola, A. Salmi and D.G. Scraba (1977). Structure of the Mengo virion. V. Distribution of the capsid polypeptides with respect to the surface of the virus particle. *Virology* **78**, 35-44.

Luo, M., G. Vriend, G. Kamer, I. Minor, E. Arnold, M.G. Rossmann, U. Boege, D.G. Scraba, G.M. Duke and A.C. Palmenberg (1987). The atomic structure of Mengo virus at 3.0Å resolution. *Science* **235** , 182-191.

McCullough, K.C., D. Parkinson and J.R. Crowther (1988). Opsonization-enhanced phagocytosis of foot-and-mouth disease virus. *Immunology* **65**, 187-191.

Muir, S., J.P. Weintraub, J. Hogle and J.L. Bittle (1991). Neutralizing antibody to Mengo virus induced by synthetic peptides. *Journal of General Virology* **72**, 1087-1092.

Ouldridge, E.J., P.V. Barnett, N.R. Parry, A. Syred, M. Head and M.M. Rweyemamu (1984). Demonatration of neutralizing and non-neutralizing epitopes on the trypsin-sensitive site of foot-and-mouth disease virus. *Journal of General Virology* **65**, 203-207.

Page, G.S., A.G. Mosser, J.M. Hogle, D.J. Filman, R.R. Rueckert and M. Chow (1988). Three dimensional structure of poliovirus serotype 1 neutralizing determinants. *Journal of Virology* **62**, 1781-1794.

Parry, N., G. Fox, D. Rowlands, F. Brown, E. Fry, R. Acharya, D. Logan and D. Stuart (1990). Structural and serological evidence for a novel mechanism of antigenic variation in foot-and-mouth disease virus. *Nature* **347**, 569-572.

Rizzo, L.V., R.H. Dekruyff and D.T. Umetsu (1992). Generation of B-cell memory and affinity maturation. Induction with Th1 and Th2 T cell clones. *Journal of Immunology* **148**, 3733-3739.

Rossmann, M.G. (1989). The canyon hypothesis. *Journal of Biological Chemistry* **264**, 14587-14590.

Rossmann, M.G., and A.C. Palmenberg (1988). Conservation of the putative receptor attachment site in picornaviruses. *Virology* **164**, 373-382.

Schwab, C. and H.R. Bosshard (1992). Caveats for the use of surface-adsorbed protein antigen to test the specificity of antibodies. *Journal of Immunological Methods* **147**, 125-134.

Tonegawa, S. (1983). Somatic generation of antibody diversity. *Nature* **302**, 575-581.

Wang, G., C. Porta, Z. Chen, T.S. Baker and J.E. Johnson (1992). Identification of a Fab interaction foootprint site on an icosahedral virus by cryoelectron microscopy and x-ray crystallography. *Nature* **355**, 275-278.

CHAPTER IV

IDENTIFICATION OF MENGO VIRUS T-HELPER CELL EPITOPES*

INTRODUCTION

Mengo virus is a member of the Cardiovirus genus of the Picornavirus family and is a natural pathogen of mice. All picornaviruses contain a positive-strand RNA genome coding for a single polyprotein; this is proteolytically processed subsequent to translation into a number of viral proteins, including the four structural proteins VP1, VP2, VP3 and VP4. Sixty copies of each of the structural proteins form the icosahedral capsid of the virus, the structure of which has been determined to a resolution of 0.30 nm (Luo *et al.*, 1987; Krishnaswamy & Rossmann, 1990). This makes it possible to correlate immunologically reactive entities (epitopes) with specific structural elements in the viral capsid.

The interaction of antibody and viral antigen has been examined in detail for a number of viruses, but this represents only one component of the adaptive immune response. The immune reaction to viral antigens, including the development of an efficient antibody response, is primarily T cell dependent. One example of this is the induction of proliferation of the major histocompatibility complex (MHC) class II restricted CD4$^+$ T-helper (Th) cells in response to antigen. These cells secrete cytokines which, in turn, mediate a variety of immune responses including the activation of antigen specific B cells (Rheinherz & Schlossman, 1981). As well, the sub population of class II restricted T-helper cells (Th1) has also been implicated in direct cell-mediated immunity including the lysis of virally infected target cells (Coffman *et al.*, 1988; Mosmann & Coffman, 1989; Palladino *et al.*, 1991).

The present study was undertaken to examine the murine Th cell response to immunization with UV-inactivated Mengo virus, to map the Th cell stimulating peptides with respect to their locations in the viral capsid, and to determine their spatial relationships with known B cell epitopes. Overlapping peptides covering the entire amino acid sequences of VP1, VP2, VP3 and VP4 were systematically evaluated for their ability to induce a proliferative response *in vitro* in lymph node cells from BALB/c mice which had been primed with inactivated virus. Peptides capable of inducing a significant proliferative response were located in proteins VP2 and VP3. Two of these, one in each

---

*A version of this chapter has been accepted for publication. Muir *et al.*, *Journal of General Virology* protein were adjacent to sequences contributing to Mengo virus B cell antigenic Sites 1 and 2. We also investigated the H-2 restriction of these epitopes in C57BL/6 and SJL/J mice. The position of the identified epitopes was examined in relation to the position of other picornavirus Th cell epitopes in mice and in relation to potential T cell epitopes identified by predictive algorithms based upon specific structural and sequence motifs.

METHODS

Mice

Relevant regulations regarding the use of animals (Canadian Council on Animal Care) were followed during the course of this research. Female BALB/c ($H\text{-}2^d$), C57BL/6 ($H\text{-}2^b$) and SJL/J ($H\text{-}2^s$) mice 6 to 8 weeks of age were bred in either the Research Institute of Scripps Clinic breeding colony, the Heritage Rodent Facility of the University of Alberta or obtained from commercial sources (Charles River, Canada or Jackson Laboratories, Bar Harbor, ME.).

Virus purification and inactivation

The M plaque variant of Mengo virus (Ellem & Colter, 1961) was produced in mouse L929 cells in roller bottle cultures and was purified as described previously (Boege *et al.*, 1986; Ziola & Scraba, 1974). Purified virus (550 µg/ml), for both immunization of mice and *in vitro* proliferation assays, was inactivated by UV irradiation (253.7 nm, 200 µW/cm^2; 10 cm from source). The minimum irradiation time required for complete inactivation was determined by standard plaque reduction assay (Ellem & Colter, 1960) of irradiated samples.

Immunization

Mice were injected subcutaneously at the base of the tail or in a foot pad with 50 µl of complete Freund's adjuvant (CFA) (Difco, Detroit, MI) emulsion into which either 5 µg of UV-inactivated Mengo virus (found to be optimal in initial experiments), 1.5 µg of isolated VP1, VP2 or VP3 capsid proteins, or 100 µg grade V ovalbumin (Sigma, St. Louis, MO.) was incorporated. The dose of individual capsid protein for immunization was chosen to represent approximately the same dose of each individual polypeptide as is given in a 5 µg injection of whole virus. For each set of ten peptides and controls, three mice were immunized and the lymph node cells were pooled from all three. All assays were done in triplicate. The response to immunization was monitored by ELISA and neutralization assays of serum collected from mice prior to sacrifice.

Detection of anti-Mengo virus antibodies

Serum samples were analyzed for the presence of anti-Mengo virus antibodies by enzyme-linked immunosorbant assay (ELISA). Microtiter plates (Fisher Scientific, Whitby, Ontario) were coated overnight with 200 ng/well of purified Mengo virus in ELISA coating buffer (13.5 mM Na_2CO_3, 35 mM $NaHCO_3$, pH 9.6). Plates were blocked for 1 hour at room temperature with 1% bovine serum albumin (Sigma) in phosphate-buffered saline (PBS) prior to the addition of test sera. Sera, serially diluted from 1:100 to 1:6400 in PBS containing 0.05% Tween 20 (Sigma) (PBS/Tween), were then added to the plates. After a 2 hr incubation at room temperature they were washed with PBS/Tween. Affinity-purified goat anti-mouse IgM+IgG+IgA alkaline phosphatase conjugate (Cedarlane, Hornby, Ontario) diluted 1:1500 in PBS/Tween was added and the plates incubated as before. After washing, the enzyme substrate disodium p-nitrophenyl phosphate (Sigma) (10 mg dissolved in 10 mL of 10% diethanolamine) was added. Following a 10 minute incubation period the absorbance at 410 nm was determined.

Serum-neutralizing assay

Murine L929 cells were continuously cultured in 1 liter spinner flasks in Modified Basal Medium Eagle (BME; Flow Laboratories, Mississauga, Ontario) to which was added 10% fetal bovine serum (Flow Laboratories), and 1% solutions of penicillin/streptomycin (200 units/ml penicillin, 100 µg/ml streptomycin). Cells were plated at 5 x 10^4 cells/well in 96-well tissue culture plates (Corning) which contained 10^4 or 10^3 PFU of Mengo virus preincubated with dilutions of test serum and negative and positive control sera. As an internal control Mengo virus alone was titrated on each plate. Plates were incubated in a humidified chamber at 37° and 5% CO_2 for 48 hr prior to serum neutralizing activity being recorded.

Peptide Synthesis

Ten to 18-mer peptides, overlapping five residues at the amino and carboxy ends, were synthesized based upon the amino acid sequence of Mengo virus capsid polypeptides (Boege *et al.*, 1991), A multiple simultaneous peptide synthesis method in polypropylene mesh "tea bags" (Houghten, 1985) or symmetrical anhydride chemistry (Hagenmaier & Frank, 1972; Merrifield, 1963) on an Applied Biosystems 430A or a Beckman Model 990 automated peptide synthesizer employing t-butyloxycarbonyl N^a - and benzyl type side-chain protection was used for peptide synthesis. Peptides were cleaved from the resin and side-chain protecting groups were removed with hydrofluoric acid. The purity of all peptides (70-90%) was determined by reverse phase high-performance liquid chromatography (HPLC) and amino acid composition verified by amino acid analysis. The majority of cleaved "tea bag" peptides were used without further purification, whereas those from commercial sources (Alberta Peptide Institute, Edmonton, Alberta; Chiron Mimotopes, Clayton, Victoria, Australia) were partially purified by ion-exchange or reversed phase HPLC and analyzed by mass spectrometry. Appendix B contains a complete list of the peptides covering the Mengo virus capsid proteins used in this study.

Isolation and purification of individual capsid proteins VP1, VP2 and VP3

Individual capsid proteins were separated by sodium dodecyl sulphate polyacrylamide gel (12%) electrophoresis. Protein was eluted from excised bands into 150 mM N-methyl morpholine (pH 8.0) and SDS was removed by extensive dialysis against PBS. Purity of individual polypeptides was assessed on polyacrylamide gels and protein concentration was estimated by the staining intensities relative to known concentrations of capsid protein.

In vitro T cell proliferation assay

Antigen specific T cell proliferation assays were performed using popliteal, superficial and deep inguinal and periaortic immune draining lymph nodes (LN). Lymph nodes were asceptically removed and a single cell suspension of LN cells was prepared, washed twice in RPMI 1640 medium containing 20 mM L-glutamine and penicillin/streptomycin (200 units/ml penicillin, 100 μg/ml streptomycin). The cells were resuspended at a concentration of 5×10^6 cells/ml in the same medium supplemented with 2% normal murine sera or fetal bovine serum (FBS) which had been screened for the absence of nonspecific proliferation activity. The cells were cultured in 0.2 ml of medium at a final concentration of 5×10^5 cells/well in 96-well flat bottomed tissue culture plates (Corning) in the presence of antigens. In all assays the non-specific mitogen concanavillin A (conA) at the experimentally determined optimal concentration of 10μg/ml was used as a positive control for lymphocyte proliferation. Cellular proliferation was measured by the incorporation of ^{3}H-thymidine (1 μCi/well; 20.00 Ci/mmol) (New England Nuclear, Boston, MA) into DNA during the last 16 hours of a 72 hour culture at 37° and 5% CO_2. All cultures were set up in triplicate, harvested onto glass fiber filter paper using a cell harvester (Skatron, Tranby, Norway) and radioactivity was counted in a Beckman LS scintillation counter. Data are presented either as mean counts per minute (CPM) or as stimulation index (SI). The stimulation index is defined as the mean CPM obtained for a given antigen divided by the mean CPM for media controls. Stimulation indices greater than three were selected as significant based on values obtained for non-Mengo virus control peptides.

Examination of VP1 and VP4 peptides was done by Dr. S. Muir.

Immunological characterization of T-lymphocyte population

The L3T4 (CD4) rat IgG2b anti-mouse monoclonal (Cedarlane) and the Ly2 (CD8) rat IgG2b anti-mouse monoclonal (generously supplied by Dr. V. Paetkau, Department of Biochemistry) were utilized for *in vitro* depletion assays. Lymph node cells ($5x10^5$ cells/ml; 100 µl/well), isolated from mice immunized with UV-inactivated Mengo virus, were plated in the presence of 1.0 and 0.1 µg/ml homologous virus and 70 to 1780 ng/well of the L3T4 or the Ly2 monoclonal antibodies. Cells not treated with either monoclonal antibody were used as a control. The plates were incubated 72 hr at 37°, 7.5% CO_2. The cells were pulsed with ^3H-thymidine (1.0 µCi/well) for 16 hr, harvested and cell associated radioactivity counted (as in the *in vitro* proliferation assay).

Computer analysis of Mengo capsid protein sequences to predict T-cell sites

The computer program, TSites (Feller & de la Cruz, 1991) was used to examine the amino acid sequences of the Mengo virus capsid proteins for predicted T cell sites. It is based on 4 different epitope searching algorithms. First, correlation between alpha-helical periodicity and amphipathicity and the antigenicity of many T cell sites (DeLisi & Berzofsky, 1985) was examined. The AMPHI algorithm (Margalit *et al.*, 1987) is used with a scanning window of 11 residues. Second a search is conducted for sequence motifs identified by Rothbard and Taylor (Rothbard & Taylor, 1988) in sequences recognized by MHC class I and class II molecules. These motifs consist of a 4 amino acid pattern of charged/glycine-hydrophobic-hydrophobic-polar/glycine residues and a 5 amino acid pattern of charged/glycine-hydrophobic-hydrophobic-hydrophobic/proline-polar/glycine residues. The final two prediction strategies search for sequences with analogy to ovalbumin peptides which are known to bind to the murine MHC class II (Ia) molecules (Sette *et al.*, 1989). Algorithm number 3 searches for peptides predicted to bind to the I-A^d molecule (the "D" motif) and algorithm number 4 identifies peptides binding to the I-E^d molecule (the "d" motif).

RESULTS

Sera from mice immunized with inactivated Mengo virus were examined for IgM, IgA and IgG content and for virus neutralization activity. Combined IgA, IgG and IgM levels in the sera of individual mice were measured by standard ELISA assay using anti-mouse combined IgA, IgG and IgM alkaline phosphatase conjugated antibodies. Sera removed from all three strains of mice the day of the assay consistently contained levels of circulating anti-Mengo antibodies detectable in ELISA tests at 1:5000 dilution. To examine whether immunization with inactivated Mengo virus could induce the production of neutralizing antibodies the sera from individual mice were tested in a micro-neutralization assay. Sera from all three strains of mice consistently neutralized Mengo virus at 1:400 to 1:800 dilutions (data not shown).

Lymph node cells, obtained from BALB/c mice injected with 5 µg of UV-inactivated Mengo virus or 100 µg ovalbumin, were stimulated *in vitro* at 7, 9, 10, and 14 days post-immunization with homologous virus or ovalbumin. The optimal response to Mengo virus was seen at 7 days post-immunization. The specificity of the T cell response to antigen was demonstrated by *in vitro* stimulation of lymph node cells with inactivated Mengo virus and ovalbumin. Lymph node cells from ovalbumin-immunized mice proliferated in response to the presence of ovalbumin, while their response to Mengo virus was essentially negligible at all antigen concentrations (Figure IV-1a). Similarly, Mengo virus induced the proliferation of lymph node cells from Mengo-primed mice whereas ovalbumin failed to stimulate them (Figure IV-1b). These results demonstrate that the T cell response *in vitro* is specific for the antigen to which the cells have been exposed *in vivo*. In all of the assays the highest level of proliferation in Mengo-primed lymph node cells was seen with 0.1 µg/ml inactivated virus. While the responses of individual mice varied considerably, the response to Mengo virus was generally about 50% of the proliferative response of lymphocytes stimulated with conA under the same conditions.

Lymphocytes from BALB/c mice inoculated with UV-inactivated Mengo virus were incubated with the optimal concentration of homologous virus and with varying concentrations of anti-CD4 or anti-CD8 monoclonal antibodies to determine which subpopulation of lymphocytes is responsible for the response in the *in vitro* proliferation assays. Addition of the anti-CD8 monoclonal antibody did not reduce the *in vitro* response to inactivated virus compared to control, whereas anti-CD4 antibody was able to reduce the response to less than 20% of control values at the highest concentration of antibody used (Figure IV-2). These results indicate that it is the $CD4^+$ helper T cell

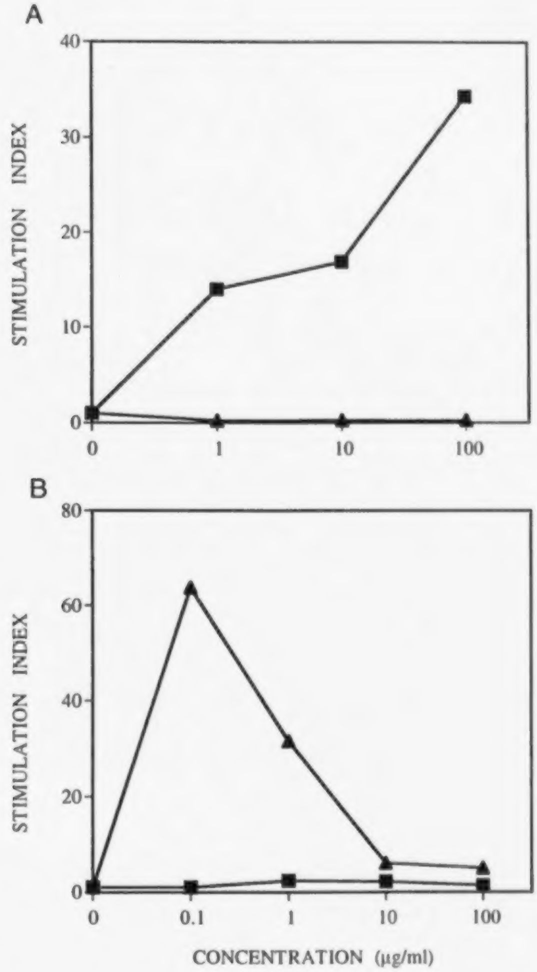

Figure IV-1. Specificity of the T lymphocyte response. BALB/c mice were immunized with either 100 µg of ovalbumin (A) or 5 µg of UV-inactivated Mengo virus (B). Seven days post-immunization the lymph node cells were stimulated in vitro with ovalbumin (■) or UV-inactivated Mengo virus (▲).

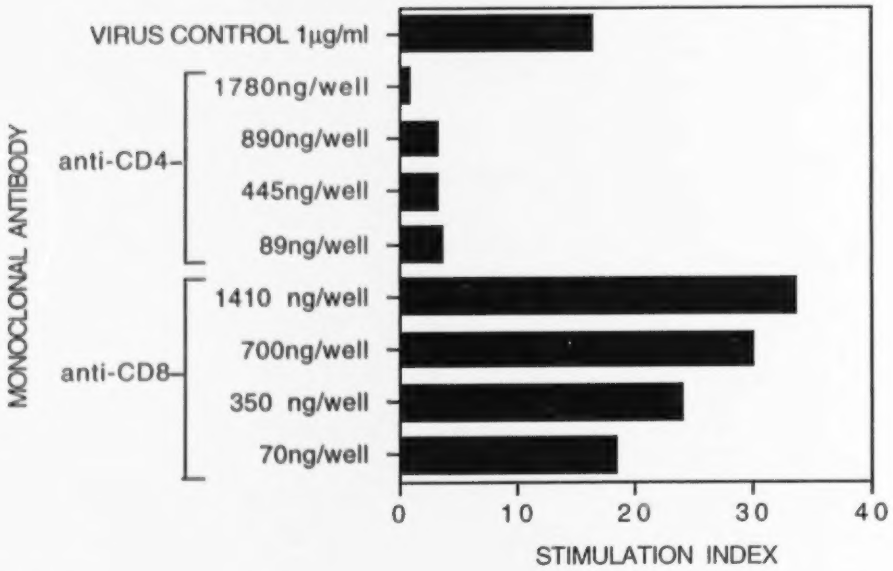

Figure IV-2. Mengo virus specific proliferation of CD4$^+$ T lymphocytes. Seven days post-immunization, lymph node cells from BALB/c mice injected with 5 μg of UV-inactivated Mengo virus, were stimulated *in vitro* with 1 μg/ml inactivated virus in the presence of anti-CD4 or CD8 monoclonal antibodies.

population of lymphocytes which is responsible for the proliferative response of the mixed lymphocyte population from lymph node-derived cultures. It is likely that the increase in proliferative response observed with increasing concentrations of anti-CD8 monoclonal antibody is due to the suppression of the activity of the subpopulation of $CD4^-CD8^+$ regulatory suppressor T lymphocytes (discussed in Baker, 1993).

Lymphocytes were isolated from BALB/c mice which had been immunized with purified Mengo capsid proteins VP1, VP2 or VP3 (it was not possible to isolate sufficient quantities of VP4 to immunize mice). Cultured LN cells were stimulated *in vitro* with UV-inactivated Mengo virus to determine whether each protein contains T cell epitopes recognized in BALB/c mice. Lymphocytes from both VP2 and VP3 injected mice proliferated in the presence of inactivated Mengo virus, but VP1 primed lymphocytes were only weakly stimulated (Figure IV-3). It was not possible to isolate sufficient quantities of the individual capsid proteins to use as antigen in the *in vitro* proliferation assay with lymphocytes from mice immunized with whole inactivated Mengo virus.

A panel of 116 synthetic peptides, each 10-18 residues in length and overlapping five residues at the amino and carboxy ends, was used to examine the ability of specific amino acid sequences in each of the four Mengo capsid proteins to induce a proliferative response in lymph node cells from mice primed with inactivated Mengo virus. The peptide panel covered the sequence of all four capsid proteins completely. Using a stimulation index of three as the arbitrarily selected minimum significant response, no Th cell epitopes were identified within peptides representing VP1 or VP4 sequences (data not shown).

For VP2, peptides designated K105, K107, K113, K120 (Figure IV-4a, Table IV-1) gave strong proliferative responses (SI > 3). In addition, a number of peptides induced low, but significant compared to controls, levels of proliferation. Peptides K89, K102 and K112 were identified as weak T cell epitopes in BALB/c mice. Table IV-1 summarizes the data for each VP2 peptide containing a T cell epitope.

For VP3, peptides designated K124, K125, K130, G135 and K151 consistently induced significant levels of lymphocyte proliferation (Figure IV-4b, Table IV-1). There were a number of other peptides in VP2 and VP3 capable of inducing low levels of proliferation, but the assay-to-assay variation in results with these peptides made it difficult to decide whether or not they represented authentic Mengo virus T cell epitopes.

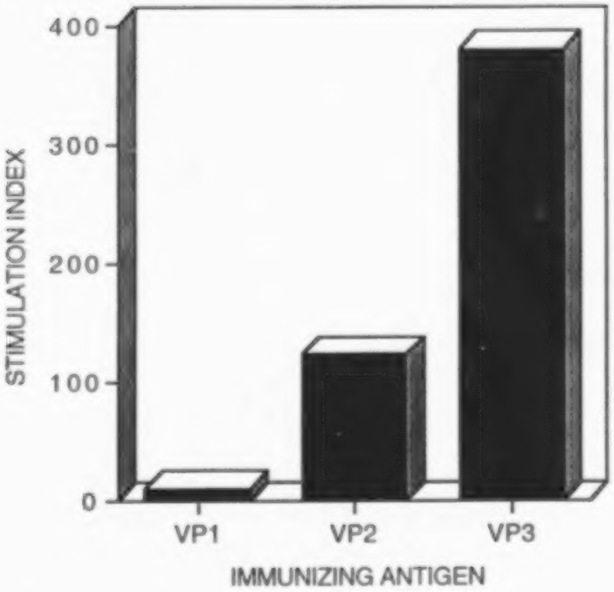

Figure IV-3. Proliferative responses of VP1, VP2 or VP3 primed lymph node cells. BALB/c mice were immunized with 1.5 µg of either capsid protein. Seven days later lymph node cells from each were stimulated *in vitro* with UV-inactivated Mengo virus.

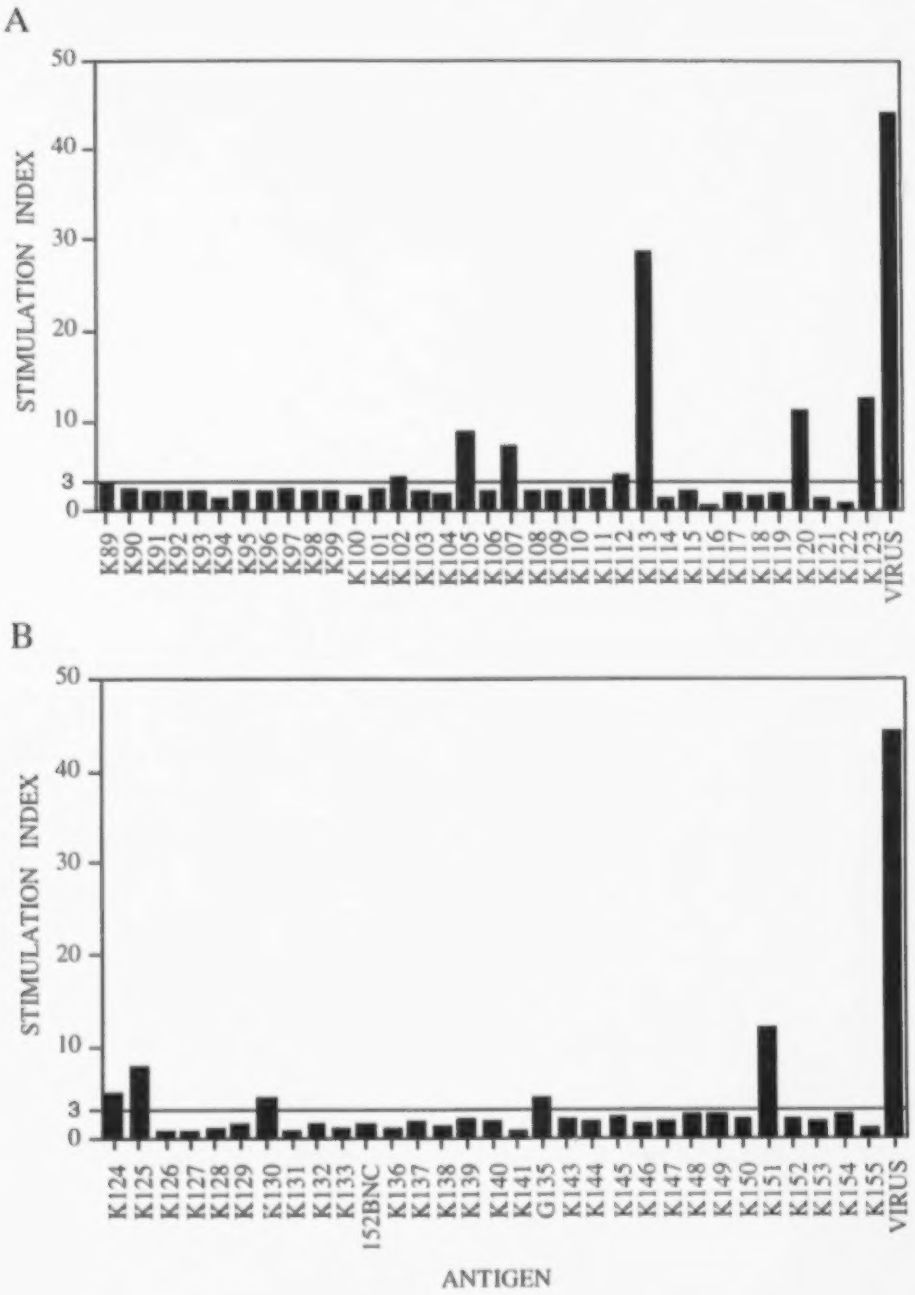

Figure IV-4. Proliferative responses of UV-inactivated Mengo virus primed lymph node cells from BALB/c mice to VP2 and VP3 synthetic peptides. BALB/c mice were immunized with 5 µg of UV-inactivated Mengo virus. Seven days later the lymph node cells were stimulated *in vitro* with VP2 (A) or VP3 (B) peptides.

TABLE IV-1

Summary of T cell epitopes in BALB/c mice

Peptide	Stimulation index	Amino acid position	Sequence
K89	3.2	2001-2015	DQNTEEMENISDRVS
K102	3.7	2099-2108	TLRRHYLVKT
K105	8.7	2118-2132	ASQFHAGSLLVFMAP
K107	7.1	2133-2147	EYPTLDVFAMDNRWS
K112	3.9	2173-2182	WQWTLYPHQF
K113	28.5	2178-2192	YPHQFLNLRTNTTVD
K120	11.1	2227-2236	GASTSLDLTA
K123	12.4	2247-2256	GLRHEVLSRQ
K124	5.0	3001-3015	SPIPVTIREHAGTWY
K125	8.0	3011-3020	AGTWYSTLPD
K130	4.5	3046-3058	EIAQIPTFIGNKM
G135	4.4	3136-3150	PTSRDQAMQATYAIW
K151	12.0	3198-3212	PPGCPTSAKILTMVS

The positions of the T cell stimulating peptides in the 3-dimensional structures of VP2 and VP3 are shown in Figure IV-5.

The positions of the previously identified B cell sites (Chapters II and III) are shown in relation to the T cell epitopes in Figure IV-6. Peptide K107 covers residues 2133-2147 of VP2 and partially overlaps the region of B-cell antigenicity at residues 2144 to 2148 (Site 1, Chapter III). As well part of B cell Site 2 in VP3 at residue 3057 is overlapped by stimulatory peptide K130 (residues 3046-3058).

To examine the H-2 restriction of the peptide-stimulated proliferative responses found in BALB/c mice, parallel *in vitro* proliferation assays were done with lymph node cells from C57BL/6 (*H-2*^{b}) and SJL/J (*H-2*^{s}) mice which had been immunized with UV-inactivated Mengo virus. In all three mouse strains the VP2 peptides K89, K102 and K113 as well as the VP3 peptides K125 and G135 were recognized as T cell epitopes (Figure IV-7). With the other peptides the pattern of recognition of T cell epitopes varied among the different strains. In C57BL/6 mice, peptides K105, K107, K120, K123 (VP2), K124 and K130 (VP3) also induced significant stimulation of cell growth. Lymph node cells from immunized SJL/J mice responded only to the five commonly recognized peptides (K89, K102, K113, K125 and G135); none of the other peptides were capable of inducing significant proliferative responses.

The amino acid sequences of all four Mengo capsid proteins were analyzed with the computer program TSites (Feller & de la Cruz, 1991) for the prediction of T cell epitopes. Figure IV-8 indicates the sequences predicted by each of the four searching strategies to be possible T cell epitopes for capsid proteins VP2 and VP3. As well, the positions of the peptides containing the experimentally identified T-cell sites in VP2 and VP3 are shown. Similarly to VP2 and VP3, VP1 and VP4 have a number of regions predicted to be T cell epitopes (data not shown) even though no T cell epitopes were identified in these capsid proteins. In all four capsid proteins the Rothbard and Taylor and "D" motif prediction strategies tended to pick out relatively restricted stretches of the proteins as potential antigenic sites, while the AMPHI program selected much more extensive regions in all the capsid proteins. The "d" motif algorithm did not select any regions in the virus capsid proteins as a site potentially capable of binding to the MHC I-E^d molecule. The VP2 peptides K89, K102, K105, K113, K120, K123 all contain significant regions of overlap with regions predicted by one or two of the algorithms to be antigenic sites. Interestingly, peptides K107 and K112 are not predicted by the TSites

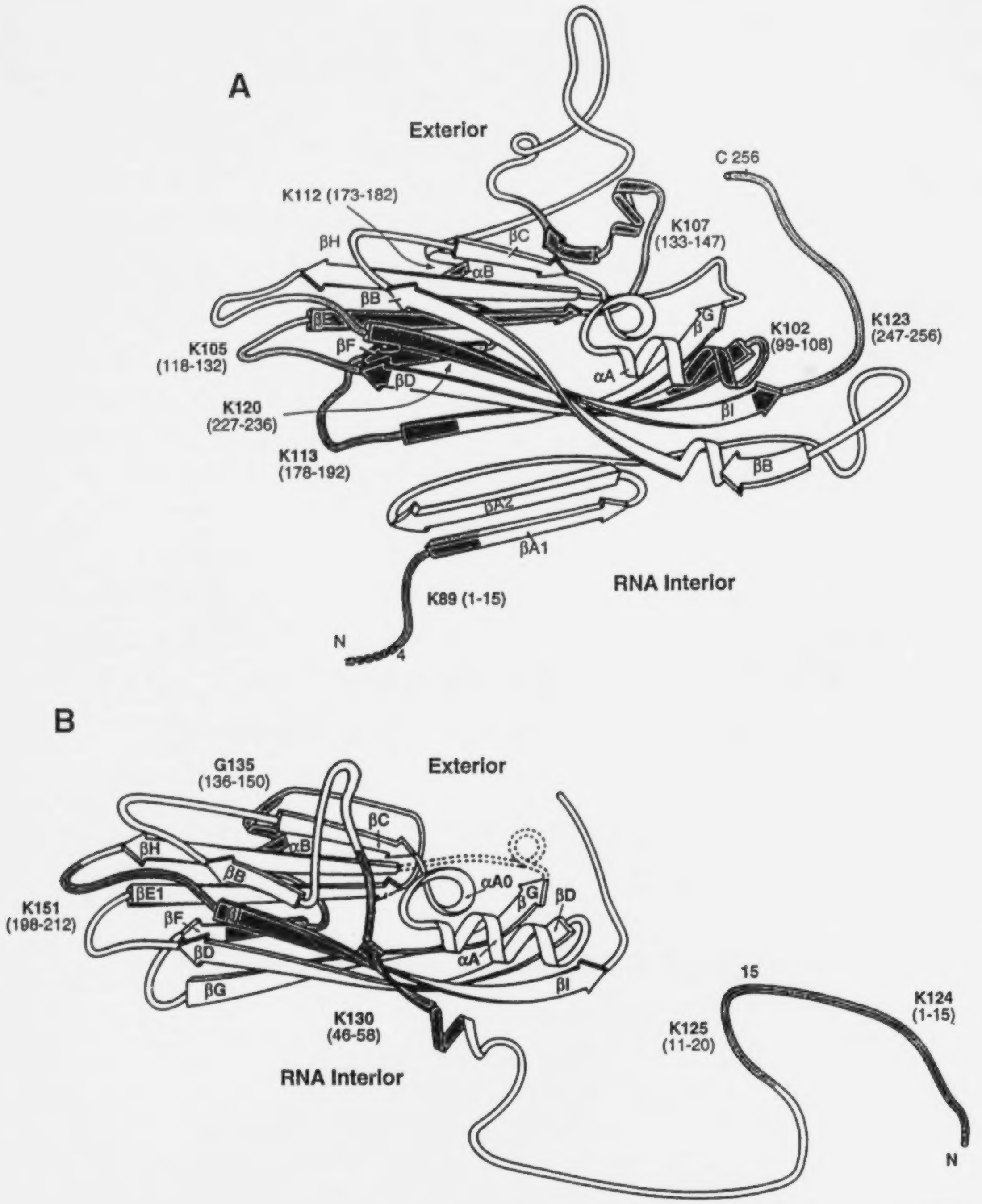

Figure IV-5. Location of T cell epitopes. Ribbon diagrams of VP2 (A) and VP3 (B) indicating the positions of the peptides containing the T cell epitopes identified in BALB/c mice in gray.

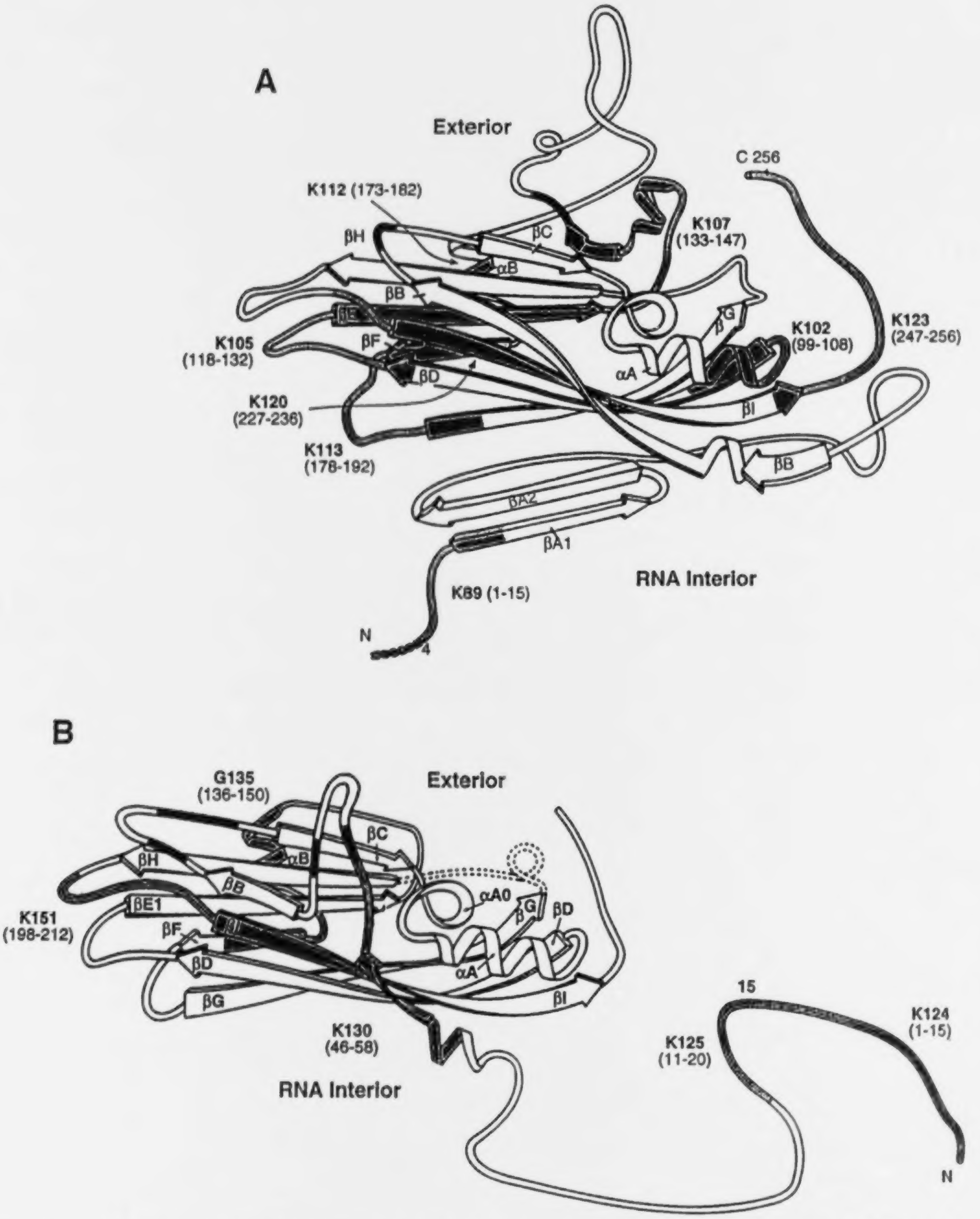

Figure IV-6. Relationship between B and T cell epitopes. Ribbon diagrams of VP2 (A) and VP3 (B) indicating the positions of the peptides containing the T cell epitopes identified in BALB/c mice (gray) with respect to the location of the B cell epitopes shown in black (VP2 residues 2075, 2144, 2145, 2147, 2148; VP3 residues 3057, 3061, 3068, 3073-3075).

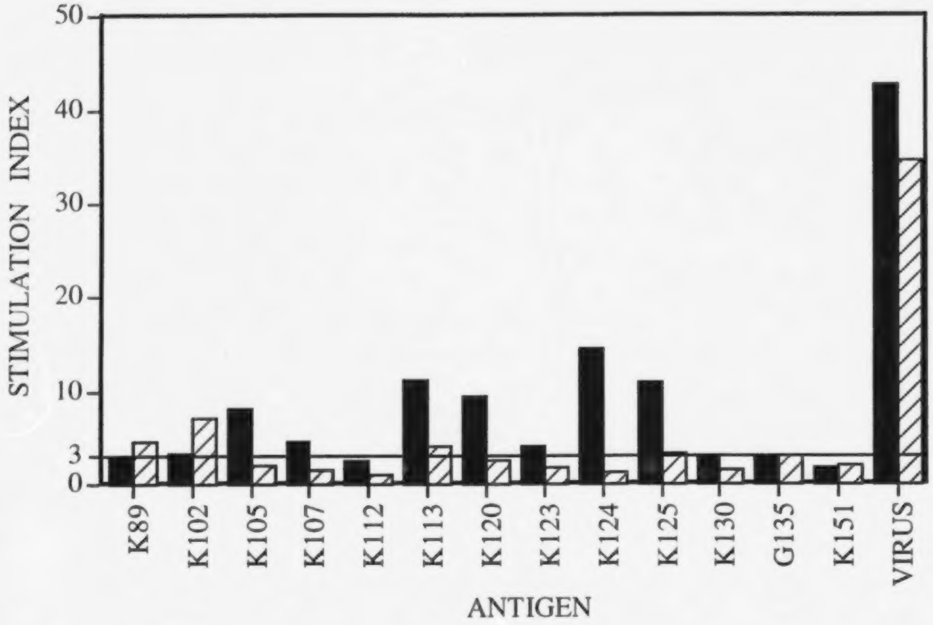

Figure IV- 7. Haplotype restriction of T cell epitopes. Proliferative responses of UV-inactivated Mengo virus primed lymphocytes (seven days post-immunization) from C57BL/6 (■) and SJL/J (▨) mice to synthetic peptides containing T cell epitopes identified in BALB/c mice.

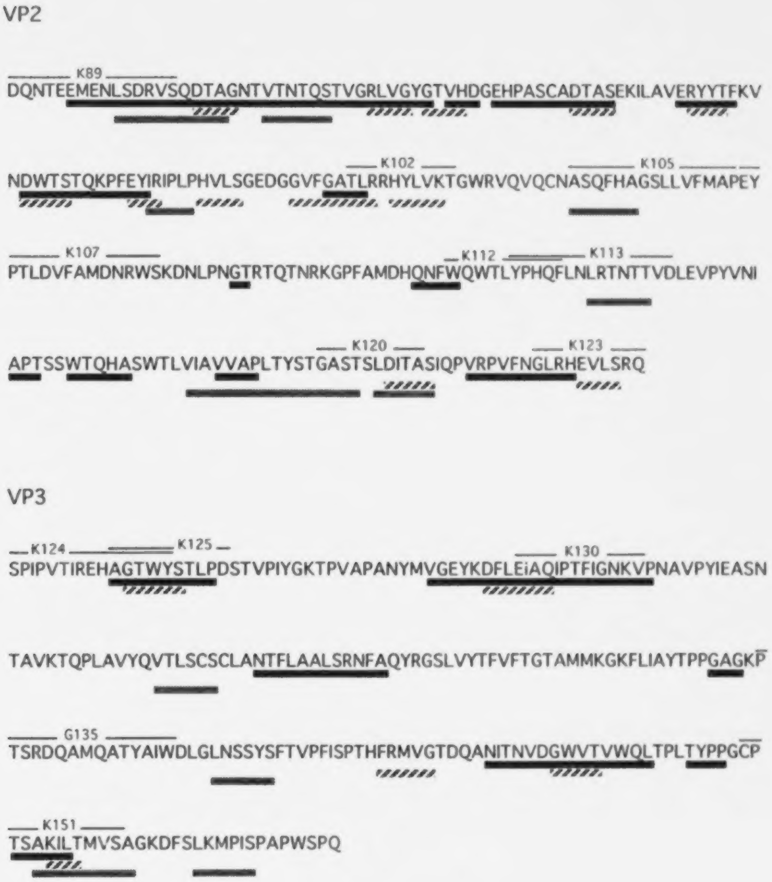
VP2
K89
DQNTEEMENLSDRVSQDTAGNTVTNTQSTVGRLVGYGTVHDGEHPASCADTASEKILAVERYYTFKV
K102
K105
NDWTSTQKPFEYIRIPLPHVLSGEDGGVFGATLRRHYLVKTGWRVQVQCNASQFHAGSLLVFMAPEY
K107
K112
K113
PTLDVFAMDNRWSKDNLPNGTRTQTNRKGPFAMDHQNFWQWTLYPHQFLNLRTNTTVDLEVPYVNI
K120
K123
APTSSWTQHASWTLVIAVVAPLTYSTGASTSLDITASIQPVRPVFNGLRHEVLSRQ
VP3
K124
K125
K130
SPIPVTIREHAGTWYSTLPDSTVPIYGKTPVAPANYMVGEYKDFLEiAQIPTFIGNKVPNAVPYIEASN
TAVKTQPLAVYQVTLSCSCLANTFLAALSRNFAQYRGSLVYTFVFTGTAMMKGKFLIAYTPPGAGKP
G135
TSRDQAMQATYAIWDLGLNSSYSFTVPFISPTHFRMVGTDQANITNVDGWVTVWQLTPLTYPPGCP
K151
TSAKILTMVSAGKDFSLKMPISPAPWSPQ

Figure IV- 8. Prediction of T cell epitopes in VP2 and VP3. Comparison of the location of T-cell epitopes predicted by the TSites AMPHI (▬), Rothbard and Taylor motif (▨) and "D" motif (▬) algorithms with peptides containing the experimentally identified T cell sites (indicated above the sequence) in VP2 and VP3.

program to be antigenic although each does stimulate a high level of lymphocyte proliferation in the *in vitro* assays. The VP3 peptides K125, K130 and K151 are predicted by one or more search strategy to be antigenic but VP3 also contains sites within peptides K124 and G135 which are not predicted by the TSites program.

DISCUSSION

We have shown that immunization of mice with inactivated Mengo virus induces a CD4$^+$ T cell response. Induction of this response is generally believed to occur through the uptake of exogenous nonreplicating and soluble antigens into the endosomal pathway by antigen-presenting cells. The antigen is processed into peptide fragments which are presented on the cell surface in association with major histocompatibility complex (MHC) class II molecules. Interaction of the peptide bound to the MHC class II molecule with the T cell receptor of CD4$^+$ T-helper cells stimulates their proliferation. Although induction of a CD8$^+$ T cell specific response to soluble antigen through peptide presentation by MHC class I molecules has been demonstrated in a number of systems (Raychaudhuri & Morrow, 1993), we observed no CD8$^+$ lymphocyte response to UV-inactivated Mengo virus.

Thirteen peptides which contain Th cell epitopes were identified in Mengo virus capsid proteins VP2 and VP3 (Figure IV-5); no epitopes were identified in VP1 or VP4. At the time the peptide panel was synthesized for this study peptides 10 to 18 residues in length were chosen. Based on more recent observations that MHC class II bound peptides tend to be 12 to 24 residues in length it is possible, depending on the positions in the peptides of residues which are critical for binding, that T cell epitopes could have gone undetected using peptides as short as 10 residues (Brown *et al.*, 1993). The immunodominance of VP2 and VP3 was confirmed by the *in vitro* stimulation of lymph node cells from BALB/c mice immunized with purified capsid proteins VP1, VP2 or VP3: *in vitro* stimulation with inactivated Mengo virus induced high levels of lymphocyte proliferation in VP2 or VP3 primed lymph node cells, whereas the proliferation of VP1 LN cells was minimal. The low level of stimulation seen with the VP1 primed lymph node cells does suggest the presence of weak T cell sites in VP1, but these were not detectable in the *in vitro* proliferation assay with peptides. It is likely that Th cell epitopes in VP1 and VP4 (as well as additional ones in VP2 and VP3) do exist but are not recognized by the H-2^d MHC molecule which binds the 13 different peptides in VP2 and VP3.

Figure IV-6 shows the positions of the known B-cell epitopes of Mengo virus together with the T cell epitopes identified in this study on ribbon diagrams of VP2 and VP3. Two linear regions of B cell antigenicity, one in each capsid protein, are each partially overlapped by a T cell epitope. This may be related to the linkage of B and T cell determinants which has been observed with several other viruses. Such studies suggest that the existence of B and T cell epitopes in close proximity is a factor in determining the efficiency of an antibody response to that site (Kutubuddin *et al.*, 1992; LeClerc *et al.*, 1991; LeClerc *et al.*, 1993). For both VP2 and VP3 the Th cell epitope is linked to the amino end of the associated B cell epitope, and there is evidence that the orientation of the T cell epitope with respect to the B cell epitope is important for promoting production of high affinity antibodies. For example, it has been demonstrated that immunization of mice with chimeric peptides composed of a T cell epitope linked to the amino terminus of a B cell epitope induces the production of higher affinity antibodies than does immunization with peptide containing the epitopes in the opposite orientation (Partidos *et al.*, 1992). This observation is potentially relevant for the design of synthetic vaccines, and it is possible that orientation of epitopes may play a role in the selection of immunodominant sites in intact pathogens.

Comprehensive studies of picornavirus T cell epitopes have been reported for rhinovirus and poliovirus (Hastings *et al.*, 1993; Mahon *et al.*, 1992). Overlapping synthetic peptides covering the entire capsid protein sequence for human rhinovirus type 1A were used to identify Th cell epitopes in BALB/c ($H\text{-}2^d$), CBA ($H\text{-}2^k$) and C57BL/10 ($H\text{-}2^b$) mice. For the BALB/c mice, only 4 Th cell epitopes (peptide S.I.>2) were found: one in VP1 (residues 211-230), one in VP2 (101-120) and two in VP3 (161-180, 181-200). The VP2 peptide 101-120 was also active in CBA mice, but not in C57BL/10 mice; the other 3 rhinovirus Th epitopes were H-2 restricted. All of these epitopes are found in elements of the 8-stranded β-barrel which comprises the interior core of each of the capsid polypeptides. None of the rhinovirus epitopes recognized by BALB/c mice correspond structurally with the Mengo virus epitopes which we have identified. Among the T cell epitopes found for poliovirus in mice (Mahon *et al.*, 1992) one is in the loop between the β-H and β-I strands of VP3; this sequence in type 1 and type 2 poliovirions also contains a neutralizing epitope (Weigers & Dernick, 1992; Patel *et al.*, 1993). The same structural region in the Mengo virion is represented by peptide K151, which has a high stimulation index for Th cells from BALB/c (but not from SJL/J or C57BL/6) mice.

A number of previous studies have suggested that variable regions of protein pathogens are preferentially recognized by T cells. For example, examination of the normal T cell response to poliovirus in humans localized most of the response to VP1 to the hypervariable regions of the capsid protein (Graham *et al.*, 1993). As well, analysis with poliovirus-specific murine CD4$^+$ T cell clones defined T cell epitopes in the variable region of VP1 adjacent to neutralizing antibody site I and in variable regions at the amino terminal and in surface regions of VP3. Mutations within the T cell epitope have been shown to abolish virus-specific CD4$^+$ and CD8$^+$ T cell responses by two possible mechanisms (Mahon *et al.*, 1992). First, recognition of the epitope by the MHC molecule or the T cell receptor can be affected by substitutions within the core of the epitope. Second, it is possible that substitutions in sequences flanking the core of the epitope prevent T-cell recognition by altering the pattern of antigen processing. In our study a number of epitopes were identified in variable stretches on the interior and exterior surfaces of capsid proteins VP2 and VP3. The amino terminal 14 residues of VP2 and 20 residues of VP3 contain Th epitopes. As well, VP2 sequences represented by peptide K107 and parts of peptides K102 and K103 are composed of surface residues. Significant portions of peptides K130 and G135, which contain Th epitopes in VP3, are found on the surface. However, we (and Hastings *et al.*, 1993) have identified epitopes in the two capsid proteins that are composed of interior residues in the protein tertiary structure, suggesting that T cell epitopes need not be confined to highly variable sites. Variation in the sequence of the internal structure of the capsid proteins cannot be ruled out as a mechanism for eluding immune surveillance, but these regions should be much less susceptible to sequence variation because of the requirement to maintain the structural and functional integrity of the capsid. Recognition of conserved regions by the T cells would be advantageous for the immune system because the virus would have only a very limited capacity to mutate these regions to avoid immune recognition. Additional support for this idea comes from the observation that VP4 of poliovirus, which is also found entirely on the interior of the capsid and important for maintaining the structural integrity of the pentameric subunits of the capsid, is recognized by Th cells in both humans and mice (Mahon *et al.*, 1992; Simons *et al.*, 1993).

Examination of the Mengo virus Th cell epitopes detected in BALB/c mice in two other strains of mice indicated that the pattern of recognition of these epitopes is dependent on the MHC haplotype (see Figure IV-7). Of the 13 epitopes which induced a proliferative response in Mengo virus primed lymph node cells from BALB/c ($H\text{-}2^d$) mice, 11 were recognized by similarly primed lymphocytes from C57BL/6 ($H\text{-}2^b$) mice, but only five were recognized in SJL/J ($H\text{-}2^s$) mice. The magnitude of the proliferative response induced by each peptide was also strain dependent. In fact, the response of

SJL/J mice to whole inactivated virus, as well as most of the peptides, was consistently less than the response of BALB/c or C57BL/6 mice. This restriction of specificity is dependent on the nature of the peptide-MHC complex or of the T cell receptor (discussed in Panina-Bordignon *et al.*, 1989). MHC molecules are highly polymorphic and studies have shown that a given peptide will generally bind to only one or a few alleles. However, the existence of promiscuous epitopes that are recognized by a large number of MHC class II molecule alleles have also been demonstrated (Panina-Bordignon *et al.*, 1989). Five of the peptides identified to contain Th cell epitopes in this study (K89, K102, K113, K125, G135) were recognized by all three strains of mice tested and may belong to the group of promiscuous epitopes. However, this would have to be tested on a large panel of mouse strains representing as many of the allelic forms of the MHC molecule as possible. Identification of such epitopes is important for understanding the restriction of T cell epitopes, and could facilitate identification of similar epitopes in infectious organisms and in the production of synthetic vaccines with broad specificity.

Considerable effort has been made to establish an *a priori* identification of immunogenic T cell epitopes, and we have examined the predictive power of the program TSites (Feller & de la Cruz, 1991) in the context of our experimental results for the Mengo virion (Figure IV-8). The TSites program identified significant portions of all the capsid proteins as potentially antigenic based on selected criteria for the correlation of T cell antigenicity to protein sequence and structure. The number of predicted sites per unit length was roughly similar for capsid proteins VP1, 3 and 4. VP2, however, had a much higher number of epitopes predicted (particularly in the first 110 residues and the last 55 residues) by all strategies. This large number of predicted sites correlates well with the observed antigenicity of VP2 which contains 8 of the 13 experimentally identified peptides corresponding to sites of T cell immunogenicity.

In VP2 and VP3, 9 of the 13 peptides experimentally determined to contain Th epitopes overlap sites which were predicted to be potentially antigenic. No one algorithm of the program appeared to have any more significant success at predicting the sites than the others, and sites predicted by more than one strategy do not appear more likely to be real epitopes than sites predicted by only one algorithm. The fact that more of the predicted sites were not identified experimentally is not necessarily indicative of any lack of predictive power or specificity of the algorithms making up the TSites program because the limited scope of our experiments only identified peptides which were recognized by the H-2^d MHC haplotype. It is more significant to note that the Th cell sites represented by peptides K107 and K112 in VP2 and by peptides K124 and G135 in VP3 were not identified by any of the predictive strategies to be potentially immunogenic. Clearly there exist recognition motifs and/or structures that cannot yet be adequately predicted by even a combination of searching strategies. Experimentally identified Th cell epitopes in VP1 of poliovirus (Kutubuddin *et al.*, 1992) have been compared with the AMPHI and the Rothbard and Taylor motif predictive strategies and no strong correlation was found between the predicted and observed epitopes. Studies with Dengue virus (LeClerc *et al.*, 1993) and the Th cell epitopes of lysozyme (Gammon *et al.*, 1991) also demonstrate the difficulties of using the available predictive strategies to identify T cell epitopes. Experimental identification of epitopes currently appears to be the only reliable way to identify T cell epitopes recognized by specific class I or class II MHC molecules of various haplotypes. The identification and characterization of many more actual epitopes is required to refine predictive strategies.

REFERENCES

Baker, P.J. (1993). Suppressor T Cells. *ASM News* **59**,123-128.

Boege, U., D. Kobasa, S. Onodera, G.D. Parks, A.C. Palmenberg, and D.G. Scraba (1991). Characterization of Mengo virus neutralization epitopes. *Virology* **181**, 1-13.

Boege, U., D.S.-W. Ko and D.G. Scraba (1986). Toward an *in vitro* system for picornavirus assembly; purification of Mengovirus 14S capsid precursor particles. *Journal of Virology* **57**, 275-284.

Brown, J.H., T.S. Jardetzky, J.C. Gorga, L.J. Stern, R.G. Urban, J.L. Strominger and D.C. Wiley (1993). Three-dimensional structure of the human class II histocompatibility antigen HLA-DR1. *Nature* **364**, 33-39.

Coffman R.L., B.W. Seynour, D.A. Lebman, D.D. Hiraki, J.A. Christiansen, B. Schrader, H.M. Cherwinski, H.M. Savelkoul, F.D. Finkelman, M.W. Bond, and T.R. Mosmann (1988). The role of helper T cell products in mouse B cell differentiation and isotype regulation. *Immunology Reviews* **102**, 5-28.

DeLisi, C. and J.A. Berzofsky (1985). T-cell antigenic sites tend to be amphipathic structures. *Proceedings of the National Academy of Sciences, U.S.A. 82*, 7048-7052.

Ellem, K.A.O. and J.S. Colter (1960). The interaction of infectious ribonucleic acid with a mammalian cell line. I. Relationship between the osmotic pressure of the medium and the production of infectious centers. *Virology* **11**, 434-443.

Ellem, K.A.O. and J.S. Colter (1961). The isolation of three variants of Mengo virus differing in plaque morphology and hemagglutinating characteristics. *Virology* **15**, 340-347.

Feller, D.C. & V.F. De La Cruz (1991). Identifying antigenic T-cell sites. *Nature* **349**, 720-721.

Gammon, G., H.M. Geysen, R.J. Apple, E. Pickett, M. Palmer, A. Ametani and E.E. Sercarz (1991). T cell determinant structure: cores and determinant envelopes in three mouse major histocompatibility complex haplotypes. *Journal of Experimental Medicine 173*, 609-617.

Graham, S., E.C.Y. Wang, O. Jenkins and K.L. Borysiewicz (1993). Analysis of the human T-cell response to picornaviruses: identification of T-cell epitopes close to B-cell epitopes in poliovirus. *Journal of Virology* **67**, 1627-1637.

Hagenmaier, H. and H. Frank (1972). Increased coupling yields in solid phase peptide synthesis with a modified carbodiimide coupling procedure. *Hoppe-Seyler's Zeitschrift für Physiologische Chemie* **353**(S), 1973-1976.

Hastings, G.Z., M.J. Francis, D.J. Rowlands and B.M. Chain (1993). Epitope analysis of the T cell response to a complex antigen: proliferative responses to human rhinovirus capsids. *European Journal of Immunology* **23**, 2300-2305.

Houghten, R.A. (1985). General method for the rapid solid-phase synthesis of large numbers of peptides: specificity of antigen-antibody interaction at the level of individual amino acids. *Proceedings of the National Academy of Sciences, U.S.A.* **82**, 5131-5135.

Krishnaswamy, S. and M.G. Rossmann (1990). Structural refinement and analysis of Mengo virus. *Journal of Molecular Biology* **211**, 803-844.

Kutubuddin, M., J. Simons and M. Chow (1992). Identification of T-helper epitopes in the VP1 capsid protein of poliovirus. *Journal of Virology* **66**, 3042-3047.

LeClerc, C., E. Deriaud, V. Mimic and S. Van Der Werf (1991). Identification of a T-cell epitope adjacent to neutralization antigenic site 1 of poliovirus type 1. *Journal of Virology* **65**, 711-718.

LeCLerc, C., E. Deriaud, F. Megret, J. Briand, M.H.V. Van Regenmortel, and V. Deubel (1993). Identification of helper T cell epitopes of Dengue virus E-protein. *Molecular Immunology* **30**, 613-625.

Luo, M., G. Vriend, G. Kamer, I. Minor, E.A. Arnold, M.G. Rossmann, U. Boege, D.G. Scraba, G.M. Duke and A.C. Palmenberg (1987). The atomic structure of Mengovirus at 3.0Å resolution. *Science* **235**, 182-191.

Mahon, B.P., K. Katrak and K.H.G. Mills (1992). Antigenic sequences of poliovirus recognized by T cells: serotype-specific epitopes on VP1 and VP3 and cross-reactive epitopes of VP4 defined by using $CD4^+$ T-cell clones. *Journal of Virology* **66**, 7012-7020.

Margalit, H., J.L. Spouge, J.L. Cornette, K.B. Cease, C. DeLisi, and J.A. Berzofsky (1987). Prediction of immunodominant helper T-cell antigenic site from the primary sequence. *Journal of Immunology* **138**, 2213-2229.

Merrifield, R.B. (1963). Solid phase peptide synthesis I. The synthesis of a tetrapeptide. *Journal of the American Chemical Society* **85**, 2149-2154.

Mosmann, T.R. and R.L. Coffman (1989). Heterogeneity of cytokine secretion patterns and functions of helper T cells. *Advances in Immunology* **46**, 111-147.

Pallidino, G., P.A. Scherle, and W. Gerhard (1991). Activity of $CD4^+$ T-cell clones of type 1 and type 2 in generation of influenza virus specific cytotoxic responses *in vitro*. *Journal of Virology* **65**, 6071-6076.

Panina-Bordignon, P., A. Tan, A. Termijtelen, S. Demotz, G. Corradin, and A. Lanzavecchia (1989). Universally immunogenic T cell epitopes: promiscuous binding to human MHC class II and promiscuous recognition by T cells. *European Journal of Immunology 19*, 2237-2242.

Partidos, C., C. Stanley and M. Steward (1992). The influence of orientation and number of copies of T and B cell epitopes on the specificity and affinity of antibodies induced by chimeric peptides. *European Journal of Immunology* **22**, 2675-2680.

Patel, V., M. Ferguson and P.D. Minor (1992). Antigenic sites on type 2 poliovirus. *Virology* **192**, 361-364.

Raychaudhuri, S. and W.J.W. Morrow (1993). Can soluble antigens induce $CD8^+$ cytotoxic T-cell responses? A paradox revisited. *Immunology Today* **14**, 344-348.

Rheinherz, E.L. and S.F. Schlossman (1981). The characterization and function of human immunoregulatory T lymphocytic subsets. *Immunology Today* **2**, 69-75.

Rothbard, J.B. and W.R. Taylor (1988). A sequence pattern common to T cell epitopes. *EMBO Journal* **7**, 93-100.

Sette, A., S. Buus, E. Appella, J.A. Smith, R. Chestnut, C. Miles, S.M. Colon and H.M. Grey (1989). Prediction of major histocompatibility complex binding regions of protein antigens by sequence pattern analysis. *Proceedings of the National Academy of Sciences, U.S.A.* **86**, 3296-3300.

Simons, J., M. Kutubuddin and M. Chow (1993). Characterization of poliovirus-specific T lymphocytes in the peripheral blood of Sabin-vaccinated humans. *Journal of Virology* **67**, 1262-1268.

Weigers, K. and R. Dernick (1992). Molecular basis of antigenic structures of poliovirus: implications for their evolution during morphogenesis. *Journal of Virology* **66**, 4597-4600.

Ziola, B.R. and D.G. Scraba (1974). Structure of the Mengo virion. I. Polypeptide and ribonucleate components of the virus particle. *Virology* **57**, 531-542.

CHAPTER V

MECHANISMS OF NEUTRALIZATION BY MONOCLONAL ANTIBODIES

INTRODUCTION

The determinants recognized by neutralizing monoclonal antibodies have been identified for a large number of picornaviruses and well characterized with respect to their location on virions. As shown in Chapters II and III antibodies bind to accessible surface structures of these virions. Additional studies with protein antigens indicate that many of the residues in the epitope contribute to stable binding but only a few of the residues are critical for the specific recognition of the epitope (Jin *et al.*, 1992). As well, recognition is enhanced by the induction of conformational changes within the combining site of the immunoglobulin molecule as well as within the epitope of the antibody (reviewed in Davies and Padlan, 1992; Rini *et al.*, 1992).

In contrast to the emphasis which has been placed on mapping and characterization of the B cell epitopes of viral antigens, less effort has been directed towards elucidating the mechanisms by which antibodies mediate the neutralization of picornavirions. A number of mechanisms have been proposed and a given antibody may utilize two or more of these mechanisms to efficiently neutralize virus. Neutralization of picornavirions can be mediated by antibody coating of the virion to sterically block its attachment to a host cell surface receptor, reduction of individual infectious units through aggregation of virions by bivalent antibody attachment, conformational changes induced by antibody binding leading to capsid dissociation and loss of the RNA genome, cross-linking of virions by the bivalent bridging of pentamers by antibody molecules so that uncoating is prevented, or locking the conformation of the virions.

In this chapter, some experimental data are presented which suggest the operative mechanism(s) by which neutralizing monoclonal antibodies produced against subviral pentamers or attenuated virus may neutralize Mengo virions.

METHODS

Antibody Purification

Monoclonal antibodies, JEL 370 (IgM) and 3A (IgA) were both purified from tissue culture supernatants by size exclusion chromatography on a 65 cm x 1.6 cm Sephacryl S-300 Superfine (Pharmacia) column. To begin purification, to approximately 100 ml of supernatant was added sufficient volume of 100% saturated ammonium sulphate solution (761g/1L, pH 7.0) to bring the saturation level of the supernatant to 60% ammonium sulphate. The supernatant was incubated overnight at 4° and then the precipitate collected by centrifugation at 3000xg for 30 minutes at 4°. The precipitate was then resuspended in 1/50 to 1/20 the starting volume of supernatant in PBS to solubilize the pellet. The entire preparation was then loaded onto the Sephacryl column and eluted in complete PBS (flow rate of 5 ml/hr). Fractions of one mL were collected until the entire sample had been eluted. Fractions were monitored for protein content by checking the absorbance of every fifth fraction at 260 nm, and the antibody peak was identified by ELISA. The antibody peak was examined for purity by SDS-polyacrylamide gel electrophoresis.

Standard plaque assay

One day before the assay 6-well tissue culture plates (Costar) were seeded with $2x10^6$ mouse L-929 cells per well in 5 mL 199 medium supplemented with 5% FCS. The virus samples were diluted in either "virus diluent" (500 mL complete PBS, pH 7.2, 0.2% bovine serum albumin (BSA), 50 µg/mL phenol red, penicillin and streptomycin), tissue culture hybridoma supernatant, or complete PBS. Medium was removed from the cell monolayers by vacuum aspiration, and 200 µl of virus sample was added to each well. The plates were incubated at 20° for 60 min and every 10 min the medium in the wells was redistributed over the cells by gentle shaking so the cells did not dry. Each well was overlayed with a mixture of equal parts of 1.6% agar in H_2O and 2x DME medium supplemented with 20% heat inactivated calf serum at 48°. The overlay was allowed to solidify for 10 min and the plates were incubated at 37° in 5% CO_2 for 24 to 48 hours before staining to visualize the plaques produced by cell lysis. To stain the wells, 2 mL of overlay mixture containing 0.01% neutral red was added to each well and incubated as before. Plaques become visible in about 12 to 24 hours.

Determination of the ND_{95} of Purified Monoclonal Antibody Preparations

Before using the purified stocks of monoclonal antibodies to study the effects of antibody attachment on virus infectivity, the neutralizing activity was standardized by determining the amount of antibody required to give 95% neutralization of a defined amount of virus (ND_{95}). A $2x10^4$ PFU/mL dilution of wild type virus was prepared in virus diluent. The virus sample was further diluted 1:10 into serial dilutions of the antibody stock also prepared in virus diluent. These samples were then incubated for 2 hr at 20° and then the remaining infectivity in the samples was assayed using the standard plaque assay procedure.

Determination of the Antibody:Virus Ratios Required For Neutralization

Using purified stocks of monoclonal antibody and Mengo virus a range of virus dilutions was made in the presence of a constant concentration of antibody. Antibody-virus mixtures were incubated 2 hr at 20° and then each mixture was diluted, in virus diluent, to a final virus concentration of $2x10^3$ PFU/mL. The number of infectious virions remaining in each sample was determined by standard plaque assay. The antibody to virus ratio in the undiluted samples was calculated based on the known concentrations of the antibody and virus stocks. For both murine IgM and IgA one absorbance unit at 280 nm is equal to 1 mg antibody/mL (Harlow and Lane, 1988). The number of molecules of antibody were then calculated from the known molecular mass of the antibody molecule and Avogadro's number. The number of Mengo virions were calculated from the relationship that one absorbance unit at 260 nm is equal to $9.5x10^{12}$ particles.

Electron microscopy of monoclonal antibody-Mengo virus complexes

Mengo virus complexes with antibodies 3A and JEL 370 were examined by electron microscopy. Virus-antibody samples were prepared by incubating 10^9 PFU/mL wild-type virus with purified monoclonal antibody at 20° for 2 hr. Samples were negatively-stained with 2% sodium phosphotungstate (pH 7.0) and photographed in a Philips EM420 electron microscope operated at 100 kV.

Attachment inhibition assays

In parallel with plaque neutralization analysis of the virus-antibody mixtures the ability of the antibody to inhibit the attachment of virus to cells was also determined. For this assay 60 mm tissue culture petri dishes were seeded with 4×10^6 cells/plate in 10 mL 199 medium supplemented with 5% FCS the day before the assay. On the day of the assay the plates were cooled to 4° and the remainder of the assay was continued on ice. The medium was removed, and 250 µl of the antibody-virus (^{3}H-labeled virus) mixture was added to the plate. The plates were incubated with occasional shaking to keep the medium distributed over the cells. After 1 hr the medium, containing all unattached virus, was collected and the cell monolayer was washed twice with 1 mL of cold PBS. The medium and washings were counted together in 10 mL of aqueous counting scintillant (Amersham) using a scintillation counter (Beckman LS 7800) to determine the total amount of labeled virus remaining unattached. To determine the amount of label associated with the cells (virus attached to cells) the cell monolayer was solubilized in 1 mL of 2% SDS in 10 mM sodium phosphate buffer, pH 7.2, collected into a scintillation vial and counted as before. The counting program used for this experiment was set up to account for the differential quenching of the radioactivity due to the different compositions of each sample.

Antigen Capture ELISA

This was a modified antigen capture assay used to assess the ability of an antibody to bind to mutant virions which escape neutralization by the selecting antibody. This assay is useful because it eliminates the need to purify each mutant virus stock for testing as would have to be done if the antigen was to be bound directly to the plate. Purified IgA (monoclonal antibody 3A) or IgM (monoclonal antibody JEL 370) at 20 µg/ml, 100µl/well in complete PBS was added to ELISA plate wells. The plates were incubated overnight at 4°. The wells were washed twice with PBS-Tween and blocked for one hour at 20° with 1% BSA in PBS. After another wash 100 µl of unpurified mutant virus stock (from 25 cm^2 flask culture stock) was added to each well. The plate was incubated 2 hr at 20° and then washed twice. Monoclonal antibody (tissue culture hybridoma supernatant) was added to the wells (100 µl/well) and incubated for 2 hr at 20°. The remainder of the procedure involved the detection of bound antibody using the appropriate anti-mouse antibody conjugated to alkaline phosphatase or horse radish peroxidase as described in Chapter III, pages 63 and 64.

RESULTS

Monoclonal antibodies JEL 370 (IgM) and 3A (IgA) were purified from tissue culture supernatants using ammonium sulphate concentrated preparations and size

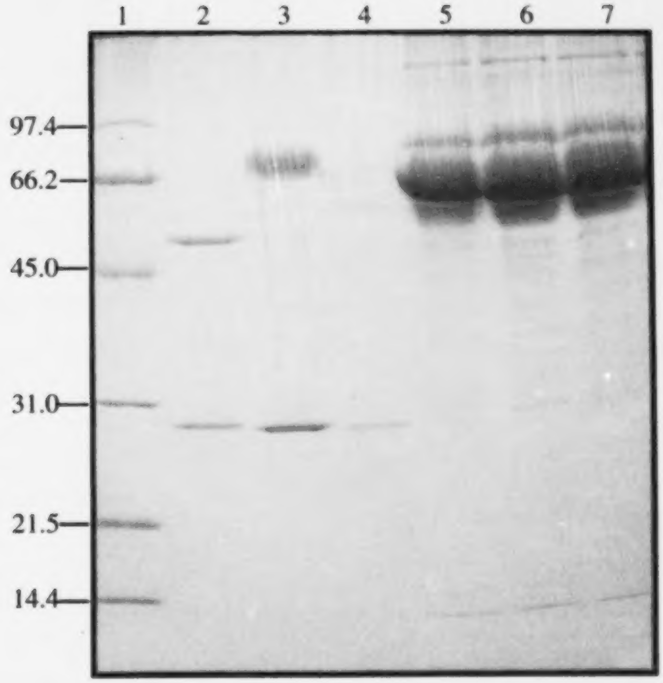

Figure V-1. Purification of monoclonal antibodies. Lane 1 contains molecular weight markers. Lanes 2, 3 and 4 contain purified monoclonal antibodies MCP5 (IgG), JEL 370 (IgM) and 3A (IgA) respectively. Lanes 5, 6 and 7 contain unpurified hybridoma supernatants from cell lines MCP5, JEL 370 and 3A respectively.

exclusion chromatography in a S300 Sephacryl column. IgM has an approximate molecular weight of 970 000 and was eluted in the void volume. Very few other proteins of this size are expected to be in the fetal bovine serum used to supplement the medium and the IgM antibody was collected free of contaminants (Figure V-1, lane 3). The bands in the denaturing gel demonstrate the presence of the 65 kDa heavy chain of the immunoglobulin and the 25 kDa light chain. IgA is also a very large molecule with molecular weight of approximately 160 000 and it too is excluded from the column free of contaminants. It is not clear why the expected heavy chain band for IgA at approximately 56 kDa was revealed as an indistinct fuzzy band (Figure V-1, lane 4), but ELISA results of the purified antibody indicate that it is immunoglobulin type A.

Antibody-Mengo virus complexes were examined by electron microscopy. Either purified monoclonal antibody 3A (IgA) or JEL 370 (IgM) was incubated with 10^9 PFU/mL of Mengo virus. Both antibodies caused extensive aggregation of virions (Figure V-2). Each IgM molecule has 10 combining sites and would be expected to aggregate virions. Antibody JEL 370-virus aggregates were loose structures, each containing several hundred virions. Antibody 3A caused the formation of large, tightly packed aggregates.

The efficiency of neutralization of Mengo virus by antibody JEL 370 was determined by incubating a series of virus dilutions in the presence of a constant concentration of the antibody. Each mixture was then diluted to a constant final virus concentration and the remaining infectivity in each was determined by plaque assay. The results are summarized in Table V-1. The optimal antibody:virus ratio was in the range of 26 to 260:1, with 95% of the virus neutralized in this range. At higher or lower antibody:virus ratios the efficiency of neutralization was decreased.

It was of interest to examine further the nature of IgA 3A-Mengo virus complexes and to determine the mechanism(s) of neutralization because antibody 3A is a very efficient neutralizing antibody. The ability of the antibody to prevent the attachment of virions to cell surface receptors was determined by adding radiolabelled virions, with or without the antibody, to monolayers of mouse fibroblast cells at 4° (Table V-2). The infectivity of each antibody-virus mixture was also determined using parallel plaque assays. Antibody 3A inhibited the attachment of virions to cells at all virus concentrations except 10^{10} PFU/mL; even at this concentration virus is able to attach to cells but infectivity is still reduced to very low levels.

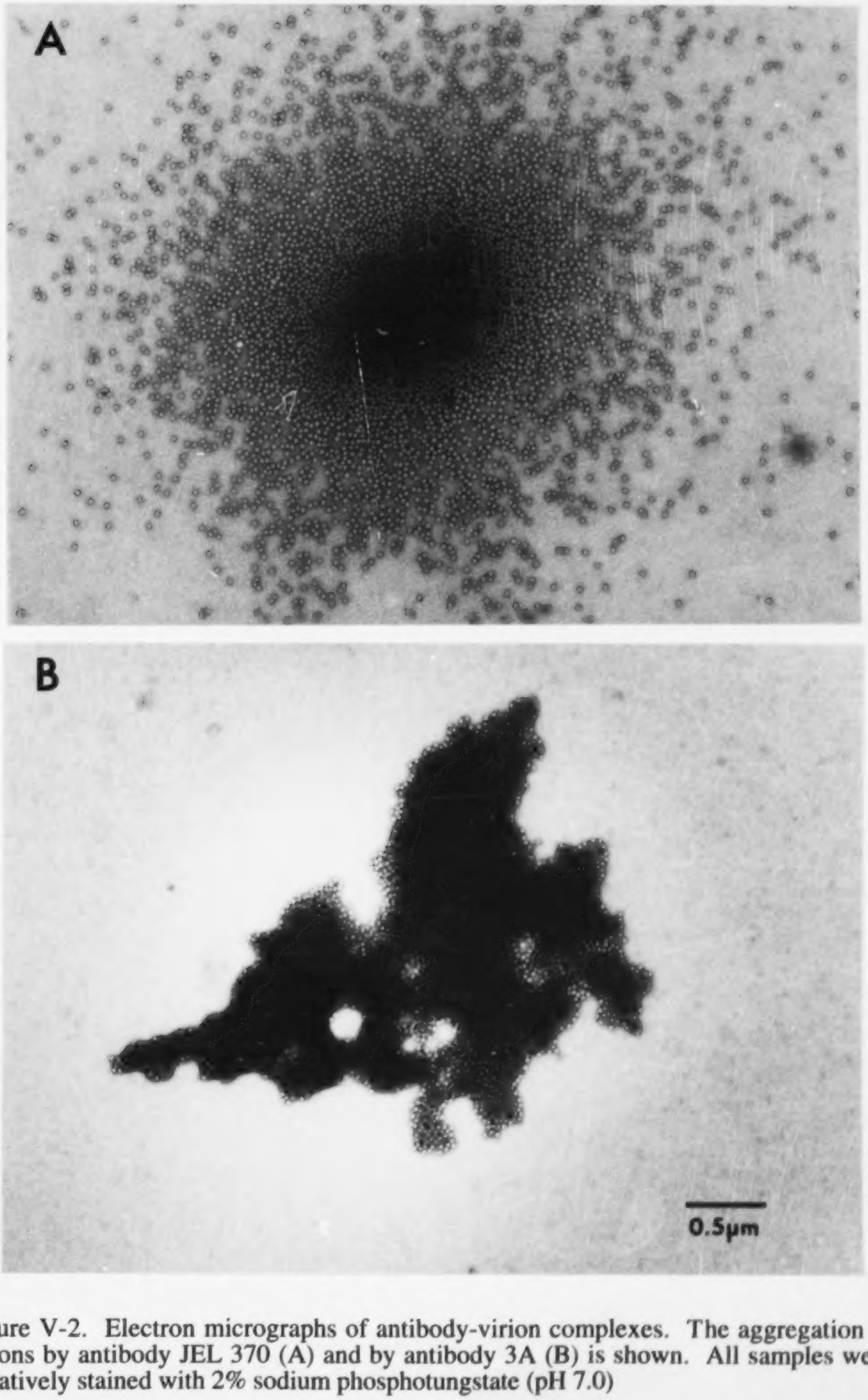

Figure V-2. Electron micrographs of antibody-virion complexes. The aggregation of virions by antibody JEL 370 (A) and by antibody 3A (B) is shown. All samples were negatively stained with 2% sodium phosphotungstate (pH 7.0)

TABLE V-1

Effect of the Antibody:Virion Ratio
on the Efficiency of Neutralization by Antibody JEL 370

Antibody:virion ratio	Percentage Neutralization
2.6:1	85%
26:1	95%
260:1	95%
2600:1	73%

TABLE V-2

Effect of Antibody 3A on Virion Attachment to Cells and Neutralization of Virions[a]

Number of plaque forming units	Attachment of virions to cells	Neutralization of virions
10^7	0%	100%
10^8	0%	100%
10^9	0%	100%
10^{10}	55%	95%

[a] Samples were prepared using a constant amount of purified antibody 3A.

The ability of a neutralizing monoclonal antibody to bind to mutants of Mengo virus selected for their ability to escape neutralization with that antibody can also be used to infer information about the mechanism of neutralization. Each mutant selected with the anti-Mengo virus monoclonal antibodies (characterized in Chapters II and III) was examined for its ability to be recognized by its selecting antibody using an antigen capture ELISA. A number of antibodies were identified which were still able to bind to at least one of their neutralization escape mutants. For example, antibody MCP4 can bind to mutants 4/01 and 4/12; both mutants 4/01 and 4/04 have a Lys→Glu mutation at residue 2075. Mutant 4/04, on the other hand, has an additional Ser→Thr mutation at residue 2147 which abolishes the binding of antibody MCP4 to the virion. Antibody MCP6 was able to bind to mutant 6/18 which has a Lys→Gln change at residue 2075. Antibody 9B was able to bind all of the mutants which were selected by their ability to escape neutralization by 9B. Mutant 352/5 was the only mutant resistant to neutralization by antibody 352 which was still recognized by the antibody. It is very interesting to observe that a single mutation in the antibody binding site on a virion can eliminate the ability of the antibody to neutralize the virion even though it can still bind to its epitope.

DISCUSSION

A series of preliminary experiments have been done to obtain information concerning the mechanism of neutralization of some of the anti-Mengo virus monoclonal antibodies generated in Chapters II and III.

The first antibody examined, JEL 370, is an IgM which recognizes VP1 in the region of residue 1100. Examination of virus-antibody complexes by electron microscopy indicated the formation of loose aggregates, as would be expected from the multiple binding sites available on the pinwheel shaped immunoglobulin. Neutralization is optimal at an antibody to virus ratio of between 26 and 260:1; in this range >95% of virions are neutralized. At higher or lower antibody to virus the efficiency of neutralization is decreased. At high antibody to virus ratios most or all of the antibody binding sites on the virions would be expected to be saturated. Because of the low level of virus present, most of the bound antibody molecules will not be associated with more that one virion and aggregation will decrease. At antibody to virus ratios below the optimal level, some aggregation of virions occurs but there is probably too little antibody available to neutralize the virus efficiently. It appears therefore that aggregation of virions by JEL 370 contributes to the efficient neutralization of Mengo virus. Although the importance of aggregation has been questioned there is at least some evidence that it can be the sole mechanism of neutralization by some antibodies and that it may at least contribute to neutralization by others although in general it does not contribute significantly to neutralization (Thomas *et al.*, 1986; Mosser *et al.*, 1989; Colonno *et al.*, 1989).

Monoclonal antibody 3A (an IgA molecule) is interesting because it is extremely efficient at neutralizing Mengo virus. It was also shown to be able to cause extensive aggregation of virions. Attachment studies showed that at high antibody to virus ratios, attachment of virions to susceptible cells is completely blocked, and as a result the infectivity of the virions is completely abolished. At low antibody to virus ratios, attachment of virions to cells does occur and the virus-antibody aggregates retain a very low level of infectivity. At high concentrations of virus it would appear that there is no longer sufficient antibody to completely coat virions so they may attach to receptors and as a consequence the large virus-antibody aggregates become associated with cells. It is probable therefore, that antibody 3A mediates the neutralization of virions by blocking their attachment to cellular receptors and that when the antibody concentration falls below that required to mask all of the receptor-binding sites on the virions they are able to bind cells and initiate an infection.

A final set of experiments concerns the information which can be inferred about the mechanism of neutralization by examining the mechanism by which some mutants are able to escape neutralization by their selecting antibody. A number of studies have shown that binding of monoclonal antibodies to proteins can be prevented by only one amino acid mutation within the epitope recognized by an antibody (Wiley and Skehel, 1987; Sherry and Rueckert, 1985; Appleyard *et al.*, 1990; Page *et al.*, 1988). Mutants of poliovirus which escape neutralization but are still bound by their selecting antibody have also been observed (Ketterlinus *et al.*, 1993; Thomas *et al.*, 1986) but the implications of these observations concerning the mechanism by which an antibody is neutralizing virus have not been examined. Most of the neutralization escape mutants selected in Chapters II and III are no longer recognized by their selecting antibody. However a subset of mutants have been identified which are capable of escaping neutralization but are still recognized by their selecting antibody.

Antibody recognition of a mutant virion which escapes neutralization provides some circumstantial evidence that the mechanism of neutralization is neither by steric blocking of cellular attachment nor by aggregation of virions. Blocking of attachment can be eliminated because antibody binding to mutant virions does not block their attachment to cell surface receptors. Aggregation can be eliminated as the only mechanism of neutralization of virions by the antibody, although aggregation of virions may contribute to neutralization. It is possible that aggregation and/or inhibition of attachment may have been utilized by these antibodies to neutralize virions, but a mutation of the epitope has resulted in reduced affinity of the antibody for the epitope such that it cannot form stable antibody-virus aggregates or effectively block attachment of virions to cells. This possibility could be investigated by using electron microscopic examination of antibody-mutant virus complexes as well as assays to determine the inhibition of attachment of the complexes to cells. Elimination of receptor blocking and aggregation as the mechanisms of neutralization by some antibodies means that these antibodies must neutralize virions by one or more of the three remaining mechanisms. It is not possible to distinguish which one or combination of these mechanisms is actually being used, but it is possible to speculate how one might further examine the nature of the interaction of antibodies with both wild-type and mutant virions which are recognized by the antibody.

Some evidence has been presented to support the idea that bivalent attachment of antibodies to a single virion could crosslink subunits so the virion is unable to uncoat (Smith *et al.*, 1993). One way that one might be able to examine whether or not an antibody is able to cause pentamer crosslinking is by the controlled formation of antibody-virus complexes. By the very slow addition of small amounts of virus to a concentrated solution of antibody intravirion bivalent interaction with virions will be preferred over aggregation of virions. With the addition of more virus, the antibody will become saturated and the equilibrium formation of aggregates with more than one virion now sharing each antibody molecule would be favored unless the antibody initially attached bivalently to the virions. It is possible that neutralization resistant mutants to an antibody which utilizes pentamer crosslinking to neutralize virions could still be bound by the antibody. Mutations within the antibody binding site may not completely abolish binding of the antibody but they may sufficiently reduce the affinity of the antibody for the virion such that it is no longer able to prevent uncoating of virions. Unfortunately, this procedure will not work for IgM or dimeric IgA molecules because each has greater than two combining sites and will always bind multiple virions per immunoglobulin molecule.

The observation that antibody binding sometimes reduces the isoelectric point of virions suggests that a conformational change may be occuring, perhaps related to that induced upon receptor binding and which eventually leads to release of the RNA genome from the virion. However the change in pI does not correlate well with the degree of neutralization and it was recently suggested that the pI change may be due to small surface conformational changes as a result of antibody binding with no large changes in overall capsid conformation occuring (Brioen *et al.*, 1985; Smith *et al.*, 1993). Delaet *et al.* (1992) reported the conversion of native poliovirions to noninfectious empty capsids by one antibody, although this required external conditions of low ionic strength and under these conditions the stability of the structure of the virion is weakened (Delaet and Boeyé, 1994). No experimental evidence has yet been presented to support the conformational locking of virions as a result of antibody binding so that they are unable to release their RNA genomes into the cytoplasm of target cells, but Wetz (1993) suggests that bivalent attachment of antibody to virions would crosslink virions subunits and stabilize them against conformational changes which would otherwise result in virus uncoating.

The same assay as outlined above to examine bivalent crosslinking of pentamers could be used to provide information concerning the ability of an antibody to disrupt virions and destroy their infectivity by causing irreversible conformational changes in the capsid. If an antibody could effect a similar conformational change in Mengo virus the result should be easily determined by electron microscopy or centrifugation of antibody-virus complexes through sucrose gradients. The contacts between pentamers in Mengo virus are not nearly as extensive as found in poliovirions and Mengo virus does not form empty capsids *in vivo* or *in vitro* (Krishnaswamy *et al.*, 1990; Scraba *et al.*, 1990). Disruption of Mengo virions to release the RNA genome would probably dissociate virions into pentamers. It is difficult to imagine how a Mengo virion with a single mutation in the binding site for an antibody which neutralized the virus by inducing a conformational change in the capsid would be able to escape neutralization by that antibody when it is still capable of binding to the virion. Presumably the reason that an antibody would induce a conformational change in the virion would be to optimize contacts between the antibody and virion. If a critical residue is changed in this binding site which lowers the affinity of the antibody for the epitope the antibody will likely no longer bind to the epitope.

The final proposed mechanism of neutralization, locking of the conformation of virions as a result of antibody binding, is not particularly easy to demonstrate experimentally. One possible way to determine whether or not an antibody is capable of locking the conformation of the capsid into an inert form would be to examine the interaction of mutant virions which escape neutralization with cell surface receptor molecules in the presence of the antibody. Presumably the antibody would neutralize virions by preventing the conformational changes which lead to uncoating in order to maintain the conformation of the epitope which the antibody recognizes. Wild type virions, bound by such an antibody, would either be unable to attach to receptor molecules or to undergo the required conformational change once bound. Using a mutant virion which escapes neutralization but still binds the antibody one would expect to observe that, upon binding of the virion to the receptor the antibody would no longer be able to prevent the conformational change because of its greatly reduced affinity for its epitope and the antibody would dissociate from the virion.

Clearly such proposals are speculative but the characterization of antibodies which still bind to neutralization escape mutants might be useful tool for dissecting the process of neutralization of virions. Knowledge of the mechanisms of neutralization is important because they may apply broadly to viruses and may be instructive in the development of more efficient new vaccines.

REFERENCES

Appleyard, G., S.M. Russell, B.E. Clarke, S.A. Speller, M. Trowbridge and J. Vadolas (1990). Neutralization epitopes on human rhinovirus type 2. *Journal of General Virology* **71**, 1275-1282.

Brioen, P., A.A.M. Thomas and A. Boeyé (1985). Lack of quantitative correleation between the neutralization of poliorivirus and the antibody mediated pI shift of the virions. *Journal of General Virology* **66**, 609-613.

Colonno, R.J., P.L. Callahan, D.M. Leippe, R.R. Rueckert and J.E. Tomassini (1989). Inhibition of rhinovirus attachment by neutralizing antibodies and their Fab fragments. *Journal of Virology* **63**, 36-42.

Davies, D.R. and E.A. Padlan (1992). Twisting into shape. *Current Biology* **2**, 254-256.

Delaet, I. and A. Boeyé (1994). Capsid destabilization required for antibody-mediated disruption of poliovirus. *Journal of General Virology* **75**, 581-587.

Delaet, I., R, Vrijsen and A. Boeyé (1992). Antigenic N to H conversion of poliovirus by a monoclonal antibody at low ionic strength. *Virology* **188**, 93-101

Jin. L., B.M. Fendly and J.A. Wells (1992). High resolution analysis of antibody-antigen interactions. *Journal of Molecular Biology* **226**, 851-865.

Ketterlinus, R., K. Wiegers and R. Dernick (1993). Revertants of poliovirus escape mutants: new insights into antigenic structures. *Virology* **192**, 525-533.

Krishnaswamy, S. and M.G. Rossmann (1990). Structural refinement and analysis of Mengo virus. *Journal of Molecular Biology* **211**, 803-844.

Mosser, A.G., D.M. Leippe and R.R. Rueckert (1989). Neutralization of picornaviruses: support for the pentamer bridging hypothesis. In: Semler, B.L. and E. Ehrenfeld (Eds.). Molecular aspects of picornavirus infection and detection. American Society for Microbiology, p 155-167.

Page, G.S., A.G. Mosser, J.M. Hogle, D.J. Filman, R.R. Rueckert and M. Chow (1988). Three dimensional structure of poliovirus serotype I neutralizing determinants. *Journal of Virology* **62**, 1781-1794.

Rini, J.M., U. Schulze-Gahmen and I.A. Wilson (1992). Structural evidence for induced fit as a mechanism for antibody-antigen recognition. *Science* **255**, 959-965.

Scraba, D.G. (1990). Functional aspects of the capsid structure of Mengo virus. *Journal of Structural Biology* **104**, 52-62.

Sherry, B. and R.R. Rueckert (1985). Evidence for at least two dominant neutralization antigens on human rhinovirus. *Journal of Virology* **53**, 137-143.

Smith, T.J., N.H. Olson, R.H. Cheng, H. Liu, E.S. Chase, W.M. Lee, D.M. Leippe, A.G. Mosser, R.R. Rueckert and T.S Baker (1993). Structure of human rhinovirus complexed with Fab fragments from a neutralizing antibody. *Journal of Virology* **67**, 1148-1158.

Thomas, A.A.M., R. Vrijsen and A. Boeyé (1986). Relationship between poliovirus neutralization and aggregation. *Journal of Virology* **59**, 479-485.

Wetz, K. (1993). Attachment of neutralizing antibodies stabilizes the capsid of poliovirus against uncoating. *Virology* **192**, 465-472.

Wiley, D.C. and J.J. Skehel (1987). The structure and function of the hemagglutinin membrane glycoprotein of influenza virus. *Annual Review of Biochemistry* **56**, 365-394.

APPENDIX A

SEQUENCING PRIMERS FOR THE CAPSID CODING REGION OF THE MENGO VIRUS GENOME

Primer	Nucleotide Position	Primer Sequence (3'→5')	Tm[a] (°C)
27	3497-3515	TTGAGACGTGTAGGACGAT	56
P4	3306-3324	AAGAAACGACCTTGCTTTG	54
33	3153-3171	TCACGGCCTGGACCATGAA	60
21	2991-3008	CACATAATATTTACACTG	46
P5	2836-2854	AGTAAAATTGTGGTCCCGG	56
32	2654-2670	ACATTGACTTTTATGTC	44
31	2567-2584	CCAATCGCGACCCTTCCT	58
30R	2388-2406	CTAGATCCAGACTTAAGAA	52
P1	2216-2234	GGATCGGCGAGAGAGGGCC	66
P3	1991-2008	AGGACTATCGTGACAAGG	54
22	1729-1745	GATTATGCTGCCATCTA	48
P6	1593-1611	TACCTGTTGTCTACCAGGT	66
26R	1424-1440	TGTACAAGATAGTCCAC	48

[a] The approximate Tm of each primer was calculated from the empirical formula $Tm = 4(G+C) + 2(A+T)$.

APPENDIX B

VP1 PEPTIDES

Peptide designation	Position	Sequence
F126	1001-1015	GVENAEKGVTENTDA
F127	1011-1020	ENTDATADFV
F128	1016-1030	TADFVAQPVYLPENQ
F129	1026-1035	LPENQTKVAF
F130	1031-1045	TKVAFFYDRSSPLGR
F131	1041-1050	SPLGRFAVKS
F132	1046-1055	FAVKSGSLES
F133	1051-1060	GSLESGFAPF
F134	1056-1070	GFAPFSNKACPNSVI
F135	1066-1075	PNSVILTPGP
F136	1071-1085	LTPGPQFDPAYDQLR
F137	1081-1090	YDQLRPQRLT
F138	1086-1100	PQRLTEIWGNGNEET
F139	1096-1105	GNEETSEVFP
F140	1101-1109	SEVFPLKTK
F141	1105-1114	PLKTKQDYSF
F142	1110-1124	QDYSFCLFSPFVYYK
F143	1120-1129	FVYYKCDIEV
F144	1125-1139	CDIEVTLSPHTSGAH
F145	1135-1144	TSGAHGLLVR
F146	1140-1152	GLLVRWCPTGTPT
F147	1148-1157	TGTPTKPTTQ
F148	1153-1167	KPTTQVLHEVSSLSE
F149	1163-1172	SSLSEGRTPQ
F150	1168-1182	GRTPQVYSAGPGTSN
F151	1178-1197	PGTSNQISFV
F152	1183-1197	QISFVVPYNSPLSVL
G314	1195-1209	SVLPAVWYNGHKRFD
F155	1200-1209	VWYNGHKRFD
F156	1205-1219	HKRFDNTGDLGIAPN
F157	1215-1224	GIAPNSDFGT
F158	1220-1234	SDFGTLFFAGTKPDI
F159	1230-1239	TKPDIKFTVY
F160	1235-1243	KFTVYIRYK
F161	1239-1248	YIRYKNMRVF
F162	1244-1258	NMRVFCPRPTVFFPW
F163	1254-1263	VFFPWPTSGD
F164	1254-1277	PTSGDKIDMTPRAGVLMLE

VP2 PEPTIDES

Peptide designation	Position	Sequence
K89	2001-2015	DQNTEEMENISDRVS
K90	2011-2020	SDRVSQDTAG
K91	2016-2030	QDTAGNTVTNTQSTV
K92	2026-2035	TQSTVGRLVG
K93	2031-2045	GRLVGYGTVHDGEHP
K94	2041-2050	DGEHPASCAD
K95	2046-2058	ASCADTASEKILA
K96	2054-2063	EKILAVERYY
K97	2059-2073	VERYYTFKVNDWTST
K98	2069-2078	DWTSTQKPFE
K99	2074-2088	QKPFEYIRIPLPHVL
K100	2084-2093	LPHVLSGEDG
K101	2089-2103	SGEDGGVFGATLRRH
K102	2099-2108	TLRRHYLVKT
K103	2104-2117	YLVKTGWRVQVQCN
K104	2113-2122	QVQCNASQFH
K105	2118-2132	ASQFHAGSLLVFMAP
K106	2128-2137	VFMAPEYPTL
K107	2133-2147	EYPTLDVFAMDNRWS
K108	2143-2152	DNRWSKDNLP
K109	2148-2162	KDNLPNGTRTQTNRK
K110	2158-2167	QTNRKGPFAM
K111	2163-2177	GPFAMDHQNFWQWTL
K112	2173-2182	WQWTLYPHQF
K113	2178-2193	YPHQFLNLRTNTTVD
K114	2188-2197	NTTVDLEVPY
K115	2193-2207	LEVPYVNIAPTSSWT
K116	2203-2212	TSSWTQHASW
K117	2208-2216	QHASWTLVL
K118	2212-2221	WTLVLAVVAP
K119	2217-2231	AVVAPLTYSTGASTS
K120	2227-2236	GASTSLDLTA
K121	2232-2246	LDLTASLQPVRPVFN
K122	2242-2251	RPVFNGLRHE
K123	2247-2256	GLRHEVLSRQ

VP3 PEPTIDES

Peptide designation	Position	Sequence
K124	3001-3015	SPIPVTIREHAGTWY
K125	3011-3020	AGTWYSTLPD
K126	3016-3030	STLPDSTVPIYGKTP
K127	3024-3035	YGKTPVAPAN
K128	3031-3045	VAPANYMVGEYKDFL
K129	3041-3050	YKDFLEIAQI
K130	3046-3058	EIAQIPTFIGNKM
K131	3054-3063	IGNKMPNAVP
K132	3059-3073	PNAVPYIEASNTAVK
K133	3069-3078	NTAVKTQPLA
152 BNC	3076-3091	PLAVYQVTLSCSCLAN
K136	3089-3103	LANTFLAALSRNFAQ
K137	3099-3108	RNFAQYRGSL
K138	3107-3116	SLVYTFVFTG
K139	3112-3126	FVFTGTAMMKGKFLI
G134	3122-3136	GKFLIAYTPPGAGKP
K141	3127-3141	AYTPPGAGKPTSRDQ
G135	3136-3150	PTSRDQAMQATYAIW
K143	3142-3156	AMQATYAIWDLGLNS
K144	3152-3161	LGLNSSYSFT
K145	3157-3167	SYSFTVPFISP
K146	3163-3172	PFISPTHFRM
K147	3168-3182	THFRMVGTDQANITN
K148	3178-3187	ANITNVDGWV
K149	3183-3197	VDGWVTVWQLTPLTY
K150	3193-3202	TPLTYPPGCP
K151	3198-3212	PPGCPTSAKILTMVS
K152	3208-3217	LTMVSAGKDF
K153	3213-3222	AGKDFSLKMP
K154	3218-3227	SLKMPISPAP
K155	3223-3231	ISPAPWSPQ

VP4 PEPTIDES

Peptide designation	Position	Sequence
K156	4001-4015	GNSTSSDKNNSSSEG
K157	4011-4020	SSSEGNEGVI
K158	4016-4030	NEGVIINNFYSNQYQ
K159	4026-4035	SNQYQNSIDL
K160	4031-4046	NSIDLSANATGSDPPK
K161	4042-4051	SDPPKTYGQF
K162	4047-4061	TYGQFSNLLSGAVNA
K163	4057-4066	GAVNAFSNML
K164	4062-4070	FSNMLPILA